HIPPARCHOS

The Hellenic Astronomical Society Newsletter

Volume 2, Issue 8

ISSN: 1790-9252

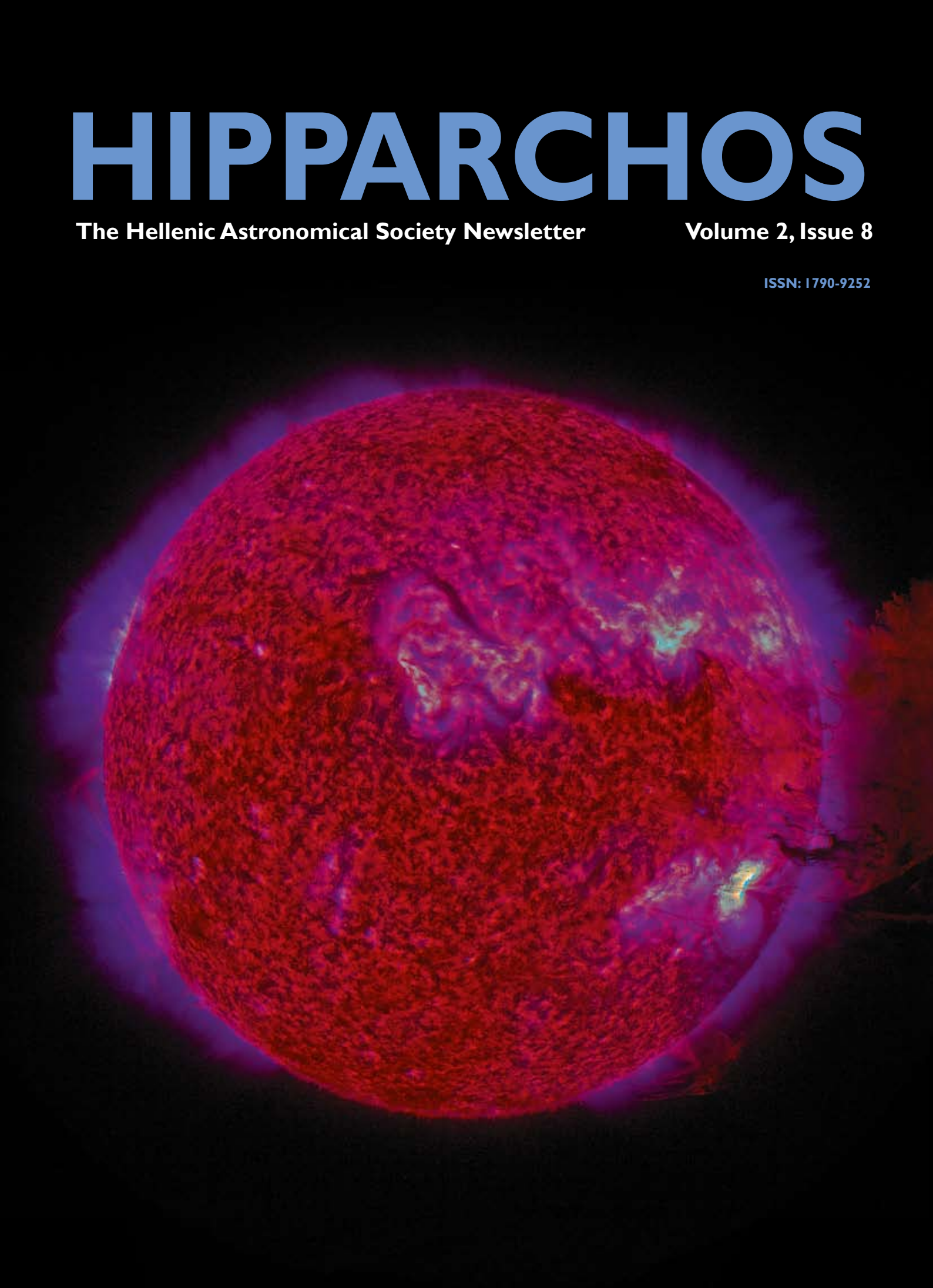

Foreground image:

The Heliophysics System Observatory (HSO) showing current operating missions, missions in development, and missions under study.

Credit: NASA

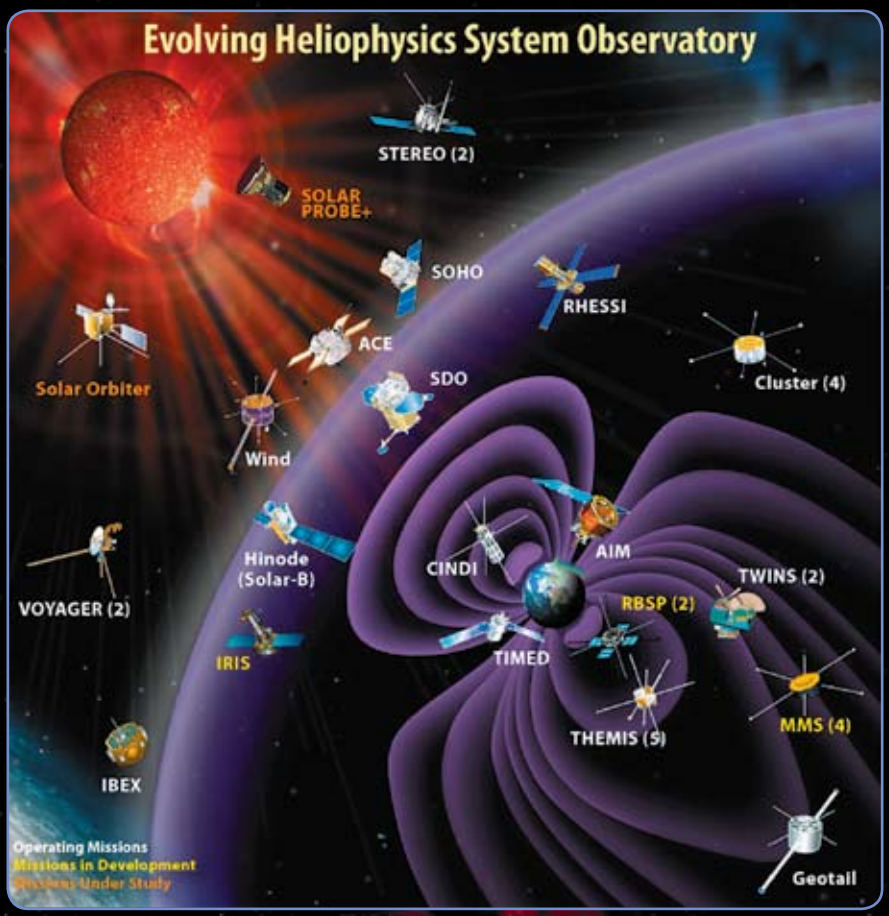

Background image:

Plasma Rain, April 19, 2010. SDO (Solar Dynamics Observatory) is the first observatory to capture both the rain and the impacts, allowing us to learn a great deal from observations like this.

Credit: NASA

Contents

HIPPARCHOS Volume 2, Issue 8 • September 2011

ISSN: 1790-9252

Hipparchos is the official newsletter of the Hellenic Astronomical Society. It publishes review papers, news and comments on topics of interest to astronomers, including matters concerning members of the Hellenic Astronomical Society.

Editorial board

- **Loukas Vlahos** (Thessaloniki)
- **Christos Efthymiopoulos** (Athens)
- **Georgia Tsiropoula** (Athens)

Contact person

Loukas Vlahos
Department of Physics,
Aristotle University,
54124 Thessaloniki, Greece
Tel: +30-2310-998044
Fax: +30-2310-995384
E-mail: vlahos@astro.auth.gr

Editorial Advisors

- **V. Charmandaris** (Crete)
- **D. Hatzidimitriou** (Athens)
- **K. Kokkotas** (Thessaloniki)
- **M. Plionis** (Athens)

Printed by ZITI Publications • www.ziti.gr

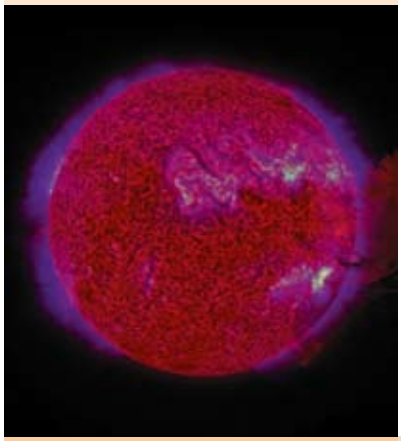

Cover image:

"The Sun like never seen before!"

Credit: Manolis K. Georgoulis

Message from the President 5

BRIEF SCIENCE NEWS

FP7 project on 'Coronal Mass Ejections and Solar Energetic Particles: forecasting the space weather impact' 6

Astronomy Education in Greek Schools 8

The Solar Dynamics Observatory Feature Finding Team (SDO/FFT): The First Massive Computer Vision Effort 11

REVIEWS

New Results from Ultra High Energy Cosmic Ray Telescopes
by Vasiliki Pavlidou 14

Planetary systems revealed through direct imaging
by Paul Kalas 22

The Cosmic microwave background radiation: the memories of the Universe revealed
by C. Sofia Carvalho 30

Recent Advances in Heliophysics from Space-Based Observations
by Angelos Vourlidas 36

Image description:

View of the spectacular solar prominence eruption of June 7, 2011, observed at 07:21 UT by the Atmospheric Imaging Assembly onboard the Solar Dynamics Observatory mission. The image is a composite, consisting of one AIA image at 304 Angstrom and one at 211 Angstrom. The gigantic eruption projects over almost the entire bottom-right (southwest) solar limb, with a projected length scale of about 1 million kilometers.

10th Hellenic Astronomical Conference

Ioannina, 5-8 September 2011

Under the Auspices of
H.E. the President of the Hellenic Republic
Dr. Karolos Papoulias

Scientific Organising Committee:
N. Kylafis (Chair)
A. Anastasiadis
T. Apostolatos
A. Bonanos
C. Efthymiopoulos
M. Metaxa
A. Nindos
I. Papadakis
D. Rigopoulou
G. Tsiropoula
N. Vlahakis
L. Vlahos
A. Zezas

Local Organising Committee:
S. Patsourakos (Chair)
A. Nindos
V. Ontiveros
V. Tsikoudi

Session 1: **Sun, Planets and Interplanetary Medium**
Session 2: **Extragalactic Astrophysics and Cosmology**
Session 3: **Dynamical Astronomy & Relativistic Astrophysics**
Session 4: **Stars, Our Galaxy and the Local Group**
Session 5: **Education in Astronomy**

Plenary Speakers:
J. Binney (Oxford University)
A. Coustenis (Paris-Meudon Observatory)
T. Piran (Hebrew University)
A Hood (St. Andrews University)

Sponsored by:
Academy of Athens (RCAAM),
National Observatory of Athens,
and University of Ioannina

Organised by:

http://www.helas.gr/conf/2011

Background Image Credits: Skinakas Observatory

Message from the President

Dear friends,

As new President of the Hellenic Astronomical Society (Hel.A.S.) and on behalf of its new Governing Council (GC) I would like to thank everyone for entrusting us to run our Society. It will be difficult to surpass the achievements of the previous GC, but we will try.

Not only our country, but also our Society is facing economic problems. Its main income comes from the annual dues of its members, which for obvious reasons are not high. Sponsors of Hel.A.S., many and generous in the past, are few and rather reserved now. Bright exceptions are the Academy of Athens and the National Observatory of Athens. The new GC of Hel.A.S. discussed extensively ways to reduce costs. Thus, small but important expenses (such as participation of its members at conferences), that were paid by the Society in the past, will not be covered until the situation changes for the better. The publication of HIPPARCHOS is a major cost for the Society. Thus, two issues per year are no longer possible. Among various proposals for the future of HIPPARCHOS, the GC decided to continue its publication, but only with one issue per year. This is the first issue under the new Editorial Board, which consists of Prof. Loukas Vlahos, Dr. Christos Efthimiopoulos, and Dr. Georgia Tsiropoula. I would like to thank the last Editor, Dr. Manolis Plionis, as well as the previous ones, for the continuous improvements.

Having painted a rather grey picture regarding the financial situation of our Society, I would like to turn to more pleasant things. The 10th Hellenic Astronomical Conference in Ioannina is a major event for our Society. I am very happy to inform you that H. E. the President of the Hellenic Republic, Dr. Karolos Papoulias, has placed our conference under his auspices.

Thanks to the members of the GC, the conveners of the sessions, and the Local Organizing Committee, the conference has been planned well. The four distinguished Plenary Speakers (Prof. James Binney, Dr. Athena Coustenis, Prof. Alan Hood, and Prof. Tsvi Piran), several Invited Speakers, and the many oral and poster contributions guarantee an exciting meeting.

The new GC of Hel.A.S. has introduced two rather innovative items for the 10th Hellenic Astronomical Conference and hopefully for the subsequent ones:

1) One of the oral contributions by a young astronomer will be presented as a Highlight Talk by a Young Astronomer. This year's Highlight Talk will be given by Dr. Dimitrios Emmanoulopoulos.
2) A full day (the last of the conference) will be devoted to the Education in Astronomy and it is meant mainly for Secondary School Teachers. Several talks and activities are planned for this day.

The GC and I are looking forward to our General Assembly in Ioannina to hear innovative ideas, as well as improvements, regarding the activities of our Society.

In closing, and in view of the start of the new academic year, I wish you health and productivity.

Nikos Kylafis
President of Hel.A.S.

FP7 project on 'Coronal Mass Ejections and Solar Energetic Particles: forecasting the space weather impact'

During an 11 year cycle the Sun goes from quiet conditions at minimum to levels of high activity at maximum. In the latter case, energetic phenomena as Coronal Mass Ejections (CMEs) and Solar Flares (SFs) accompanied by explosive releases of mass, magnetic flux and Solar Energetic Particles (SEPs) are common. Ensuring the safety of astronauts and space assets from the extreme conditions of space, especially the energetic particle environments, is a key goal for both ESA and NASA. The analysis, the risk management, the forecasting of such events and the mitigation of hazards constitutes the scientific field of Space Weather. Space Weather is thus a highly relevant field of research for our modern society.

The Carrington event in 1859– named after the British astronomer Richard Carrington who observed the intense white-light flare associated with the subsequent geomagnetic storm – is by several measures the most severe space weather event on record. It produced several days of spectacular auroral displays even at unusually low latitudes. Given the state of the technology at the time the effect was limited to significant disruption telegraph services around the world. If such an event occurred today the story would be totally different. Modern society depends heavily on a variety of technologies that are vulnerable to the effects of intense geomagnetic storms and SEP events. Strong auroral currents can disrupt and damage electric power grids and may contribute to the corrosion of oil and gas pipelines. Magnetic storm-driven ionospheric density disturbances interfere with high-frequency and ultra-high-frequency radio communications and navigation signals from GPS satellites. Exposure of spacecraft to energetic particles during SEP events and radiation belt enhancements can cause temporary operations anomalies, damage critical electronics, degrade solar arrays, and blind optical systems such as imagers and star trackers. SEPs can penetrate astronaut uniforms, damage human DNA and cause cell replications. Intense sporadic SEP events (Figure 1) thus present a significant radiation hazard for astronauts on the International Space Station as well as for future human explorers of the Moon, Mars and asteroids who will be unprotected by Earth's magnetic field. Therefore, Europe urgently needs to have access to space weather predictions *at all times* in order to protect its citizens and services that

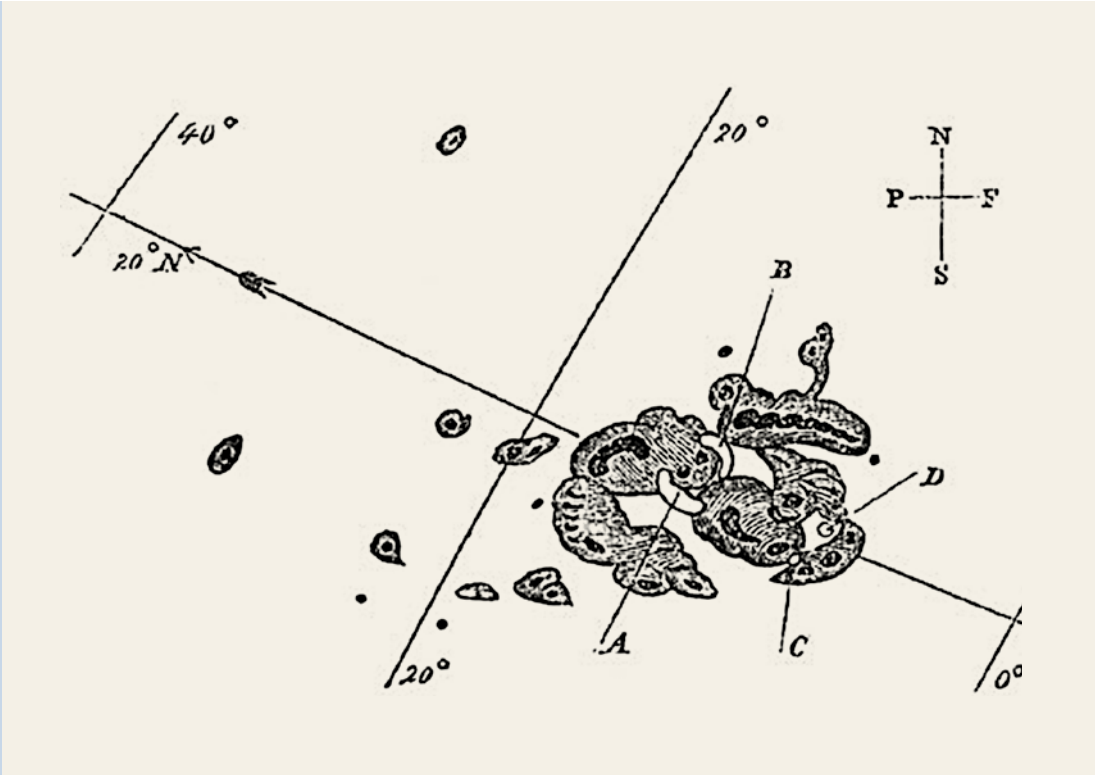

Figure: Sunspots of September 1, 1859, as sketched by Richard Carrington. A and B mark the initial positions of an intensely bright event, which moved over the course of 5 minutes to C and D before disappearing.

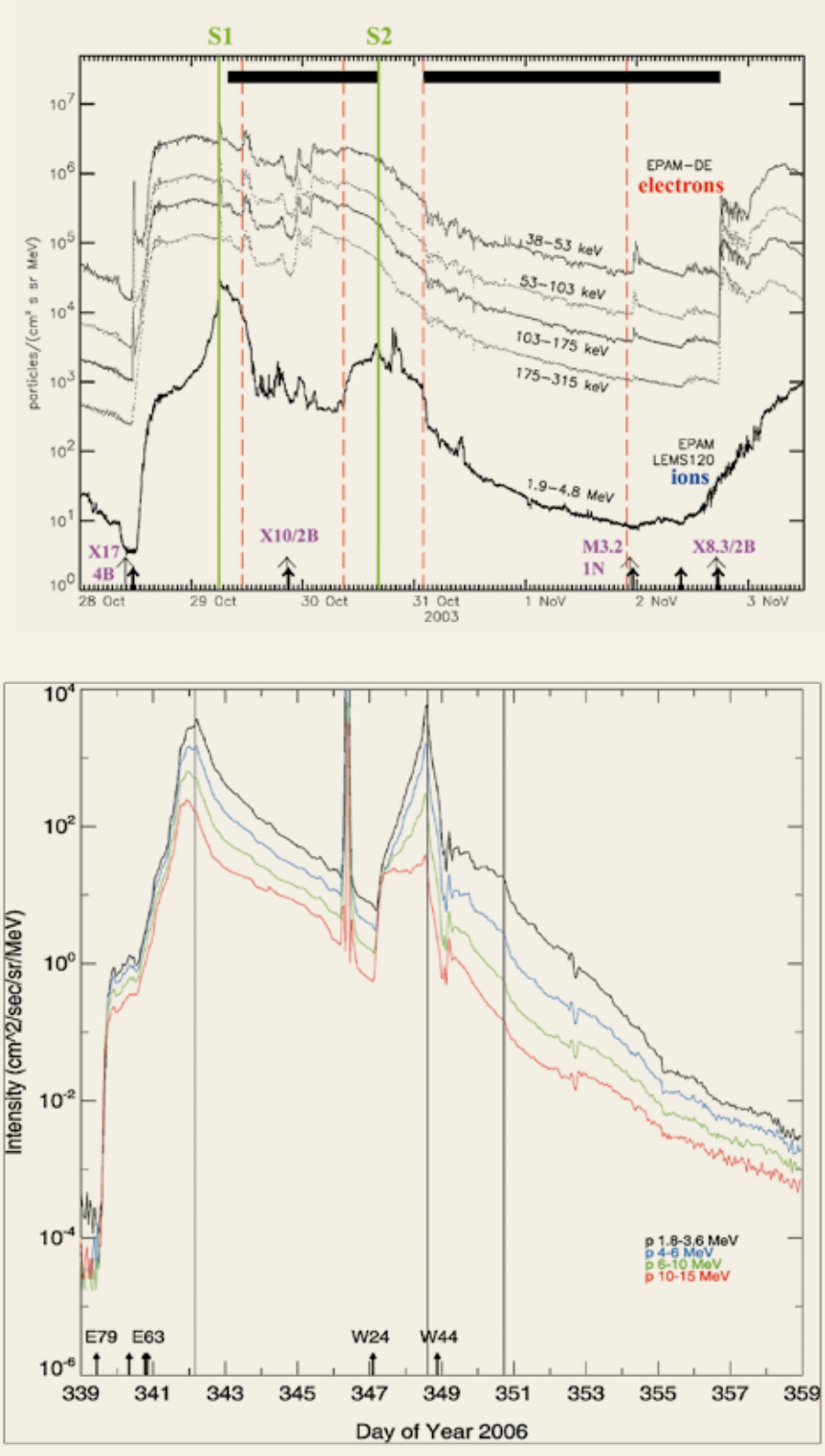

Figure: *(Top)* In late October and early November 2003 the Sun produced some of its strongest eruptive activity in the last three decades, which produced intense SEP events and triggered severe geomagnetic storms. 1-min averaged differential electron and ion intensities as measured by the ACE/EPAM experiment near the Earth are shown. The arrows indicate the occurrence of solar events, solid lines the passage of shocks whereas the black horizontal bars indicate the passage of ICMEs over ACE (*Malandraki et al.*, J. Geophys. Res., 110, A09S06, 2005).

(Bottom) 1.8-15 MeV proton intensities as measured by the LET instrument onboard STEREO-B are shown during the intense solar activity of December 2006 (*Malandraki et al.,* Astrophys. J., 704, 469, 2009).

support daily life and that rely on systems vulnerable to Space Weather.

The Institute of Astronomy and Astrophysics (IAA) of the National Observatory of Athens (NOA), apart of its involvement in the 'SEPServer' FP7 project, is currently strongly involved in a collaborative project funded by the seventh framework program of the European Union, namely: 'COMESEP: Coronal Mass Ejections and Solar Energetic Particles: forecasting the space weather impact'. The co-ordinating Institute is Institut d'Aeronomie Spatiale de Belgique with partners from Austria, Denmark, Croatia, and the UK. Principal Investigator on behalf of IAA/NOA is Dr. Olga Malandraki, member of staff, expert in the National Delegation team representing Greece to the ESA 'Science Programme Committee' and also the National Co-ordinator of the worldwide 'International Space Weather Initiative' (ISWI) under the auspices of the United Nations. The COMESEP team comprises Dr. Lun C. Tan, Dr. Gareth Dorrian and Dr. Kostas Tziotziou hired at the post-doctoral/researcher level at IAA/NOA. Within COMESEP, by analysis of historical data, complemented by the extensive data coverage of solar cycle 23, the key ingredients that lead to magnetic storms and SEP events and the factors that are responsible for false alarms will be identified. In order to enhance our understanding of the 3D kinematics and interplanetary propagation of CMEs, the structure, propagation and evolution of CMEs will be investigated. In parallel, the sources and propagation of SEPs will be examined and modelled. In collaboration with Dr. Allan Tylka in the Naval Research Laboratory, Space Science Division in the USA, IAA/NOA is strongly involved in the scientific investigation of the so-called 'reservoir effect', whereby SEP intensities follow a common decay at locations very far apart in space, as well as the impact of the large-scale structure of the IMF on the SEP profiles and its space weather implications. These important processes need to be understood in order to allow the event's duration (which determines the overall fluence) to be forecast. Based on the insights gained, COMESEP is set out to develop and optimise forecasting tools for SEP radiation storms and geomagnetic storms. These forecasting tools will be incorporated into an automated operational European Space Weather Alert system, which is the 'COMESEP' primary goal.

by Olga Malandraki
Institute of Astronomy and Astrophysics, National Observatory of Athens

Astronomy Education in Greek Schools

Astronomy provides a unique environment for educators from Kindergarten to Lyceum. It is the oldest of the natural sciences and it has a multidisciplinary character since over the years it has developed strong links with Physics, Chemistry, Biology, Ecology and Earth Sciences. Furthermore, the cultural and philosophical role of Astronomy is undisputed. Studying the Universe is a way of searching for our own origin, learning to situate ourselves within cosmic infinity and developing a sense for the beauty and fragility of our planet Earth. It allows us to keep a critical approach towards irrational pseudo-sciences. Astronomy is extremely popular and there is a great public interest for topics such as eclipses, meteor showers, space missions, discovering new planets and more exotic phenomena such pulsars and black holes (Metaxa, 2009).

Professional astronomers and their societies have traditionally played a key role in providing information and train-

Figure: *Simulating the detection of an exoplanet with the transit method in the school laboratory of the 2nd Lyceum of Echedoros.*

ing for the educators since the excitement at the school level about astronomy affects the recruitment and training of future astronomers and influences the awareness, understanding and appreciation for astronomy of the taxpayers and politicians who support astronomy. In other words we have an obligation to share the excitement and the significance of our work with students and the public. (Percy, 1995)

Astronomy education takes place in many cases besides the formal classroom. Of the most important cases are the planetariums and museums, the public media (newspapers, television, popular books, internet etc) and the recently developed, in many cities around Greece, amateur astronomical societies. All the above reinforce Astronomy education and suggest that students are also influenced by what is usually called "informal" education. (Pasachoff and Percy, 1990)

In the past the curriculum and the books written for the Greek secondary education were full of details and in some cases the material was extremely complicated even for the majority of the teachers. The subject of "Astronomy" was until 1998, obligatory in the second year of the Lyceum (one hour per week). From 1999 until last year, Astronomy was an elective course (two hours per week). The number of students attending Astronomy the last ten years had a steady increase (Dormatzidis, 2011 for details). Unfortunately school teachers (mostly with diploma in mathematics) did not have many opportunities to attend in service training which would assist them in the teaching of Astronomy, although they recognize that astronomy can inspire many students to pursue carrier in sciences and technology. In the meantime Greek Ministry of Education supported and disseminated in the Greek schools information about innovative international and European Large Scale astronomical projects. Teachers and students found ways for creative activities e.g. astronomy-on-line, Venues transit, sea and space etc, in their schools.

All these inspiring Large Scale projects were welcomed by the educational community all over Europe. In Greece as well these unique projects had a great appeal and more than 800 students from about 80 schools from all over the country had participated. A permanent link of cooperation between secondary school teachers and university teachers was also established through these activities. The summer school for students at the National Observatory of Athens and the Astronomy contests were established (Metaxa, *2009*). Hellenic Astronomical Society, recognizing the important role of astronomy education in the Greek schools, in the past years, had organized educational sessions for school teachers and students within its decennial conferences. The University of Athens offered to the elementary education student teachers a course dedicated to Astronomy which was entitled «our cosmos: basic concepts of astronomy and earth sciences » through which the future teachers would learn more about astronomy (Halkia, 2006).

Astronomy Education varies in European countries. In some of them "Astronomy" is taught either as a separate subject and in others it is part of the

Figure: *Students at Arsakeio High School created and constructed an exact galactic garden at their School using accurate data from the latest map of NASA/JPL-CALTECH/R. Hurt, 2008.*
The solar system and the most prominent nebulae, black holes, supernova etc are situated at the right place so the visitor can understand the dimensions and structure of the Galaxy walking around.

physics books. Additionally, in Europe, students learn more about astronomy through specific projects in a very effective way.

From all the above it becomes obvious that we have to search for an effective way to teach Astronomy in our schools, starting from kindergarten through the end of secondary education. In order to enhance Astronomy education we should build and implement a model which may include collaboration between teachers-researchers-students. In addition, as research has shown, by introducing technical innovations into the classroom, we could produce a dramatic redefinition of the traditional roles for teachers by emphasizing the collaborative work between teachers and learners. Also, the use of technology in the classroom could foster the formation of an environment that reflects more closely the processes that scientists use in doing research (Metaxa, 2002). Astronomy is undoubtedly a subject that can easily bring technical innovations into the classroom.

The recent national reform introduced recently by the Greek Ministry of Education under the name "The New school," where the science curriculum provides guidelines which call for (a) integration of science with mathematics, (b) more time devoted to inquiry and long-term projects, (c) more group work and cooperative learning, (d) effective application of existing technical tools such as plotting data using special software and microcomputer-based laboratories, and (e) realistic assessment tied to non-academic outcomes. The purpose of this new reform is to make the classrooms more exciting places to learn and apply science (Metaxa, 2002).

Figure: *Students of The Gymansium Lyceoum Nikiforos, observing through the school´s telescope, assisted by the Amateurs´Club of Drama, Pigasos.*

We believe that introducing Astronomy in the area of the "Research project" (which is one of the innovations of the "New School") will have many unique characteristics: (a) will cover all levels of education and unify the formal and informal education, (b) will have a Multi-Disciplinary character (involving Physics, Technology, Environment etc) (c) will foster collaboration to manage scientific work, and (d) will stress both the scientific and the social components. Thus by developing and promoting the teaching of Astronomy in the broadest possible way we can introduce students to science in a very pleasant way and can easily focus on preparing them for a "life–long learning" journey (Metaxa, 2006, Kallery, 2007). Thus it's a unique opportunity to involve Astronomy in the NEW LYCEOUM which has been planned to start form the new academic year and to make it part of the science curriculum in a most effective way, as it is in other countries.

References

1. Dormatzidis, M. (2011), Diploma Thesis, School of Natural Sciences, Open University (in Greek)
2. Halkia, C. (2006). The Solar System inside the Universe, University of Crete Press (in Greek)
3. Kallery, M. (2007). Science Fair: An alternative way to learning and developing scientific skills and attitudes. *Contemprary Education,* (in Greek), Vol. 149, pp. 111-121.
4. Metaxa, M. (2002), "Teaching Astronomy in the Modern Classroom", Communicating Astronomy, Tenerife, ed. T.J. Mahoney
5. Metaxa, M. (2002), "International Schools Education Networks for Light Pollution Control", Light Pollution: the Global view, Chile, ed. H.E. Schwarz
6. Metaxa, M. (2006), Light pollution: A tool for astronomy education**,** Innovation in Astronomy education, p.85, ed. J.M.Pasachoff, R.M.Ros, IAU GA in Prague
7. Metaxa, M. (2009), Astronomy Education: a challenge for contemporary Education, Advances in Hellenic Astronomy During the IYA09, *ASP* Vol.424, p.483, *2009, Athens*
8. Percy, J.R. (1995c), Fifth International Conference on Teaching Astronomy, ed. R.M. Ros, Universidad Politecnica de Catalunya, 63.
9. Pasachoff, J.M., Percy, J.R. (1990), "The Teaching of Astronomy", Cambridge, Cambridge University Press. 1.

by Margarita Metaxa
Philekpaideutiki Etaireia, Arsakeio High school
Loukas Vlahos
Department of Physics,
Aristotle University, 54124 Thessaloniki, Greece

The Solar Dynamics Observatory Feature Finding Team (SDO/FFT): The First Massive Computer Vision Effort

In the mid-morning hours of February 11, 2010, a flagship NASA mission lifted off the grounds of Cape Canaveral: it was the Solar Dynamics Observatory (SDO), designed to succeed the historic Solar and Heliospheric Observatory (SoHO) mission, arguably the most successful heliophysics mission ever launched. The SDO payload philosophy is simpler but its observing plan is incomparably more detailed and data-intensive than SoHO's (Figure 1). The SDO includes basically three suites of instruments: the Helioseismic and Magnetic Imager (HMI), the first full-Sun space-borne solar vector magnetograph, the Atmospheric Imaging Assembly (AIA), an ultraviolet, extreme ultraviolet (EUV), and X-ray imager of the Sun's corona, and the Extreme Ultraviolet Variability Experiment (EVE), a full-Sun EUV spectrograph and photometer combination. Take the daily data harvest of HMI and AIA and you have a volume that would appear inconceivable just a few years ago: nearly 1.5 TerraBytes of data are collected by SDO every single day and are archived at the storage facilities of the Joint Science Operation Center (JSOC) between the Lockheed Martin Solar and Astrophysical Laboratory (LMSAL), for AIA, and Stanford University, for HMI.

The above staggering amount of data needs to be processed and scientifically analyzed. Obviously, this cannot be accomplished manually regardless of workforce committed to the task. Realizing this in time, NASA selected in the Fall of 2008 two international consortia with a four-year period of performance and an objective to devise the appropriate automatic software tools able to process, classify, and analyze the AIA and HMI data. These projects have no precedent as the massive SDO data will be automatically processed and scientifically analyzed at the instruments' pipeline, that is, just as the data are down-linked from space. One of the selected teams focused on analyzing the HMI's helioseismology data; the other, self-proclaimed the *SDO Feature Finding Team (SDO/FFT)*[1] will analyze the SDO's solar atmospheric data and is the main topic of this article.

The SDO/FFT comprises of researchers from five (5) European and seven (7) US universities and research institutes. It is coordinated by a joint team from Harvard and the Montana State (MSU) universities with the Principal Investigator being MSU's Dr. Petrus Martens. There is Greek participation in the SDO/FFT involving the Academy of Athens' Research Center for Astronomy and Applied Mathematics (RCAAM).

The SDO/FFT has converged on a series of thirteen (13) modular scientific algorithms that are currently operating or are being optimized for implementation onto the AIA and HMI pipelines. In random order, these modules are the following:

- A solar flare detection method, led by Harvard's Dr. P. Grigis.
- A solar active region and coronal hole detection method, led by Dr. V. Dellouille of the Royal Observatory of Belgium.
- A solar filament identification and characterization method, led by Dr. P. Bernasconi of the Johns Hopkins University Applied Physics Laboratory.

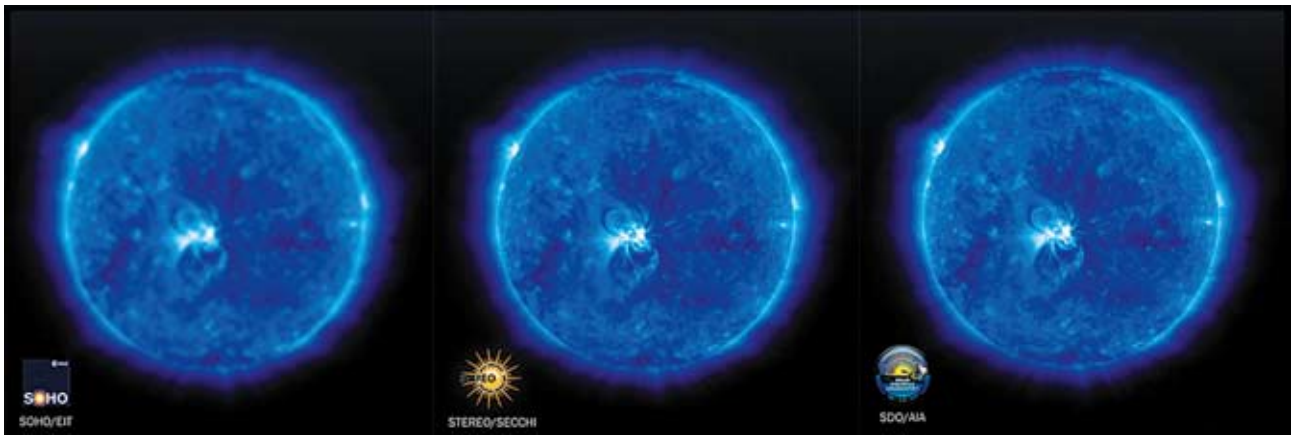

Figure 1: *Improvement in image clarity and resolution brought by the SDO mission: three nearly simultaneous images of the EUV solar corona as observed by SoHO (left), STEREO (middle), and SDO (right) missions. With a SoHO cadence of 12 min per wavelength and an image analysis of 2 arcsec per pixel, the SDO will collect one image per wavelength with analysis 0.6 arcsec per pixel every 10 s. [Courtesy: NASA/SDO].*

– A solar X-ray sigmoid finder, led by RCAAM's Dr. M. Georgoulis.
– An emerging magnetic flux detector, led by Dr. C. DeForest of the South-West Research Institute.
– A coronal dimming's detector, led by Harvard's Dr. A. Davey.
– A EUV-wave tracker, led by Harvard's Dr. M. Wills-Davey.
– A coronal bright point detector, led by Harvard's Dr. S. Farid.
– A jet detector within solar coronal holes, led by Dr. A. Savcheva of Boston University.
– A magnetic polarity inversion line mapping method, led by Harvard's Dr. A. Engel.
– A coronal oscillations detector, led by Dr. J. McAteer of the New Mexico State University.
– A global solar nonlinear force-free magnetic field extrapolator, led by Dr. T. Wiegelmann of the Max-Planck Institute at Lindau.
– An artificial intelligence trainable module, led by MSU's Dr. R. Angryk.

Evidently the selected modules address a wide variety of quiescent and eruptive phenomena of the solar coronal zoo. Timely, automated results can also affect positively ongoing efforts for space-weather forecasting, another central objective of the SDO mission. Of particular interest is the ambitious automatic trainable module that can be trained to identify solar features not already addressed by other modules. By the project's expiration, in the Fall of 2012, the results of all modules will be freely accessible online.

To facilitate the dissemination process, the SDO/FFT software is part of the SDO Event Detection System (EDS) operating at JSOC[1]. The core objective of the EDS is the automatic analysis of AIA and HMI pipeline data including the generation of space-weather alerts, quicklook images and movies, and other helpful community tools. Emphasis has also been given to versatility: the EDS will allow the inclusion of future tools and modules to accommodate forthcoming advances in the automatic scientific analysis of solar data.

Each EDS module, and hence the SDO/FFT modules, produce uniform VOEvent object metadata in XML format that are stored and displayed at the freely accessible Heliophysics Events Knowledgebase (HEK)[2] (Figure 2). The HEK further provides data to the Virtual Solar Observatory (VSO) or to the Helioviewer[3] (Figure 3). This is another unprecedented, joint ESA-NASA effort for a common, user-friendly desktop tool able to gather, synthesize, and visualize in a sophisticated manner SDO and other space- and ground-base data.

In this era of massive data acquisition, assimilation and efficient visualization without human intervention have naturally assumed central roles. But these tasks cannot be possibly achieved by a single team, let alone by a single scientist. The best response to the needs of our times is to seek and forge synergies with groups worldwide pursuing the formation of international partnerships with diverse skills and sufficient expertise to address the complexity of the tasks at hand. It is of hope and promise that ESA, NASA, JAXA and perhaps other space agencies seem to have realized this and are moving in concerted steps where necessary.

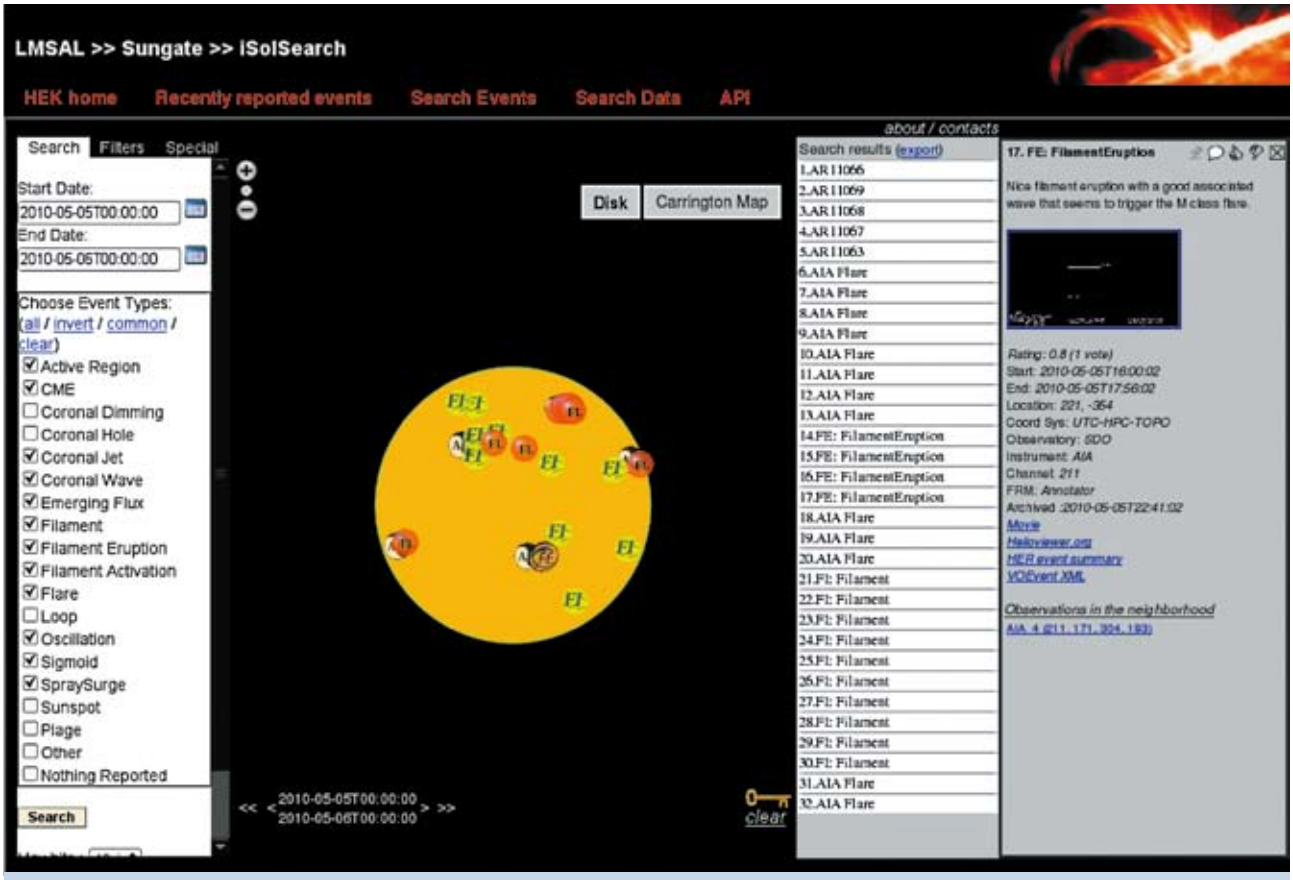

Figure 2: *HEK interface screenshot. Features identified by SDO/FFT modules have been placed on a featureless solar disk via their respective symbols. A list of the features found and elements from the VOEvent metafiles are given in the right [Courtesy: LMSAL].*

Figure 3: *Desktop screenshot from Helioviewer depicting two AIA images (in 171 Å and 304 Å) that have been blended in observing an eruptive solar prominence [Courtesy: NASA].*

Acknowledgements:

I thank the HIPPARCHOS Editors for the opportunity to present and discuss the SDO/FFT Project. During my tenure at the Johns Hopkins University Applied Physics Laboratory this work was funded by NASA's grant NNX09AB03G. In Europe my work is partially supported by a Marie Curie Fellowship of the European Union's Seventh Framework Programme (FP7/2007 – 2013) under grant agreement n° PIRG07-GA-2010-268245.

References

1. Martens, P. C. H., et al.: "Computer Vision for the Solar Dynamics Observatory (SDO)", *Solar Phys.* 2011, in press, DOI: 10.1007/s11207-010-9697-y
2. Hurlburt, N., et al.: "Heliophysics Events Knowledgebase for the Solar Dynamics Observatory (SDO) and Beyond", Solar Phys. 2011, in press, DOI: 10.1007/s11207-010-9624-2
3. Hughitt, V. K., et al.: "Helioviewer: A Web 2.0 Tool for Visualizing Heterogeneous Heliophysics Data", AGU Fall Meeting 2008, abstract #SM11B-1617

by Manolis K. Georgoulis
Research Center
for Astronomy and Applied Mathematics
of the Academy of Athens

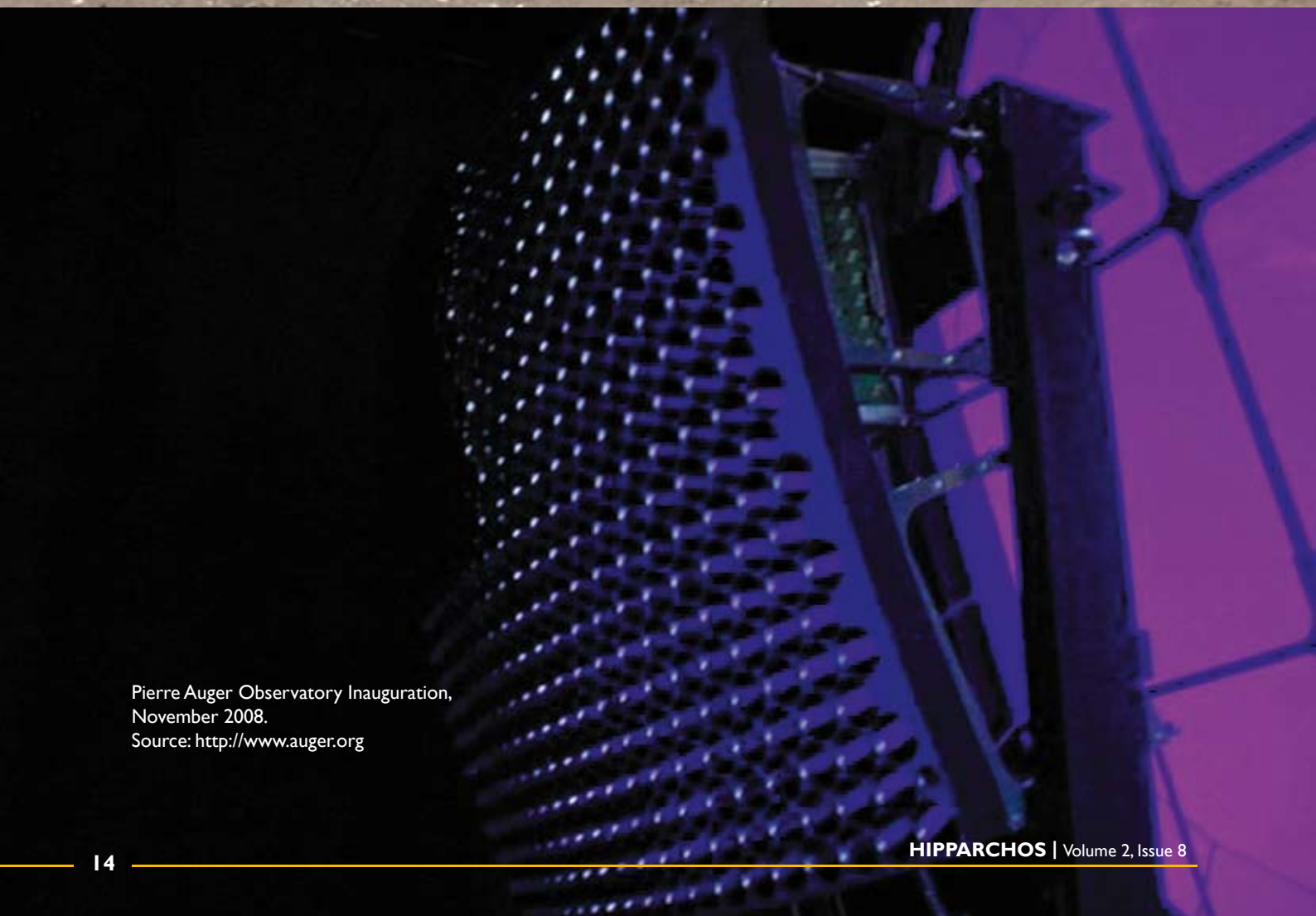

Pierre Auger Observatory Inauguration,
November 2008.
Source: http://www.auger.org

New Results from Ultra High Energy Cosmic Ray Telescopes

by Vasiliki Pavlidou

Astronomy Department, California Institute of Technology, USA, & Department of Physics, University of Crete, Greece

Abstract

Ultra-High-Energy Cosmic Rays (UHECR) are the most energetic particles in the Universe, with energies reaching 10^{20} eV. Their sources, which are nature's most powerful accelerators, are still unknown; however, UHECR experiments have achieved tremendous progress over the past decade. In particular, a wealth of unprecedented quality new data on the UHECR spectrum, composition, and arrival directions have been collected and presented during the past few years. Here, we briefly review the significant progress that high-quality data from state-of-the-art observatories have allowed us to make, as well as the new big questions in UHECR physics that the new data have posed.

Ultra High Energy Cosmic Rays: Challenges and Promise

Ultra-high–energy cosmic rays (UHECR) are the most energetic particles in the Universe. With energies over 10^{18} eV, they pack the energy equivalent of an aggressively served tennis ball in a single subatomic particle. Questions such as their origin, their composition, and the extreme physical mechanisms that get them to such high energies remain, to this day, open and highly debated. This is not due to lack of effort, but rather due to severe practical difficulties hindering their study.

First of all, UHECR cannot be detected directly. They interact in the Earth's atmosphere and produce extended air showers of secondary particles (see Fig. 1), including electrons and positrons, photons, muons, and neutrinos, which, by the time they reach the ground, have a footprint of enormous scale – its size depends on the nature and energy of the primary incoming particle and the shower inclination, but at the highest energies typically reaches diameters of several to tens of kilometers.

Second, the flux of UHECR at the highest energies is extremely low. At energies above a few times 10^{18} eV the flux is at one particle per km^2 per year, while at the highest energies (above a few times 10^{19} eV) it falls to one particle per km^2 per century (see Fig. 2): UHECR study is a sport only for those who have extremely large patience or extremely large detectors.

Third, UHECR are charged particles, and as a result they are deflected by the Galactic and intergalactic magnetic fields, so their apparent arrival directions cannot be directly traced back to their sources. For a source at a given distance, the angular extent of the UHECR deflections depends on the particle energy and charge, and on the magnetic field magnitude and coherence length. Even if intergalactic magnetic fields, the magnitude of which remains highly uncertain, turn out to be very low, and even if UHECR are composed exclusively of protons, deflections in the magnetic field of the Galaxy alone can reach, at the highest energies (above a few times 10^{19} eV), a few degrees (e.g., Abraham et al. 2007). These deflections will only increase for higher Z particles, lower energies, and appreciable intergalactic magnetic fields.

Fourth, this deflective motion within magnetic fields also renders impossible the use of temporal coincidences of UHECR spikes with transient or flaring sources. The reason is that while photons from a presumed UHECR-accelerating event will travel to the observer along null geodesics, the charged particles will be deflected in the magnetic field and cover a much longer path on their way to the observer, and as a result they will take a much longer time to arrive there (e.g., Alcock & Hatchett 1978). Again, under the assumption of proton-only UHECR of energies a few times 10^{19} moving in the magnetic field of the Galaxy alone, the associated time-delays between the photon and the particle signal would be of the order of a century.

Finally, hadronic collision physics at the highest UHECR energies has not been studied in the lab, and is not well-understood: the collisions initiating the UHECR showers have center-of-mass energies of 100 TeV, an order of magnitude higher than the energies probed by the Large Hadron Collider (LHC) at CERN. As a result, the reconstruction of the energy and the charge of the primary particle from the distribution of particles reaching the ground involve systematic uncertainties that cannot be accounted for or controlled in a satisfactory manner (Abraham et al. 2010b).

Despite these observational challenges, the motivation for studying UHECR is very strong and diverse.

First of all, UHECR pose a unique challenge to theoretical astrophysics: their energies lie at the very edge of the energy range that any astrophysical accelerator can even in principle reach (Hillas 1984; Ptitsyna & Troitsky 2010). The very basic requirement to accelerate particles at high energies starting from lower-energy particles in any single astrophysical system is to be able to confine the particle within the system. This requirement in turn can be translated in a requirement on the combination of said system's size and magnetic field. Only a handful of extreme systems, such as neutron stars,

active galactic nuclei and their jets, gamma-ray bursts, and intergalactic structure formation shocks, have appropriate combinations of sizes and magnetic fields to be able to reach, even in principle, such high energies. But accelerating the particles is not enough – it is then necessary to get them out of the source, without them suffering severe energy losses. This is also challenging, as UHECR undergo losses through photopion production in strong photon fields, or even in diluted photon fields (such as the cosmic microwave background, or the extragalactic infrared, optical, and ultraviolet background light produced by galaxies) if they propagate over large enough distances. The first effect poses severe challenges for candidate accelerators that are very luminous. The latter effect poses challenges for scenarios involving multi-site acceleration or acceleration in very rare sources: at the highest energies, UHECR that have traveled distances over a few tens of Mpc start experiencing severe energy losses; the highest-energy particles have to have originated in the local universe.

Second, exactly because of their travel through intergalactic magnetic fields, UHECR present a unique tool for studying and mapping these fields. Should individual point sources of UHECR be identified, the effective "point spread function" induced on the arrival directions of particles from each source through magnetic deflections would be a cumulative measure of the magnetic fields and their coherence lengths intervening between observer and source. If, on the other hand, a *class* of UHECR sources is identified, then the intergalactic and Galactic magnetic fields in various directions could be assessed statistically, comparing the level of anisotropies in the highest-energy UHECR with the known distribution of nearby source counterparts in various wavelengths.

Third, because UHECR experience energy losses as they travel through the infrared, optical, and ultraviolet extragalactic background light, a study of the way their energy spectrum is affected and altered by these losses provides a way to study the extragalactic background light itself. This is very important as this background light is produced by, and in turn probes, star-formation through cosmic time.

Fourth, in the process of photopion losses of UHECR on the extragalactic background light and on the cosmic microwave background, charged pions, and later neutrinos, are produced, among other particles and photons. These neutrinos, commonly referred to as cosmogenic neutrinos, comprise the only guaranteed astrophysical high-energy neutrino signal in the universe. Their detection could provide the first long-sought detection of high-energy astrophysical neutrinos (note that neutrinos which have been detected up to now from astrophysical sources, i.e. neutrinos from the Sun and from supernova 1987A, all have relatively low energies, much lower than the TeV thresholds typically applicable to current and under development km^3 astrophysical neutrino detectors, such as IceCube and KM3NeT). A combined study of the UHECR spectrum and the spectrum of cosmogenic neutrinos could provide valuable information about the distribution of UHECR sources in the universe, their cosmological evolution, and the single-source spectrum (see, e.g., Kotera & Olinto 2011 for a recent review of candidate accelerators and the astrophysics of UHECR propagation).

Finally, exactly because particle physics at the highest center-of-mass energies probed by UHECR collisions in the Earth's atmosphere cannot be studied in any other way at present, UHECR observations can probe new physics at these highest energies. Still, to this day, nature's accelerators dwarf any accelerators we have built on Earth (although, as we already discussed, the UHECR fluxes and hence the associated effective beam luminosities are very low).

Observational Techniques

Since UHECR cannot be directly detected, their observation relies on techniques that involve gathering information about the air shower they induce in the atmosphere, and reconstructing the energy, the type (photon, neutrino, or nucleus, and, in the latter case, charge), and the arrival direction of the primary. These can be generally classified in fluorescence, ground particle detection, and hybrid techniques. For detailed reviews of UHECR observing techniques see recent reviews by, e.g., Letessier-Selvon & Stanev (2011) and Beatty & Westerhoff (2009).

Fluorescence Detection

Fluorescence techniques rely on energy losses of air shower particles as they propagate in the Earth's atmosphere: the air shower particles excite nitrogen atoms, which, during their de-excitation, emit fluorescent light in ultraviolet wavelengths. The detection of this light by telescopes specially designed to "look" at the atmosphere for such air shower tracks can be used to deduce information about the incoming UHECR that induced the shower.

The advantages of fluorescence techniques lie in their excellent potential for deducing the energy of the primary without having to rely on simulations of the air shower development: rather, the energy of the primary can be calculated directly from the total energy deposited in the atmosphere during the shower development, and the main uncertainty entering the calculation comes from the uncertainty in our knowledge of the fluorescent yield of the atmosphere. In addition, because fluorescent telescopes allow us to monitor directly how the shower develops as it propagates in the atmosphere and when this development reaches its maximum, it enables us to reconstruct the penetration depth of the primary particle in the atmosphere, and from it its interaction cross-section, which in turn can reveal the type of the incoming particle, allowing us to perform composition studies. Fluorescence techniques can also be used to reconstruct the arrival direction of the primary with good accuracy, provided that the air shower is detected *in stereo* (by two different telescopes, from two different viewing angles, at the same time).

Disadvantages of fluorescence techniques are associated with their effective area and their event acceptance: fluorescent telescopes can only operate during the night and are affected by weather, so their duty cycle is low, and the event acceptance as a function of energy is in general complicated to calculate. Uncertainties thus induced on the calculation of the observatory exposure propagate in turn to the calculation of the UHECR flux and its energy spectrum.

Past UHECR detectors such as Fly's Eye (Baltrusaitis et al. 1985) and High Resolution Fly's Eye (HiRes, Boyer et al. 2002), as well as future space observatories (e.g. JEM-EUSO[1]) are based on fluorescence techniques.

Ground Particle Detection

Ground particle detection techniques generally rely on arrays of particle detec-

1 http://jemeuso.riken.jp/en/index.html

tors (e.g. scintillators or water Cerenkov tanks), which detect the number and energy of particles in several points of the air shower footprint on the ground. From the number of detectors triggered, the energy deposited in each detector, and the order in which the detectors are triggered, the energy and the arrival direction of the primary can be reconstructed.

Advantages of the ground particle detection technique involve the large effective area that can be achieved by extending the array over large ground surface areas, the high duty cycle (ground detectors operate day and night, and they are not affected by weather), and the extremely well-defined exposure and its energy dependence. The arrival direction reconstruction is also generally very good, and this is true for a very high percentage of the incoming showers, in contrast with the fluorescence technique, which achieves comparable angular accuracy in the path reconstruction of the primary only for the fraction of events that are observed in stereo.

However, the ground detection technique has severe disadvantages when it comes to energy calibration. Because only a fraction of air shower particles reach the ground, the reconstruction of the energy of the primary relies on Monte Carlo simulations of the shower development from its entry point all the way to the ground, and these involve severe systematic uncertainties, especially so since the center-of-mass energies involved in the first interaction are either poorly studied or not studied at all in the lab, and as a result it is difficult to assess how well simulations perform in these cases. In addition, composition studies are generally not possible with ground arrays alone.

The Akeno Giant Air Shower Array (AGASA, Chiba et al. 1992) was the largest (100 km^2) ground-detection array of scintillators operating in the 1990s.

Hybrid Detectors

The hybrid technique benefits from the best features of each of the two techniques discussed above (see Fig. 1). Hybrid detectors consist of a ground detector array overlooked by several fluorescence telescopes. The ground detector array ensures a high duty cycle and an excellent knowledge of the detector effective area and exposure. At the same time, showers that are simultane-

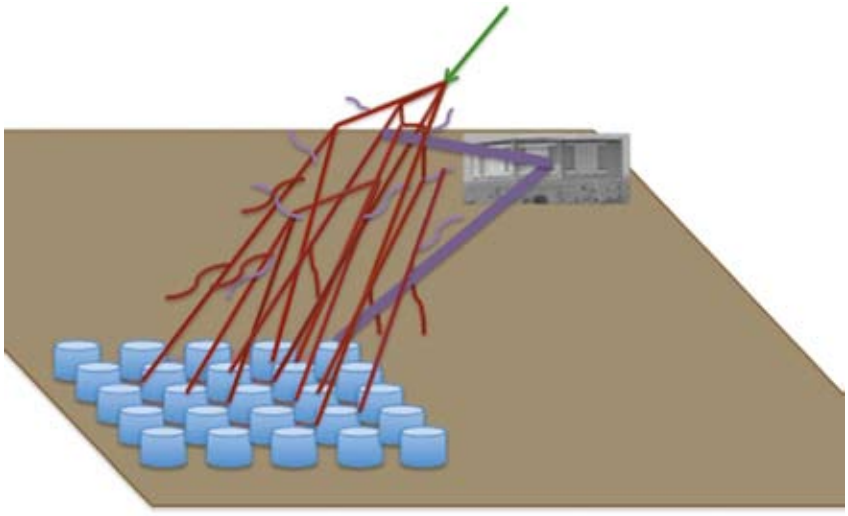

Figure 1. Cartoon representation of UHECR observing techniques: the primary path is shown in green, and air shower particles and photons in red; isotropically emitted fluorescence photons are shown in purple. Particles on the ground are detected by the ground array (here represented by the blue "tanks"), while fluorescent light is detected by fluorescent telescopes; here one of the buildings housing Auger fluorescence detectors is shown in the background.

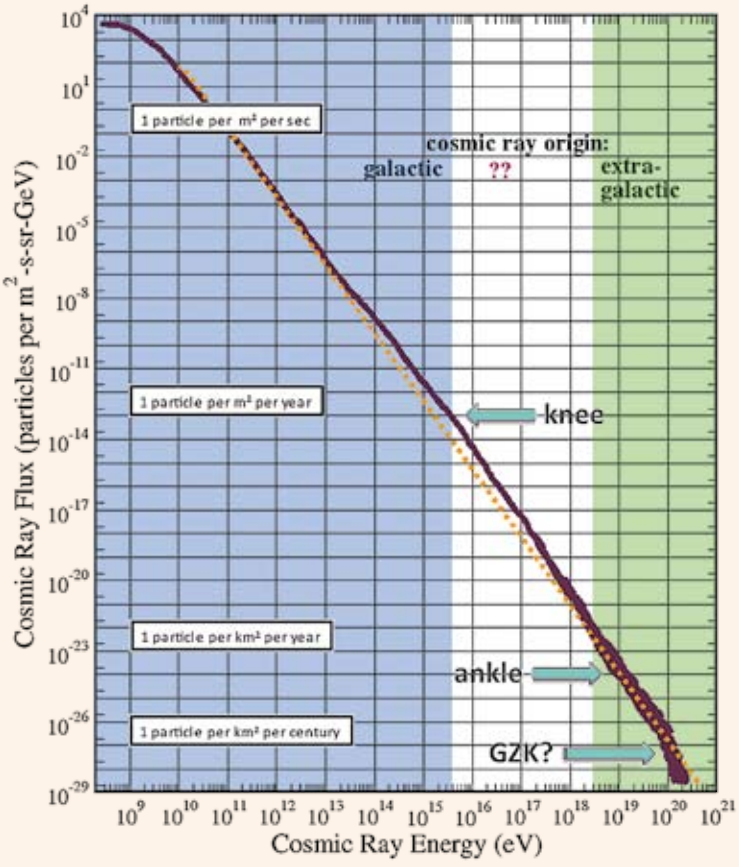

Figure 2. Broadband cosmic ray energy spectrum ("Swordy Plot", see Cronin, Gaisser & Swordy 1997, Swordy 2001, and references therein); data updated to include Auger (Abraham et al. 2010a) and HiRes (Abbasi et al. 2009) measurements above 10^{18} eV. The increased width of the shaded area at higher energies corresponds to the increased statistical uncertainties at these energies. The orange dotted line represents a power law with a slope of –2.7.

ously observed by both the ground array and the fluorescent telescopes can be used to calibrate the energy scale of the ground array, independently of any air shower simulations, and they enable composition studies.

The Pierre Auger Observatory in the southern hemisphere (covering 3000 km^2 in Argentina, Abraham et al. 2004) and the Telescope Array in the northern hemisphere (covering 762 km^2 in the United States) are currently operating hybrid detectors.

Recent Results

Energy Spectrum

The energy spectrum of cosmic rays is in general remarkably featureless over ten orders of magnitude (see Fig. 2), with their flux (number of particles per unit surface area-time-energy-solid angle) falling approximately as a power law with a slope close to –3.

At "low" energies (above 10^9 eV) the energy spectrum slope is –2.7, and cosmic rays at these energies have been shown to be of Galactic origin. The argument that settled this debate came from gamma-ray observations, and it is straightforward: if low-energy cosmic rays were of extragalactic origin, then their flux would be roughly the same in nearby galaxies (such as the Large and the Small Magellanic Clouds) as it is in the Milky Way. Cosmic rays interacting with the interstellar gas produce neutral pions which decay into gamma-rays primarily in the MeV-GeV range, which can be detected with past and current space telescopes such as the Energetic Gamma-ray Experiment Telescope aboard the Compton Gamma-ray Observatory which operated during the 1990s, and the Large Area Telescope on board the currently operating Fermi Gamma-ray Space Telescope. These experiments have confirmed that the gamma-ray flux of the Large and Small Magellanic Clouds is inconsistent with what would be expected given the gas content of these galaxies and a cosmic-ray flux equal to that of the Milky Way, beyond any uncertainties in our observational knowledge of the gas content of these galaxies (Sreekumar et al. 1993; Abdo et al. 2010). Therefore the cosmic-ray flux should be different (lower) in these galaxies, and the origin of 10^9 eV cosmic rays should be local to each galaxy.

The Galactic cosmic-ray accelerators start "running out of steam" at energies about 4×10^{15} eV, where a steepening known as the "knee" is observed in the cosmic-ray energy spectrum; the slope above the knee is equal to -3. That this feature in the energy spectrum is most likely due to the Galactic accelerators that contribute dominantly to high energies reaching the maximum energy is most strongly supported by studies of the composition of cosmic rays at these energies. The pioneering KASCADE experiment (e.g., Kampert et al. 2004) showed that the steepening in slope is caused by a falloff in the flux of light nuclei, with this falloff occurring later for heavier nuclei, and the energy of the falloff being approximately proportional to the charge of the nucleus – as would be expected for a class of accelerators reaching their maximum energy, which is proportional to the nuclear charge of the accelerated particles. Alternatively, the knee could be the result of a more efficient confinement of heavier nuclei in the Galaxy by the Galactic magnetic field.

Above energies of 3×10^{18} eV (the "ankle"), the cosmic-ray energy spectrum becomes again shallower (slope of -2.6; for recent measurements in this range see, e.g., results from HiRes, Abbasi et al. 2009, and Auger, Abraham et al. 2010a). At these energies cosmic rays are expected to be of extragalactic origin. The transition between Galactic and extragalactic cosmic rays is expected to occur somewhere between the knee and the ankle. Two interpretations have been suggested for the ankle: if the cosmic-ray composition at these energies is either mixed or dominated by heavy nuclei (iron), then the ankle signifies the transition from Galactic cosmic rays, cutting off as the Galactic accelerators can no longer produce particles at these energies, to extragalactic cosmic rays, starting to dominate as the Galactic cosmic rays drop out (Allard et al. 2007); if, on the other hand, cosmic rays at the "ankle" are pure protons, the "ankle" could really be a "dip," produced due to pair production energy losses during propagation (e.g., Berezinsky et al. 2006). In the latter case, the transition from Galactic to extragalactic cosmic rays is assumed to have occurred at lower energies, between the "knee" and the "ankle."

Finally, at energies above 3×10^{19} eV, the cosmic-ray energy spectrum has been long expected to show a suppression due to energy losses caused by the interaction of cosmic rays propagating in the intergalactic medium with the CMB (the Greisen-Zatsepin-Kuzmin, GZK, effect, Greisen 1966; Zatsepin & Kuzmin 1966). The dominant energy loss mechanism on the CMB is photopion production for protons, and photodissociation for heavier nuclei. The existence of a suppression has been long debated, as AGASA and early HiRes results in the past decade were conflicting, with AGASA observing no flux suppression (Takeda et al. 1998) and HiRes results observing a flux consistent with the existence of the GZK cutoff (Abbasi et al. 2004). As a result, many scenarios in which the sources of UHECR were local rather than located at cosmological distances were proposed during that time, to explain a potential absence of the propagation-induced GZK cutoff. The issue however was settled in 2008, when both HiRes and Auger confirmed the existence of a suppression (Abbasi et al. 2008, Abraham et al. 2008). However, it is still not easy to verify whether the observed flux suppression is truly caused by propagation (the GZK effect), or by extragalactic accelerators reaching their maximum energy (see Kotera & Olinto 2011 for a detailed discussion).

Composition

At ultra-high energies where cosmic-ray detection is necessarily indirect, the cosmic-ray composition can be deduced by measuring the penetration depth of the primary in the atmosphere. The trend is that heavier primaries have a bigger cross-section, they experience their first interaction earlier (higher), and their interaction depth fluctuates less. The quantity used to probe UHECR composition is $\langle X_{max} \rangle$, the mean atmospheric depth (in units of g/cm^2) when the shower reaches its maximum development (maximum number of particles) . $\langle X_{max} \rangle$ depends both on the energy of the primary, E, and its atomic mass, A, with an approximate scaling $\langle X_{max} \rangle \sim \ln(E/A)$ (see discussion in Letessier-Selvon & Stanev 2011).

As the UHECR energy approaches the "ankle", both HiRes (Abbasi et al. 2010) and Auger (Abraham et al. 2010b) have reported a trend of $\langle X_{max} \rangle$ values toward lighter composition than right above the "knee," where, as we have discussed, the relative abundance of heavier nuclei increases. This is consistent with the idea that the contribution of extragalactic sources dominates around the ankle.

However, at energies above 10^{19} eV and up to 4×10^{19} eV, Auger data (Abraham et al. 2010b, left panel of Fig. 3) indicate a reversal of this trend, with primary composition, as deduced from $\langle X_{max}\rangle$ observations, tending to heavier atomic masses. HiRes data on $\langle X_{max}\rangle$ at similar energies remain consistent with light composition. Differences in the shower reconstruction methods between Auger and HiRes can account for the discrepancy, and results from the two experiments are consistent within errors. The composition at energies $>10^{19}$ eV is therefore unclear based on observations of the average depth of shower maximum as a function of energy alone.

Additional information on UHECR composition can be obtained using two independent measures. The first one is the *spread* in X_{max} for showers of the same energy (quantified, for example, by the root-mean-square, RMS, X_{max}). The X_{max} of light-primary showers at a given energy fluctuates about $\langle X_{max}\rangle$ more than that of heavy-primary showers. Auger data show that above 10^{19} eV the RMS X_{max} does exhibit a significant trend toward lower values, consistent with the $\langle X_{max}\rangle$ data indicting a transition to heavier composition at these energies (Abraham et al. 2010b, right panel of Fig. 3).

The second measure is anisotropies in the UHECR arrival directions. As we will discuss in the next section, Auger data do show some deviation from isotropy at the highest energies, which is a general indication of light composition (since heavier nuclei have higher charge and are deflected and isotropized more by the Galactic and intergalactic magnetic fields). However, the anisotropy level detected by Auger is not incompatible with the injection of heavier nuclei at the source. Besides, the reader should keep in mind that the cosmic ray energies for which anisotropies set in are higher than the energies where $\langle X_{max}\rangle$ and RMS X_{max} measurements are currently possible. The reason is statistics: a measurement of the X_{max} requires monitoring of the shower development by fluorescence telescopes, which have a much lower effective area than the ground detectors. Ground detectors on the other hand can reconstruct well the arrival directions of cosmic rays, and for this reason they can be used for anisotropies studies even at energies for which the fluorescent telescopes run out of events.

The indicators are thus conflicting, and the situation with the composition of UHECR at energies above 10^{19} eV remains unresolved.

If anisotropies persist and give an unambiguous indication of light composition, the Auger data on $\langle X_{max}\rangle$ and RMS X_{max} may be an indication of new physics: our expectations for the $\langle X_{max}\rangle$ and RMS X_{max} values for various primaries are based on shower simulations at energies which have not been studied in accelerators (Abraham et al. 2010b) – they are an extrapolation of our understanding of hadronic interaction physics into energies that constitute unknown territory. It is therefore not inconceivable that new physics effects may become important at these energies and our interpretation of this data may be mistaken.

If the composition at the highest energies is indeed heavy, then this raises questions on the nature of the UHECR accelerators. Large-scale extragalactic accelerators such as AGN jets would be expected to be accelerating intergalactic, low-metallicity material, so lighter composition is preferred in such models. These considerations have revived interest in the potential contribution of Galactic accelerators (see Kotera & Olinto 2011 for a discussion of candidate accelerators and acceleration models).

Finally, it is also conceivable that the trend toward heavier composition is due to the extragalactic accelerators having reached their maximum acceleration energy for protons, similarly to the Galactic accelerators reaching their maximum energy for protons around the knee. In this case, the suppression in the spec-

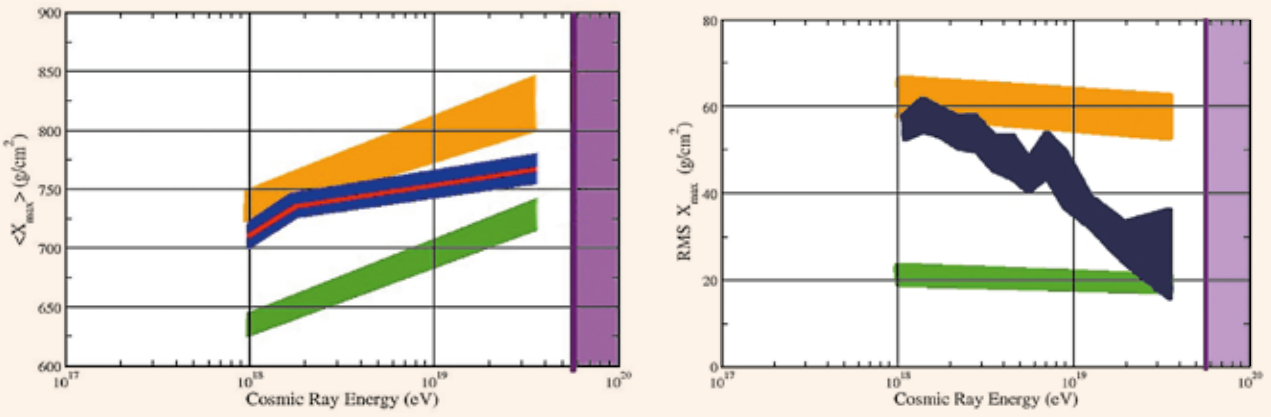

Figure 3. Left panel: $\langle X_{max}\rangle$ as a function of energy. Red line: best-fit broken power law representing Auger data (Abraham et al. 2010b). The blue band represents the systematic uncertainties on the measurement. The orange and green bands are the range of predictions, based on shower simulations, for the behavior of $\langle X_{max}\rangle$ with energy for protons and iron respectively. HiRes results (Abbasi et al. 2010) are consistent with the Auger measurement within their uncertainties and Auger systematics, however they do not exhibit the break seen in the Auger trend with energy. Right panel, blue band: Auger measurement (Abraham et al. 2010b) of RMS $\langle X_{max}\rangle$ (the band indicates 1σ statistical uncertainty). Orange and green bands are simulation results for protons and iron, respectively. Note that the Auger measurement of arrival direction anisotropies occurred at higher energies (indicated with the purple shaded areas in both cases).

trum at the highest energies observed by Auger and HiRes could be due to the accelerators reaching their maximum capabilities for iron nuclei, instead of, or in addition to, the GZK effect (e.g., Allard et al. 2008; Aloisio et al. 2011).

Anisotropies

If the flux suppression above 4×10^{19} eV is indeed due to he GZK effect, this would imply that trans-GZK events must originate from increasingly nearby sites as the energy increases and the mean free path for interaction with cosmic microwave background photons decreases (it is about 100 Mpc at ~5×10^{19} eV). At the same time, at these energies the deflection angle for propagation in the Galactic magnetic fields becomes relatively small for protons (a few degrees). Therefore, assuming light primaries and weak intergalactic magnetic fields, the combination of the two effects would be expected to result in anisotropic arrival directions. If the number of contributing sources is low, and again assuming weak magnetic fields, a certain level of anisotropy could also be expected for heavy nuclei.

The reasoning is as follows. The distribution of matter in the local Universe is anisotropic. If local-universe accelerators are therefore correlated with the local large-scale structure (as one would expect for pretty much any astrophysical accelerator), and if the background of UHECR that come from cosmological distances and are therefore isotropic is suppressed by the GZK effect, then the cosmic rays that do reach us at the highest energies should also be anisotropically distributed and spatially correlated with the local large-scale structure (see Fig. 4).

Indeed, Auger data at energies above 6×10^{19} eV do show a deviation from isotropy, and a spatial distribution of arrival directions more consistent with local large-scale structure than a uniform (after accounting for the spatially-dependent exposure) distribution. The statistical technique employed by the Auger Collaboration used the distribution of local AGN (e.g., Abraham et al. 2007). The test was designed to find whether UHECR of $E>5.5\times10^{19}$ eV tended to have arrival directions within some angular distance (~3°) of local (<75 Mpc) AGN more frequently than expected from an isotropic source distribution. The answer was "yes," and the significance of this result is currently 3σ (Abreu et al. 2010). It is currently estimated that, if the deviation from isotropy persists, in order to increase this significance to 5σ four more years of Auger data would be required.

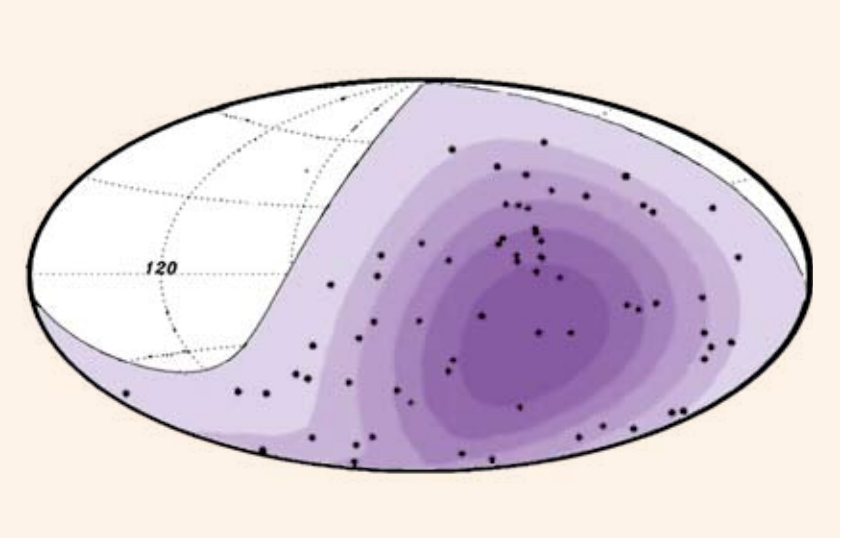

Figure 4. Auger sky map (Galactic coordinates, Aitoff-Hammer projection). The purple gradient visualizes the exposure of the Auger ground array (darker colors represent higher exposure). The black dots are the 69 events with $E>5.5\times10^{19}$ eV detected by Auger up to the end of 2009 (Abreu et al. 2010). An isotropic distribution of arrival directions would result in higher density of events (within Poisson uncertainties) in the direction of the sky with higher exposure. Instead, the density of points is higher in the directions of local extragalactic matter, with the significance of the discrepancy currently at 3σ.

Note however that, because of the nature of the test (which checked for consistency with isotropy rather than for agreement of the distribution of arrival directions with a particular distribution of sources), as well as its angular scale, even if the result persists, the implication would be that the UHECR are correlated with large-scale structure (which AGN also follow), rather than that AGN themselves are necessarily the preferred acceleration sites.

Outlook

Despite the enormous progress that has been achieved over the past decade in the field, major questions in UHECR physics, including their composition and the nature of their sources, remain unanswered. Although the positive detection of the spectrum suppression at the energies where the GZK effect is expected to set in represents a tremendous success, it also implies that the flux of trans-GZK events is very low, and that collecting the necessary statistics to resolve the outstanding issues at the highest energies is going to be difficult.

Future ground observatories (e.g., Auger North[2]) and space experiments (which will also use the Earth's atmosphere as a detector but will observe it from above, e.g. JEM-EUSO) promise to increase the collecting area of current experiments by an order of magnitude or more. This next generation of experiments holds the promise of even more exciting discoveries and is expected to pave the way for the new field of charged-particle astronomy.

Acknowledgements

The author gratefully acknowledges insightful comments by Dr. Kumiko Kotera that improved this review, and valuable discussions over the years with the University of Chicago Auger group and the Auger Collaboration. She thanks the editors of Ipparchos for their interest in UHECR astrophysics. The author's work is supported by NASA through Einstein Postdoctoral Fellowship grant number PF8-90060 awarded by the Chandra X-ray Center, which is operated by the Smithsonian Astrophysical Observatory for NASA under contract NAS8-03060.

2 http://www.augernorth.org/

References

1. Abbasi, R. U. et al. "Measurement of the Flux of Ultrahigh Energy Cosmic Rays from Monocular Observations by the High Resolution Fly's Eye Experiment." *Physical Review Letters* 92 (2004): 151101.
   http://adsabs.harvard.edu/abs/2004PhRvL..92o1101A
2. Abbasi, R. U. et al. "First Observation of the Greisen-Zatsepin-Kuzmin Suppression." *Physical Review Letters* 100 (2008): 101101.
   http://adsabs.harvard.edu/abs/2008PhRvL.100j1101A
3. Abbasi, R. U. et al. "Measurement of the flux of ultra high energy cosmic rays by the stereo technique." *Astroparticle Physics* 32 (2009): 53-60.
   http://adsabs.harvard.edu/abs/2009APh....32...53T
4. Abbasi, R. U. et al. "Indications of Proton-Dominated Cosmic-Ray Composition above 1.6 EeV." *Physical Review Letters* 104 (2010): 161101. http://adsabs.harvard.edu/abs/2010PhRvL.104p1101A
5. Abdo, A. A., et al. "Detection of the Small Magellanic Cloud in gamma-rays with Fermi/LAT." *Astronomy & Astrophysics* 523 (2010):,A46.
   http://adsabs.harvard.edu/abs/2010A%26A...523A..46A
6. Abraham, J. et al. "Properties and performance of the prototype instrument for the Pierre Auger Observatory." *Nuclear Instruments and Methods in Physics Research Section A* 523 (2004): 50-95. http://adsabs.harvard.edu/abs/2004NIMPA.523...50A
7. Abraham, J. et al. "Correlation of the Highest-Energy Cosmic Rays with Nearby Extragalactic Objects." *Science* 318 (2007):938.
   http://adsabs.harvard.edu/abs/2007Sci...318..938T
8. Abraham, J. et al. "Observation of the Suppression of the Flux of Cosmic Rays above 4×10^{19}eV." *Physical Review Letters* (2008) 101: 061101.
   http://adsabs.harvard.edu/abs/2008PhRvL.101f1101A
9. Abraham, J. et al. "Measurement of the energy spectrum of cosmic rays above 10^{18} eV using the Pierre Auger Observatory." *Physics Letters B* 685 (2010a): 239-246.
   http://adsabs.harvard.edu/abs/2010PhLB..685..239A
10. Abraham, J. et al. "Measurement of the Depth of Maximum of Extensive Air Showers above 10^{18} eV." *Physical Review Letters* 104 (2010b): 091101.
    http://adsabs.harvard.edu/abs/2010PhRvL.104i1101A
11. Abreu, P. et al. "Update on the correlation of the highest energy cosmic rays with nearby extragalactic matter." *Astroparticle Physics* 34 (2010): 314-326.
    http://adsabs.harvard.edu/abs/2010APh....34..314T
12. Alcock, C. & Hatchett, S. "The effects of small-angle scattering on a pulse of radiation with an application of X-ray bursts and interstellar dust." *Astrophysical Journal* 222(1978): 456-470.
    http://adsabs.harvard.edu/abs/1978ApJ...222..456A
13. Allard, D., Parizot, E., & Olinto, A.V. "On the transition from galactic to extragalactic cosmic-rays: Spectral and composition features from two opposite scenarios" *Astroparticle Physics* 27 (2007): 61-75.
    http://adsabs.harvard.edu/abs/2007APh....27...61A
14. Allard, D., Busca, N. G., Decerprit, G., Olinto, A. V. & Parizot, E. "Implications of the cosmic ray spectrum for the mass composition at the highest energies." *Journal of Cosmology and Astroparticle Physics* 10 (2008): 33.
    http://adsabs.harvard.edu/abs/2008JCAP...10..033A
15. Aloisio, R., Berezinsky, V. & Gazizov, A. "Ultra high energy cosmic rays: The disappointing model." *Astroparticle Physics* 34 (2011): 620-626.
    http://adsabs.harvard.edu/abs/2011APh....34..620A
16. Baltrusaitis, R. M. et al. "The Utah Fly's Eye detector." *Nuclear Instruments and Methods in Physics Research Section A* 240 (1985): 410-428.
    http://adsabs.harvard.edu/abs/1985NIMPA.240..410B
17. Beatty, J. J. & Westerhoff, S. "The Highest-Energy Cosmic Rays." *Annual Review of Nuclear and Particle Science* 59 (2009): 319-345.
    http://adsabs.harvard.edu/abs/2009ARNPS..59..319B
18. Berezinsky, V., Gazizov, A., & Grigorieva, S. "On astrophysical solution to ultrahigh energy cosmic rays." *Physical Review D* 74 (2006): 043005.
    http://adsabs.harvard.edu/abs/2006PhRvD..74d3005B
19. Boyer, J. H. et al. "FADC-based DAQ for HiRes Fly's Eye." *Nuclear Instruments and Methods in Physics Research Section A 482* (2002): 457-474.
    http://adsabs.harvard.edu/abs/2002NIMPA.482..457B
20. Chiba, N. et al. "Possible evidence for >= 10 GeV neutrons associated with the solar flare of 4 June 1991." *Astroparticle Physics* 1 (1992): 27-32.
    http://adsabs.harvard.edu/abs/2010APh....34..314T
21. Cronin, J.W., Gaisser, T. K. & Swordy, S. P. "Cosmic rays at the energy frontier." *Scientific American* 276 (1997): 32-37.
    http://adsabs.harvard.edu/abs/1997SciAm.276a..32C
22. Greisen, K. "End to the Cosmic-Ray Spectrum?" *Physical Review Letters* 16 (1966): 748-750.
    http://adsabs.harvard.edu/abs/1966PhRvL..16..748G
23. Hillas, A. M. "The Origin of Ultra-High-Energy Cosmic Rays." *Annual Review of Astronomy & Astrophysics 22* (1984): 425-444.
    http://adsabs.harvard.edu/abs/1984ARA%26A..22..425H
24. Kotera, K. & Olinto, A.V. "The Astrophysics of Ultrahigh Energy Cosmic Rays." *Annual Review of Astronomy and Astrophysics* 49 (2011). http://arxiv.org/abs/1101.4256
25. Kampert, K.-H., et al. "Cosmic Ray Energy Spectra and Mass Composition at the Knee Recent Results from KASCADE." Nuclear Physics B Proceedings Supplements 136 (2004): 273-281.
    http://adsabs.harvard.edu/abs/2004NuPhS.136..273K
26. Letessier-Selvon, A. & Stanev, T. "Ultrahigh Energy Cosmic Rays." Reviews of Modern Physics (2011).
    http://arxiv.org/abs/1103.0031
27. Ptitsyna, K.V. & Troitsky, S.V. "Physical conditions in potential accelerators of ultra-high-energy cosmic rays: updated Hillas plot and radiation-loss constraints." *Physics Uspekhi* 53 (2010): 691-701. http://adsabs.harvard.edu/abs/2010PhyU...53..691P
28. Sreekumar et al. "Constraints on the cosmic rays in the Small Magellanic Cloud." *Physical Review Letters* 70 (1993): 127-129,
    http://adsabs.harvard.edu/abs/1993PhRvL..70..127S
29. Swordy, S. P. "The Energy Spectra and Anisotropies of Cosmic Rays." *Space Science Reviews* 99 (2001): 85-94.
    http://adsabs.harvard.edu/abs/2001SSRv...99...85S
30. Takeda, M. et al. "Extension of the Cosmic-Ray Energy Spectrum beyond the Predicted Greisen-Zatsepin-Kuz'min Cutoff." *Physical Review Letters*, 81 (1998): 1163-1166.
    http://adsabs.harvard.edu/abs/1998PhRvL..81.1163T
31. Zatsepin, G. & Kuzmin, V. "Upper Limit of the Spectrum of Cosmic Rays." *Journal of Experimental and Theoretical Physics Letters* 4 (1966): 78.
    http://adsabs.harvard.edu/abs/1966JETPL...4...78Z

Sunset with Moon
Date: 08/17/2004
Credit: Gemini Observatory

This view of the Gemini South Telescope shows the open dome with the telescope visible through the three story high vents. This late twilight shot also shows the crescent moon in the western evening sky.
Source: http://www.gemini.edu/gallery/v/gs/exterior/GSSunset18.jpg.html

Planetary systems revealed through direct imaging

by Paul Kalas

University of California, Berkeley, &
SETI Institute, Mountain View, California

Abstract

The direct imaging of extrasolar planets recently achieved the following remarkable milestone: more extrasolar planets than solar system planets have now been discovered through direct imaging. In a few years we will increase the number of direct detections by an order of magnitude. Here we review a few aspects of the currently detected exoplanets, and briefly describe the capabilities of the "Gemini Planet Imager".

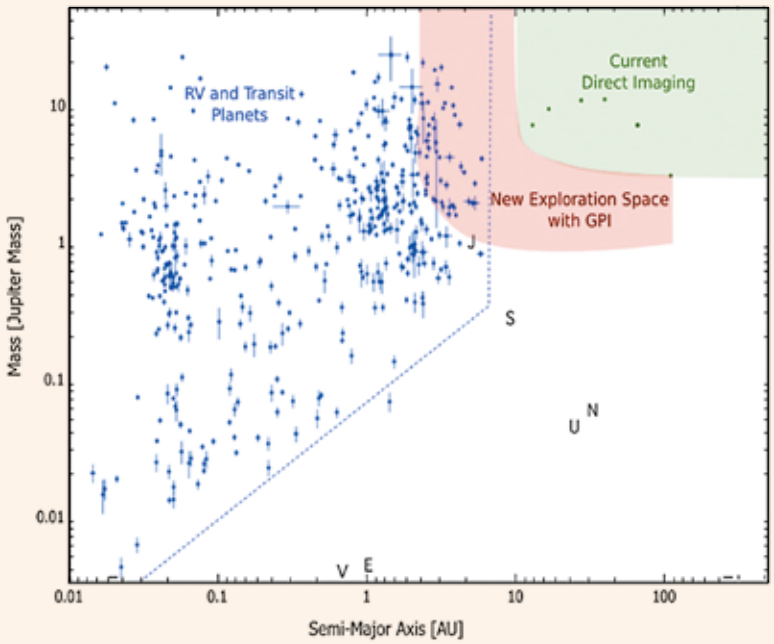

Figure 1. Discovery space for direct imaging versus RV and transit techniques. (Credit: Bruce Macintosh and James Graham).

The discovery space of direct imaging

The first detections of extrasolar planets were accomplished through pulsar timing (Wolszczan & Frail 1992) and the radial velocity (RV) technique (Mayor & Queloz 1995). Microlensing and transit searches yielded even more detections, including the recent 10^3 planet candidates announced by the *Kepler* (transit search) team (Borucki et al. 2011).

Each of these techniques has strengths and weaknesses when considering the discovery space plot of planet mass versus semi-major axis (Figure 1). The transit technique obviously requires planetary systems that are viewed edge-on to our line of sight. So too, because the RV technique detects the line of sight reflex motion of a star, edge-on systems yield the strongest RV signal, whereas face-on systems yield zero RV signature. Given a search program with a finite duration a few years, both the RV and transit techniques are most sensitive to planets with an orbital period of a few years. Therefore the majority of extrasolar planets detected reside within a few AU of their host star (Figure 1).

Direct imaging struggles within this few AU region due to angular resolution and contrast requirements. Instead, direct imaging has thus far detected planets that are somewhat analogous to our gas giants in terms of mass and semi-major axis, but not in age. The current state of technology does not permit the detection of extrasolar planets via reflected light. Instead, exoplanets must be self-luminous due to their youth. Therefore Figure 1 represents two age populations, where the RV and transit detected planets have Gyr ages, and the direct planet detections to the upper right originate from 10-100 Myr old systems.

Direct imaging is therefore the prime observational window for understanding the formation and early dynamical evolution of giant planets. The 10-100 Myr old age range corresponds to the dynamically active epoch of our solar system that included a Moon-forming impact event, the formation of the Oort

cloud, and planetesimal-driven migration of the gas giants that may lead to dynamical instabilities before the system settles into a long-lived configuration (Tsiganis et al. 2005). RV and transit techniques are fundamentally limited in this domain because young stars have significant variability that is the dominant astrophysical noise source in spectroscopy and photometry. With large telescopes and interferometric techniques, direct imaging can even explore the 1-10 Myr old range where forming gas giants are still embedded within the primordial circumstellar disk (e.g. Bonavita et al. 2010).

How do we know it's a planet?

The key hurdles to finding an exoplanet with imaging include suppression of starlight, proving that a point source adjacent to a bright star is a real astrophysical feature rather than an instrumental artifact, showing that the source is physically related to the central star, and determining that the object has the mass of a planet rather than that of a brown dwarf.

There are several techniques for starlight suppression of which coronagraphy is the most well known (Lyot 1939). An occulting spot at the telescope focal plane artificially eclipses the star, preventing light from scattering within the optics of the science camera (additionally, a Lyot stop suppresses diffracted light at a pupil plane). Since we expect to find gas giant planets relatively close to stars, a key challenge is making the radius of the spot as small as possible, and this is determined by the image quality. Though image quality is often thought of as the image sharpness, an additional goal is to create a temporally stable image so that the light contained in the halo of the point spread function can be subtracted with data taken at later times. The *Hubble Space Telescope* has several cameras with coronagraphic capability and superb image quality, but the last decade has witnessed significant advances in ground-based adaptive optics that rival *HST* images.

After suppressing starlight, instrumental artifacts may masquerade as point sources near the star, such as the quasi-static speckles that plague both ground-based and *HST* images of bright stars. One solution, called spectral differencing, is to image the scene at multiple wavelengths. The spatial locations of instrumental artifacts are wavelength-dependent, whereas an astrophysical source will remain stationary in images taken through different filters. A second solution is to rotate the field relative to the instrument frame of reference. For example, Bernard Lyot manufactured coronagraphs that rotate around the optical axis. With *HST*, we can roll the telescope by as much as 30° during an observation. In this case, instrumental features remain stationary, while astrophysical features appear to rotate around the optical axis.

After a faint point source near a star is verified as real, the next step is to show that it is a physical companion to the star. The literature contains several cases where a putative planet is found to be a background object as multi-epoch data are later obtained or a spectrum reveals it to be a background star. An indispensable resource for determining common proper motion is the *Hipparchos Catalog*.

The final step to finding an exoplanet is often the one creates the greatest controversy. Even though the object in question is shown to be real, and shown to be physically linked to the star, is it a planet? At this stage a typical study must estimate the age of the system, the luminosity of the object, and apply a theoretical model of planet evolution that gives the predicted planet luminosity at a given age for a given planet mass. If the result is $M < 13\ M_J$, the object is deemed a planet, otherwise it is a brown dwarf (Burrows et al. 1995). Given the various uncertainties and the model-dependent nature of this exercise, many objects are considered "candidate planets", and occasionally they are dropped from the catalogs of extrasolar planets when they are determined to be a brown dwarf instead. The section below will describe a few more details concerning this topic.

Current inventory of directly imaged exoplanets

Table 1 summarizes a few of the key facts concerning directly imaged exoplanets, ordered by heliocentric distance. As early as 2004, Gael Chauvin and his colleagues, using the *VLT* and adaptive optics, surveyed objects in the young association TW Hydrae. One of the targets, a 25 solar mass brown dwarf 2M1207 was found to have a faint companion with

Host	SpT	Distance (pc)	Separation (AU)	Mass (M_J)	Age (Myr)	Reference
Fomalhaut	A3V	7.69	119	<3.0	100-400	Kalas et al. '08
Beta Pic	A5V	19.3	8	7-11	8-20	Lagrange et al. '09
HR 8799	A5V	39.4±1.0	68, 38, 24, 15	5-13	30-160	Marois et al. '08, '10
AB Pic	K2V	45.5±1.8	258	11-16	30	Chauvin et al. '05
2M1207	L2	52.4±1.1	41	2-10	2-12	Chauvin et al. '04
GQ Lup	K7	156±50	100	4-39	<2	Neuhauser et al. '05
1RXJ160929	K7	145±20	330	6-11	4-6	Lafreniere et al. '10
CT Cha	K7	160±30	440	11-23	<4	Schmidt et al. '08

Table 1. Properties of directly detected exoplanet candidates

mass 5 ± 2 M_J. Despite the fact that the 2M1207b mass was firmly established below the 13 M_J limit, the fact that the host object was a brown dwarf and not a star, and the fact that the projected (i.e. minimum) separation is 41 AU, gave rise to the notion that planets could form by the process of gravitational collapse like stars, and not by core accretion within a circumstellar disk of gas and dust, like planets. Thus we return to the final topic of the previous section that alludes to the debate concerning the definition of a planet. Is the process of formation relevant to the definition of a planet (e.g., see Basri and Brown 2006)?

The age column in Table 1 reveals that the youngest planet candidates found to date orbit pre-main sequence stars such as GQ Lup and CT Cha that are located beyond the local bubble in star forming regions. In other young clusters, such as σ Orionis, IC 348 and Trapezium, several objects not listed in Table 1 have been identified as possible free floating planets (e.g. Zapatero Osorio et al. 2000).

Within the local bubble, the luminous A stars Fomalhaut, β Pic and HR 8799 have yielded a total of six extrasolar planets. A characteristic held in common is that all three planetary systems include debris disks or belts that were previously known from infrared and direct imaging studies. The significance is that planet masses can be estimated not only by measuring their luminosity, but also by interpreting the dynamics of the planets with the debris belts (e.g., Chiang et al. 2009).

β Pic b is the most "Jupiter-like" planet in Table 1 given that the ~8 AU semi-major axis corresponds to the approximate ice line of the system. Historically, β Pic could be considered the first main sequence star where orbiting solid material was first discovered through imaging. After Aumann et al. (1984) announced the discovery of thermal infrared excess around main sequence stars from *IRAS* observations, Smith & Terrile (1984) used a ground-based coronagraph to image an edge-on debris disk surrounding the star. They noted that central region of the debris disk is depleted from dust, possibly because of a planetary system sweeping the inner region clear of dust. Kalas & Jewitt (1995) then found that contrary to expectations, the entire debris disk appears asymmetric. *HST* observations of these asymmetries included the finding of a warped midplane a few tens of AU from the star that could be due to a planetary perturbation (Burrows et al. 1995; Heap et al. 2000). Several other lines of evidence pointed to a planetary system, and Mouillet et al. (1997) dynamically modeled the midplane warp, giving quantitative limits to the planet mass given planet-disk interactions. New *HST* observations of the warp region revealed the appearance of two edge-on debris disks surrounding β Pic, with a minor disk midplane inclined by 5° relative to the major disk midplane (Golimowski et al. 2006).

Thus a key question with the discovery of β Pic b is whether or not this is the planet that creates the 5° warp, or is there a yet-to-be-detected planet, β Pic c, that creates the warp. Because of its ~16 year orbital period and the 9 year observational baseline, images of b Pic b include its location on both sides of the star. Most recently, Currie et al. (2011) analyzed the VLT archive data and conclude that the orbital plane of β Pic b lies within the main disk midplane. These tentative results suggest that the dynamical source of the midplane warp may be an analog to Saturn beyond the orbit of β Pic b.

HR 8799 (HD 218396) certainly came as a surprise with a total of four gas-giant planets imaged within the region 15 to 68 AU from the star (Marois et al. 2008; 2010). The star was previously flagged for its debris disk (Sadakane & Nishida 1986). More recent measurements with the *Spitzer Space Telescope* reveal an inner warm disk between 6 and 15 AU, a dust depleted gap between 15 and 90 AU, and an extended disk beyond 90 AU radius (Su et al. 2009). Thus the four planets reside within the disk gap. Using the *HST*, we will soon attempt to image the HR 8799 dust disk in scattered light. Direct imaging in this case will give the precise location of the dust belt edges, reveal any non-axisymmetric resonant structures, and ultimately inform a more comprehensive dynamical model for the system.

With the discovery of the first three HR 8799 planets, dynamicists immediately seized the opportunity to determine if the system is stable. The basic result is that stability can be preserved for long timescales if planets b, c, d ("b" is the outermost at 68 AU) reside in a 1:2:4 Laplace resonance (Reidemeister et al. 2009, Fabrycky and Murray-Clay 2010). But, this configuration also requires that the "planets" have planet masses, since brown dwarf masses would render the system unstable. The stability analysis demands an estimate for the age of the system, which generated significant debate. Using various age indicators, Marois et al. (2008) cited an age of 30-160 Myr. Given the measured planet luminosities, the model-dependent masses are M < 13 M_J. However, if the age was instead closer to 1 Gyr, the objects detected via imaging are brown dwarfs. Moya et al. (2010) highlighted the significant uncertainties in the Marois et al. (2008) age estimate, and then suggested that an age of 1 Gyr is consistent with astroseismology observations. The Moya et al. (2010) arguments were then countered by Moro-Martin et al. (2010) who reinforced the notion that it is dynamically impossible to have three brown dwarfs orbiting in the observed configuration for a Gyr timescale. HR 8799 must be young (10-100 Myr) and the detected objects must have planet masses. With the discovery of the innermost (14.5 AU) fourth planet, HR 8799 e, Marois et al. (2010) produced a new stability analysis and found that there are stable solutions for "e" given the double resonance between b, c, and d preserves the dynamical stability of the outer planets.

The closest to the Sun and the oldest of the stars with a directly imaged planet is Fomalhaut. The age has been typically quoted as 200±100 Myr (Barrado y Navascues 1998), though more recent estimates suggest that 400 ± 50 Myr is plausible (E. Mamajek, private comm.). As with β Pic, this was one of the early *IRAS* main-sequence stars that exhibited excess far-infrared emission, though significantly fainter due to the older age. Fomalhaut's circumstellar dust was resolved as having an extended toroidal geometry at 850 microns using *JCMT/SCUBA* (Holland et al. 1998). The inner, cleared region of this toroidal configuration therefore provided compelling justification to conduct a planet-search with *HST* when the *Advanced Camera for Surveys* (*ACS*) was installed in 2002. The *ACS* consists of three "channels" that are three separate cameras. The *High Resolution Channel* (*HRC*) was built with a coronagraphic mechanism containing both a focal plane occulters and a pupil-plane Lyot stop. As a result of the Lyot stop, *ACS/HRC* data result in the only *HST* images where diffraction spikes due to the secondary support spider are not present. Despite

the fact that the *ACS/HRC* was an optical camera, planet evolution models suggested that planets more massive than 5 M_J would be detectable with the *ACS/HRC* at 0.8 microns.

The first *HST* images of Fomalhaut in 2004 with the *ACS/HRC* revealed the toroidal dust belt in scattered light (Kalas et al. 2005). Two measurements suggested that an unseen planet was indeed dynamically perturbed by a planet: (1) The geometric center of the belt was offset from the star by 15 AU, an effect that is attributable to the secular perturbation of an eccentric sub-stellar companion (Wyatt et al. 1999), and (2) The inner edge of the belt is consistent with a knife-edge, as if the perturber lies relatively close to the inner edge and sweeps clear material in a manner analogous to Neptune's effect on the Kuiper Belt (Moro-Martin & Malhotra 2002).

In 2006 we observed Fomalhaut again with *HST*, but this time a collection of deeper integration times revealed a faint point source, Fomalhaut b, located 119 AU from the star, and about 18 AU interior to the inner edge of the dust belt. The 2004 data also contained this point source, but the data were insufficient to prove that it was a real astrophysical feature instead of a quasi-static speckle. Indeed, how do we know that Fomalhaut b is a real astrophysical feature? First, I had designed the observing program so that Fomalhaut would be imaged behind two different focal plane occulting spots in the *ACS/HRC* field. This is equivalent to dithering, and the speckle pattern changes as the star is placed on different parts of the field. If Fomalhaut b were a speckle, it would be detected in one imaging position and not the other. This was a crucial test, which ultimately verified the reality of Fomalhaut b. Second, we made the same observation in a different filter, and Fomalhaut b was detected at both 0.6 and 0.8 microns. Third, since the "detection" is essentially made by eye, I had one of my colleagues reduce the same data set from scratch, and report his results independently from my findings. Again Fomalhaut b was confirmed.

But is it a planet? Certainly the apparent optical brightness of Fomalhaut b is inconsistent by an order of magnitude with the theory of evolving planet luminosity. Therefore we reported several plausible sources of optical luminosity, including the possibility of a planet seen in reflected light due to a circumplanetary ring. In this case, the Fomalhaut b ring system would have to be approximately 30 planetary radii in size. Since our solar system did not have an analogous ring system, publishing this suggestion seemed risky. Nevertheless, about a year later, Verbiscer et al. (2009) announced the thermal infrared discovery of a new ring surrounding Saturn extending over a 100 planetary radii, and thus making the proposed Fomalhaut b ring seem somewhat puny in size. Saturn's "Phoebe ring" is supplied by the erosion of a single, small satellite of Saturn, Phoebe. Dust released from the moon's surface encounters solar radiation forces (Poynting-Robertson drag) and spirals inward to the planet, resulting in a tenuous circumplanetary ring. It is certainly plausible that at ages <1 Gyr, when the solar system had a more significant population of interplanetary dust and planetesimals, the Phoebe ring would have a greater optical depth and dominate the reflected-light flux from Saturn. Thus, with the study of Fomalhaut b, we may be exploring a somewhat new domain of empirically understanding the early evolution of Saturn analogs.

A Phoebe-like ring is not the only explanation for the optical luminosity of Fomalhaut b. In exploring the origin of the irregular satellites of the giant planets Kennedy and Wyatt (2011) extended their analysis to suggest that instead of a flattened ring, the irregular satellites surrounding a planet would produce a significant dust cloud. Such a dust cloud surrounding Saturn has an hourglass shape and as viewed from Earth, has a larger diameter than the Moon.

Obtaining a third epoch detection of Fomalhaut b proved challenging – the ACS electronics failed in January 2007. Though the last servicing mission to Hubble fixed the other two cameras on ACS, the portion with the coronagraph (*HRC*) remains inoperable. Eventually, in September 2010, we observed Fomalhaut with the optical camera *HST/STIS* in a relatively brief observation that recovered a source near the expected location of Fomalhaut b. The "expected" position has Fomalhaut b following an orbit interior to the dust belt. However, the STIS data show that Fomalhaut b will cross through the belt over the next few decades, reach apastron at >200 AU, and then cross back through the belt for a periastron near 50 AU. The eccentricity for this orbit is 0.69, and the 99%-confidence upper limit on e is 0.86. This seems puzzling at first, but it could solve other problems. In particular, it is difficult to form a planet 119 AU from a star.

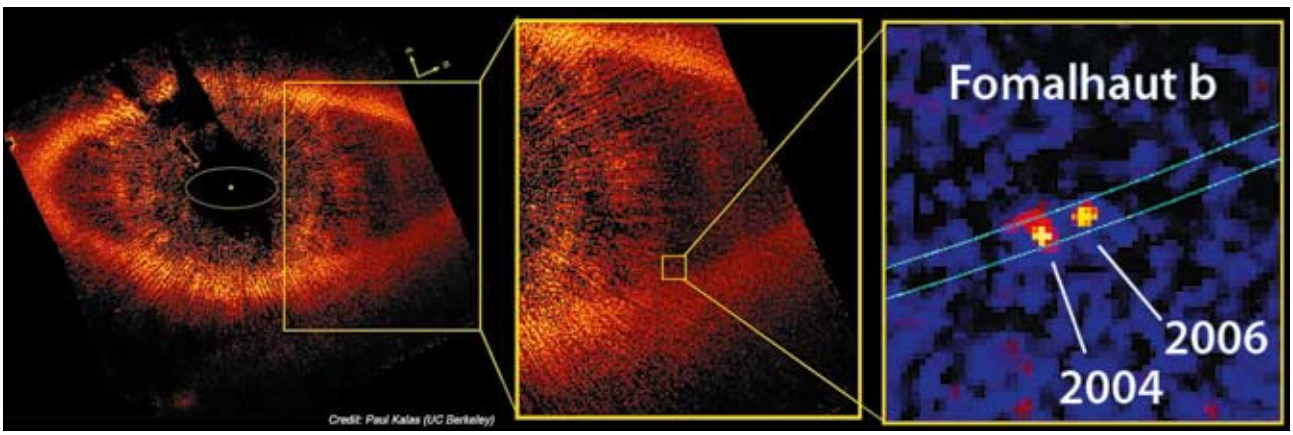

Figure 2. Hubble Space Telescope images of the Fomalhaut system at 0.6 microns (Kalas et al. 2008). The dust belt is inclined to our line of sight by 66 degrees and the inner edge has a semi-major axis of 133 AU. Fomalhaut b lies 119 AU northwest of the star. The ACS data show a counterclockwise orbital motion, though the third epoch obtained with STIS gives a highly eccentric orbit that crosses the dust belt.

The eccentric orbit allows the planet to have its formation site at 50 AU, and then as a result of planet-planet scattering or some other dynamical instability, ends up with an eccentric orbit (Rasio & Ford 1996, Veras et al. 2009). In this picture, there is a second planet, Fomalhaut c, that remains to be discovered.

Fortunately we have been awarded more time with *HST* to obtain a fourth epoch with *STIS* to validate, or refute, the eccentric orbit. Because our current orbit depends on detections with two different instruments, the possibility remains that an uncorrected systematic error accounts for the unexpected third epoch astrometric position. Also with *Hubble* we will attempt to image Fomalhaut with the new camera *WFC3/UVIS*. Compared to the other optical detectors aboard *HST*, *UVIS* has excellent blue sensitivity. If the optical light from Fomalhaut b is truly due to reflection from a circumplanetary dust belt or cloud, then we should be able to detect it at 0.3 microns using *UVIS*.

The near future: The Gemini Planet Imager

What would we learn about the formation of planetary systems, the evolution of their atmospheres, and the diversity of orbital configurations if we could expand Table 1 by 100 rows? Within the next few years a handful of advanced, ground-based adaptive optics systems with coronagraphic capability will come online, targeting stars of various spectral types within the local neighborhood for planetary systems. The key European effort is the *SPHERE* instrument for the *VLT* (Beuzit et al. 2008), the Japanese will be commissioning *SCExAO* for the *Subaru* 8-m (Martinache & Guyon 2009), others have produced *Project 1640* for the Palomar 5-m (Hinkley et al. 2011), and the *Gemini Planet Imager* (*GPI*) will have first light on the 8-m Gemini South telescope in early 2012.

Let us consider *GPI* as an example of these new exoplanet-imaging capabilities (Macintosh et al. 2008). The adaptive optics (AO) system senses the wavefront using a conventional Shack-Hartmann sensor. The wavefront is controlled by a MEMS deformable mirror operating at 1.5 kHz with 43x43 illuminated actuators. The rapid atmospheric correction requires very bright stars as the wavefront reference source, and thus *GPI* and the other plant-imaging projects will be limited to bright targets (e.g., <9th magnitude for *GPI*). Also, the angular region of superb atmospheric correction is relatively small, about 1.3 arcseconds wide in the case of *GPI*. The imaging of large-separation exoplanet such as Fomalhaut b will not benefit from these instruments. The image quality delivered by the AO system means that the coronagraphic spots can be very small. The sensitivity to planets begins a few λ / D radius from the star (about 0.12 arcseconds radius for *GPI*) and direct imaging begins to overlap in sensitivity to the transit and RV techniques (Figure 1). The science camera in *GPI* is a near-infrared (0.9-2.4 micron) integral field spectrograph that provides an image cube where the third dimension is a low-resolution spectrum (R ~ 45). Moreover, *GPI* is capable of dual channel polarimetry which provides a means to detect the faint polarization signal of circumstellar dust.

What do we expect to achieve with GPI in a 900-hour survey of 600 stars in the southern hemisphere? Under the worst-case assumptions of instrument performance and the frequency of giant planets as a function of semi-major axis, 25 new exoplanets will be imaged, their orbits estimated, with low resolution spectra of their atmospheres. As many as 50 discoveries are possible, and additional planets may be inferred via the analysis and dynamical modeling of debris disk structure, as was the case with Fomalhaut and β Pic.

Figure 3 demonstrates the current best image of HR 8799 from the *Keck II* telescope and its adaptive optics system, versus the predicted *GPI* image of the same system. The simulated *GPI* ob-

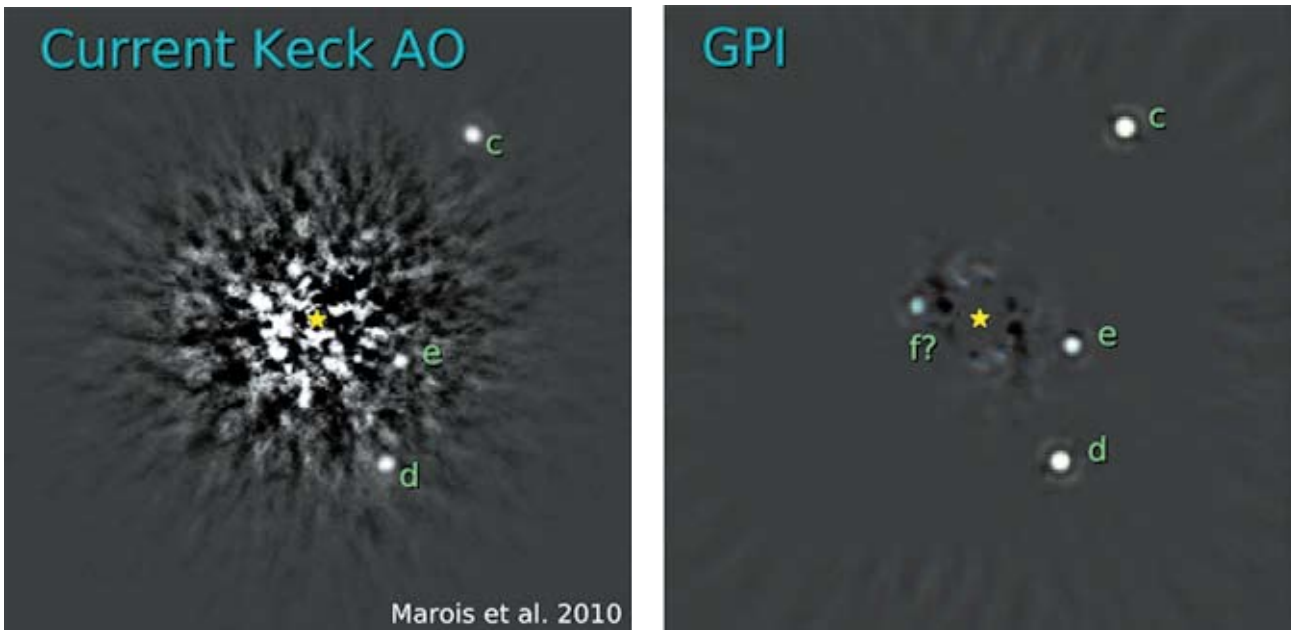

Figure 3. LEFT: Adaptive optics observations of HR 8799 and the detection of three inner planets at 2.2 microns, from Marois et al. (2010). RIGHT: Simulation of *GPI* data at 1.6 microns, with a hypothetical 5 Jupiter mass planet "f" inserted inward of HR 8799 e. (Figure courtesy Bruce Macintosh and the GPI planet survey team.)

servation drives the region of sensitivity inward towards the star where a hypothetical 5 M_J planet (HR 8799 f) would be detectable.

Figure 4 shows the *GPI* sensitivity relative to planet luminosities and several of the currently detected exoplanets. Most importantly, two types of planet evolution models are displayed on the figure that give significantly different predictions for planet luminosities at ages $<10^8$ yr. The models predicting lower luminosities ("cold-start models") assume that gas infalling onto a growing planet should pass through a shock, dissipating heat, and therefore arrive at the planet surface cold (Marley et al 2007). The higher luminosity models ("hot-start") assume that planet formation begins from a hot, adiabatic sphere (Burrows et al. 1997). Thus with direct imaging searches a key science driver is to determine which of the planet formation and evolution models are empirically validated.

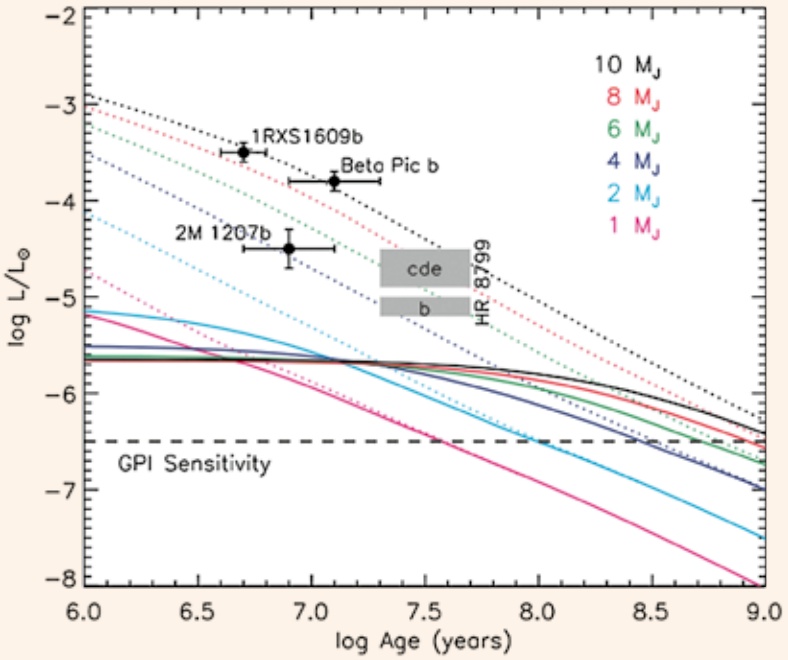

Figure 4. The measured luminosities of several extrasolar planets from Table 1 compared to theoretical tracks. The solid lines represent the cold-start models where gas accretion passes through a shock that dissipates heat such that the gas arrives on the planet surface cold. The horizontal dashed line marks the approximate sensitivity of *GPI*. (Figure courtesy Bruce Macintosh and the *GPI* planet survey team).

Summary

The study of extrasolar planets through direct imaging has succeeded in recent years and promises to be data-rich over the next decade. Direct images touch on numerous scientific disciplines such as planet formation, planetary system dynamics, the chemical composition of atmospheres and the origin of our solar system. This article provided a brief introduction to some of these topics, summarizing the current state-of-the-art and highlighting future prospects. For the far-future, the development of very large, 30 meters or larger, ground-based optical telescopes will push the sensitivity of direct imaging even closer to stars. Such an advance will permit the detection of Jupiter-analogs in reflected light around nearby stars, as well as provide snapshots of planets forming within their circumstellar disks in more distant star-forming regions. The direct detection and characterization of exo-Earths will have to wait somewhat longer for the launch of a space mission specifically designed for this purpose. We expect that the scientific findings from the upcoming generation of instruments will provide the strong motivation and technological demonstration to take on this most challenging goal.

References

1. Aumann, H.H., Gillett, F.C., Beichman, C.A., et al. 1984, *ApJ*, **278**, L23.
2. Barrado y Navascues, D. 1998, *A&A,* **339**, 839.
3. Basri, G. & Brown M.E. 2006, *ARAA*, **34**, 193.
4. Beuzit, J.-L., Feldt, M., Dohlen, K., et al. 2008, *Proc. SPIE*, 7013, 701418.
5. Bonavita, M., Chauvin, G., Boccaletti, A. et al. 2010, *A&A,* **522**, A2.
6. Borucki, W.J., Koch, D.G., Basri, G., et al. 2011, *ApJ*, **736**, 19.
7. Burrows, C.J., Krist, J.E., Stapelfeldt, K.R., et al. 1995, *BAAS*, **27**, 1329.
8. Burrows, C.J., Saumon, D., Guillot, T., Hubbard, W.B., & Lunine, J.I. 1995, *Nature*, **375**, 299.
9. Burrows, C.J., Marley, M., Hubbard, W.B., et al. 1997, *ApJ*, **491**, 856.
10. Chauvin, G., Lagrange, A.-M., Dumas, C., et al. 2004, *A&A*, **438**, L25.
11. Chauvin, G., Lagrange, A.-M., Dumas, C., et al. 2005, *A&A*, **425**, L29.
12. Chiang, E., Kite, E., Kalas, P., Graham, J.R., and Clampin, M. 2009, *ApJ*, **693**, 734.
13. Currie, T., Thalmann, C., Soko, M. et al. 2011, *ApJL*, in press.
14. Fabrycky, D. C. & Murray-Clay, R.A. 2010, *ApJ*, **710**, 1408
15. Golimowski, D.A., Ardila, D.R., Krist, J.E., et al. 2006, *AJ*, **131**, 3109.
16. Heap, S.R., Lindler, D.J., Lanz, T. M., Cornett, R.H. & Hubeny, I. 2000, *ApJ*, **539**, 435.
17. Hinkley, S., Oppenheimer, B.R., Zimmerman, N., et al. 2011, *PASP*, **123**, 74.
18. Holland, W.S., Greaves, J.S., Zuckerman, B., et al. 1998, *Nature*, **392**, 788.
19. Kalas, P. & Jewitt, D. 1995, *AJ*, **110**, 1008.
20. Kalas, P., Graham, J. & Clampin , M. 2005, *Nature*, **435**, 1067.
21. Kalas, P., Graham, J.R., Chiang, E., et al. 2008, *Science*, **322**, 1345.
22. Kennedy, G.M. & Wyatt, M.C. 2011, *MNRAS*, **412**, 2137.
23. Lafreniere, D., Jayawardhana, R. & van Kerkwijk, M. H. 2010, *ApJ*, **719**, 497.
24. Lagrange, A.-M., Gratadour, D., Chauvin, G., et al. 2009, *A&A*, **493**, L21.
25. Lyot, B. 1939, *MNRAS*, **99**, 538.
26. Macintosh, B.A., Graham, J.R., Palmer, D.W., et al. 2008, *SPIE*, **7015**, 31.
27. Marley, M.S., Fortney, J.J., Hubickyj, P. et al. 2007, *ApJ*, **655**, 541.
28. Marois, C., Macintosh, B. Barman, T., et al. 2008, *Science*, **322**, 1348.
29. Marois, C., Zuckerman, B., Konopacky, Q.M., et al. 2010, *Nature*, **468**, 1080.
30. Moro-Martin, A. & Malhotra, R. 2002, *AJ*, **123**, 2305.
31. Moro-Martin, A., Rieke, G.H., & Su, K.Y.L, 2010, *ApJ*, **721**, L199.
32. Martinache, F. & Guyon, O. 2009, *Proc. SPIE*, 7440, 744000
33. Moya, A., Amado, P.J., Barrado, D., et al. 2010, *MNRAS*, **405**, L81.
34. Mayor, M. & Queloz, D. 1995, *Nature,* **378**, 355.
35. Mouillet, D., Larwood, J.D., Papaloizou, J.C.B. and Lagrange, A.M. 1997, *MNRAS*, **292**, 896.
36. Neuhauser R., Guenther, E.W., Wuchterl, G., et al. 2005, *A&A*, **435**, L13.
37. Rasio, F.A. and Ford, E. B. 1996, *Science*, **274**, 954.
38. Reidemeister, M., Krivov, A.V., Schmidt, T.O.B., et al. 2009, *A&A*, **503**, 247.
39. Sadakane, K. & Nishida, M. 1986, *PASP,* **98**, 685.
40. Schmidt, T.O.B, Neuhauser, R., Seifahrt, A., et al. 2008, *A&A*, **491**, 311.
41. Smith, B.A. & Terrile, R. 1984, *Science*, **226**, 1421.
42. Su, K.Y.L, Rieke, G. H., Stapelfeldt, K. R., et al. 2009, *ApJ*, **705**, 314.
43. Tsiganis, K., Gomes, R., Morbidelli, A., & Levison, H.F. 2005, *Nature,* 435, 459.
44. Veras, D., Crepp, J.R. & Ford, E.B. 2009, *ApJ*, **696**, 1600.
45. Verbiscer, A.J., Skrutskie, M.F., & Hamilton, D.P. 2009, *Nature*, **461**, 1098.
46. Wolszczan, A. & Frail, D.A. 1992, *Nature*, **355**, 145.
47. Wyatt, M.C., Dermott, S.F., Telesco, C.M. et al. 1999, *ApJ*, **527**, 918.
48. Zapatero Osorio, M.R., Bejar, V.J.S., Martin, E. L., et al. 2000, *Science*, **290**, 103.

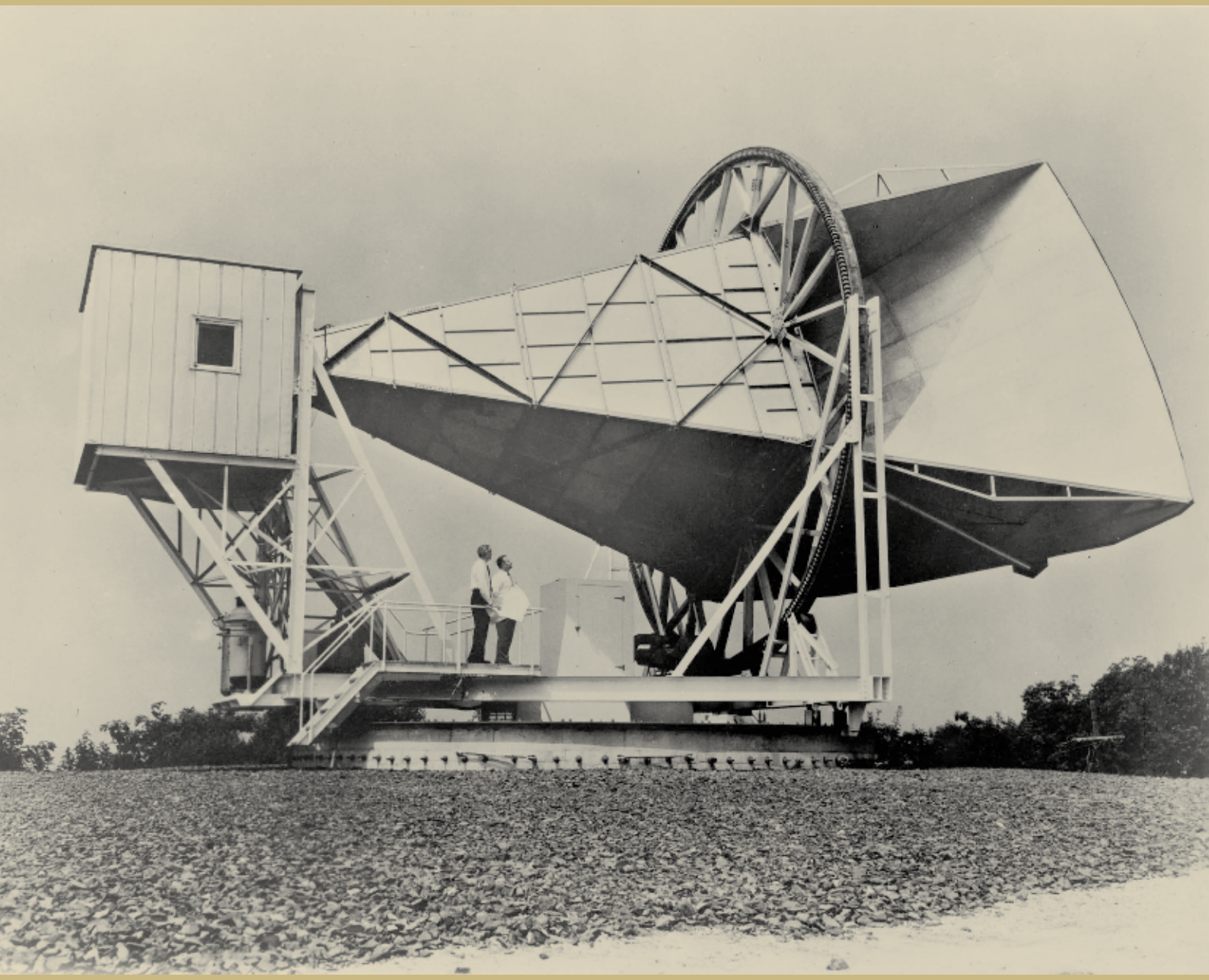

The Holmdel Horn Antenna on which Penzias and Wilson discovered the cosmic microwave background.
Source: http://dayton.hq.nasa.gov/IMAGES/LARGE/GPN-2003-00013.jpg

The Cosmic microwave background radiation: the memories of the Universe revealed

by C. Sofia Carvalho

Instituto de Plasmas e Fusão Nuclear, Instituto Superior Técnico, Av. Rovisco Pais 1, 1049-001 Lisboa, Portugal & Research Center for Astronomy and Applied Mathematics, Academy of Athens, Soranou Efessiou 4, 11-527 Athens, Greece

ἐν ἀρχῇ ἐποίησεν ὁ θεὸς τὸν
οὐρανὸν καὶ τὴν γῆν

ἡ δὲ γῆ ἦν ἀόρατος
καὶ ἀκατασκεύαστος καὶ σκότος
ἐπάνω τῆς ἀβύσσου καὶ πνεῦμα θεοῦ
ἐπεφέρετο ἐπάνω τοῦ ὕδατος

καὶ εἶπεν ὁ θεός γενηθήτω φῶς
καὶ ἐγένετο φῶς

Gen 1,1:3

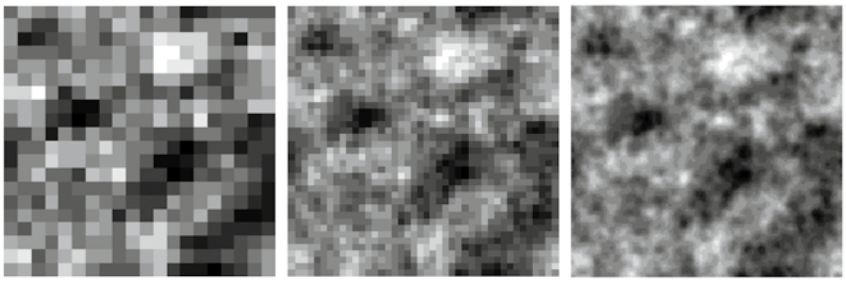

***Figure 1.* A 5 × 5 deg^2 patch of a simulated CMB map for three experiments with different angular resolution.** The full width at half maximum (fwhm) is a measure of the size of the beam, and thus of the resolution of the experiment. Left panel, WMAP: fwhm = 15′ /pixel; Middle panel, PLANCK space probe: fwhm = 7.2′ /pixel; Right panel, ACT: fwhm = 1.4′ / pixel. As the resolution increases, finer and finer structures in the CMB anisotropy maps become discernible, pinpointing astrophysical objects.

I. Introduction

The universe is the most perfect example of a black body ever observed. As discovered by Penzias and Wilson [1], the universe is permeated by the cosmic microwave background (CMB), a bath of radiation with temperature T = 2.725 ± 0.001 K (95%CL), homogeneous to one part in 10^4 and isotropic to one part in 10^5, as first revealed by the Cosmic Background Explorer (COBE) [2].

The discovery of the CMB marks the beginning of modern cosmology. Cosmology, as the study of the origin and evolution of the universe, has been promoted from a theoretical field, occasionally ridiculed as speculative, to a quantitative field supported by data of ever-increasing precision capable of testing the theories. Since we have access to one universe only, experimentation in cosmology is impossible and data can be gathered from observations only. The analysis of the CMB, which started at degree scales as probed by COBE ($\text{fwhm}_{\text{COBE}}$ = 7°), has known a formidable advance with the improvement of detectors for space probes such as the Wilkinson Microwave Anisotropy Probe (WMAP) ($\text{fwhm}_{\text{WMAP}}$ = 15′) and PLANCK ($\text{fwhm}_{\text{PLANCK}}$ = 7.2′), and for ground-based telescopes such as the Atacama Cosmology Telescope (ACT) (fwhm_{ACT} = 1.4′) and the South Pole Telescope (SPT) (fwhm_{SPT} = 1.0′). Cosmology is now entering the arcminute scale (milimeter wavelengths) and thus overlapping with the scales of interest for astrophysics. In Fig. 1 we illustrate the effect of the beam size (the fwhm) in the resolution of the same region of a simulated CMB map. The enormous range of physical scales involved in cosmology makes the synthesis of information challenging. Parallel to the improvement in detectors, computational power has increased, allowing to gather and process quantities of information unimaginable not too long ago.

Cosmology is an interesting field because many pressing questions to the understanding of the Universe are still open. To answer questions such as: *Did cosmic structure form solely via gravitational instability? What is the mass of the neutrino and how does it affect the structure formation? How does galaxy distribution relate to the mass distribution? What is the nature of the dark matter and the dark energy? What is the origin of the density perturbations? Is there an ingredient missing from the cosmological model?* we need experiments that can probe the corresponding scales. Data of unprecedented precision, entering astrophysical scales, are now becoming available and turning cosmology into a precision science. Hence cosmology is also a promising field because the possibility of answers is real and attainable.

This article, aimed at the astronomy community, attempts to update on the recent progress in the understanding of the universe derived from the study of the CMB, and convince that the CMB is a unique and powerful tool not only for cosmology but also for astrophysics.

II. A black-body spectrum

The high degree of homogeneity and isotropy of the CMB radiation suggests that the universe was once small enough for all the patches in the sky to be in causal contact and that the universe eventually expanded to the pres-

ent size. As the universe expanded, the photon wavelengths stretched and hence redshifted, whereas the particle number density diminished, resulting in the low photon temperature and density observed today. We thus infer that the universe was once in a hot dense state, formed by a plasma of hydrogen and helium almost homogeneously distributed in space. The interactions between the particles led the universe to a state of thermal equilibrium at a redshift $z \sim 10^7$. (The redshift z measures the relative difference of the observed and observed wavelengths. In a homogeneous and isotropic universe, it can be expressed as a function of the scale factor at observation and emission, respectively a_{obs} and a_{em}, as $z = a_{obs}/a_{em} - 1$.) Due to the scattering from the free electrons, the mean free path of the photons was then small compared to the cosmological scales, i.e. the universe was opaque. As the universe expanded, the plasma cooled, the helium ions first and the hydrogen ions next captured the free electrons and the photons became free, i.e. the universe became transparent. This happened at a redshift $z \sim 10^3$, which is about 380,000 years after inflation. It is from this time, which defines the surface of last-scattering, that the CMB dates. At the time of decoupling, the photons had a black-body spectrum of the same temperature as that of the plasma, i.e. of order 3000 K. The fact that we see a black-body spectrum today means that all wavelengths were stretched by the same factor. The thermal radiation spectrum of the CMB is thus the most compelling evidence of the premise of universal expansion of the big-bang theory.

Since the CMB photons have travelled from the last-scattering surface until today, they are a powerful probe of the large-scale structure and the thermal history of the universe. The small deviations from homogeneity and isotropy of the CMB are evidence of the premise of a homogeneous and isotropic universe, moreover confirmed by the average large-scale structure mapped by various surveys [3].

III. Temperature anisotropies

The deviations from the Planck law describe temperature anisotropies which appear as higher order moments. These anisotropies were produced by processes in the primordial plasma (the primary anisotropies), as well as by gravitational interactions of the CMB photons with the baryons on their way to us (the secondary anisotropies). In particular, the dipole contains a Doppler shift which measures the peculiar motion of the Sun with respect to the comoving reference frame. It corresponds to a temperature of 3.355 ± 0.008 mK which implies a solar system peculiar velocity of 369.0 ± 0.9 km s^{-1} along the direction (l, b) = (263.99 ± 0.14, 48.26 ± 0.03) deg in galactic coordinates, respectively (longitude, latitude) [4]. Higher order moments contain imprints of the primordial plasma and of the regions from where the photons last scattered, in particular information on the gravitational potential, the velocity along the line of sight and the density fluctuations. (For further details, see Ref. [5].)

While the primary anisotropies provide information on cosmological parameters and the physics of the early universe, the secondary anisotropies provide information on the dynamics and geometry of the expanding universe. Consequently, the two types of anisotropies are complementary, rendering the CMB a robust probe of all accessible scales. Here we will focus on scalar perturbations and on temperature anisotropies only. Tensor perturbations and polarization will not be discussed.

The nature of the CMB anisotropies is different depending on the scale where they are manifested. (In the following, we will be using the multipole index ℓ of the Fourier mode expansion as a measure of distance, which relates with angular distance θ (in radians) by $\ell \approx \sqrt{4\pi}/\theta$.)

At large angular scales, i.e. θ > 5′ or multipoles $\ell < 2500$, the primary anisotropies dominate, which are due to small linear perturbations in the primordial plasma's density and velocity. These perturbations cause the plasma to undergo acoustic oscillations until it decouples. The acoustic oscillations consist of waves of density and velocity, where regions of maximum compression correspond to potential wells and regions of maximum rarefaction correspond to potential peaks. These oscillations grew by gravitational collapse and provided the seed for the formation of the large-scale structure in the universe (i.e. galaxies and clusters of galaxies) that we observe today. The CMB contains an imprint of the acoustic oscillations averaged over the surface of last-scattering. This is because, after decoupling, Thomson scattering of photons off of electrons sourced a global reionization which rendered the surface of last-scattering to have a finite thickness in redshift between $z \sim 10^3$ and $z \sim 10$. Moreover, temperature anisotropies on the surface of last-scattering reflect density variations of the same order in the primordial plasma. Hence, the temperature observed in a given direction of the sky is the weighted average of the temperature on the $z \sim 10^3$ surface which lies in the past light cone of the point on the $z \sim 10$ surface from which the photons streamed almost freely until reaching us today.

At small angular scales, i.e. θ < 5′ or multipoles $\ell > 2500$, the primary anisotropies become negligible due to photon diffusion which suppresses fluctuations in the density distribution of wavelengths smaller than the mean free-path of the photons. This effect, called Silk damping, sets the scale for the thickness of the last-scattering surface and causes a modulation of the anisotropies by an exponential cutoff on small angular scales. Non-linear effects from more recent epochs become all the more important as secondary sources of perturbations. There are three major non-linear contributions at small scales angular, as summarily described below.

The **thermal Sunyaev–Zel'dovich (tSZ) effect** consists of the scattering of CMB photons from hot electrons in clusters, which creates a spectral distortion of photons to higher energies in the form of a deficit of photons below ν ≈ 217 GHz and an excess above this frequency. Since the thermal distortion of the spectrum remains unaltered as the photons propagate freely, the tSZ signal depends on the cluster mass and temperature, and not on the cluster redshift. This effect has been successfully used to detect galaxy clusters, whose tSZ signature is stronger than that of the CMB, and to study the structure and physics of clusters [6].

The **kinetic Sunyaev–Zel'dovich (kSZ) effect** and **the Ostriker–Vishniac (OV) effect** consist of the scattering of CMB photons from ionized gas with peculiar velocity, which is due to the velocity–density coupling. The kSZ signal is concentrated in galaxy clusters and can be removed using the spacial distribution of the tSZ signal. In contrast, the OV effect extends over the entire field of view, generating fluctuations

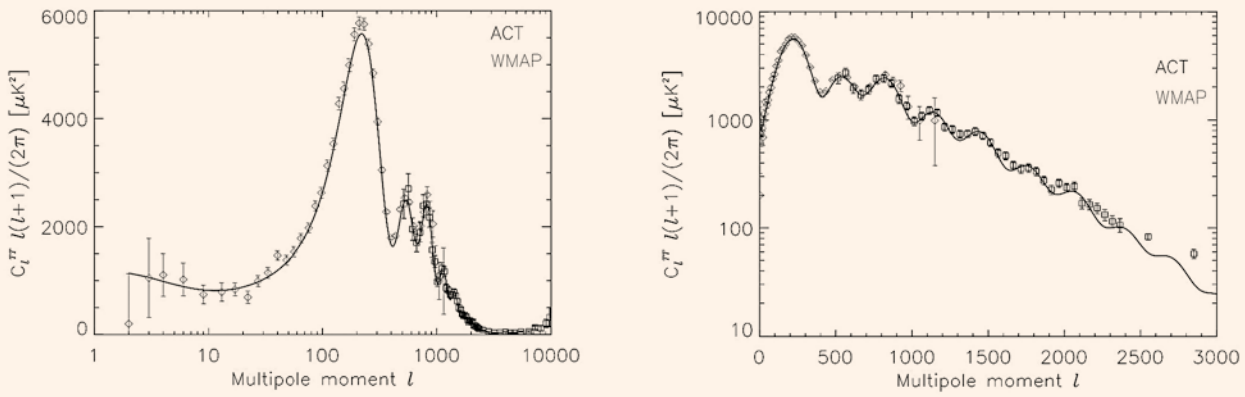

Figure 2. **The temperature power spectrum from the WMAP 7-year data and the ACT 148 GHz data.** The gray diamonds are the data points from WMAP, the black squares are the data points from ACT. The dark gray curve is the theoretical power spectrum. Right panel shows a detail of the left panel for a better visualization of the acoustic peaks.

about the black-body spectrum of a few μK on arcminute angular scales. These fluctuations are sensitive to inhomogeneities in the reionization of the Universe, and thus give information on the depth of reionization epoch. This effect, which has so far eluded detection in the CMB, might be detected in arcminute-resolution maps.

The **weak gravitational lensing** consists of the deflection of CMB photons by matter fluctuations along the line of sight. The characteristic deflection angle is a few arcminutes, being coherent over a few degrees. This deflection causes a smearing of the acoustic peaks in the power spectrum, as well as the generation of small scale power wherever there are temperature gradients. This effect, being sensitive to mass fluctuations, is a most promising probe of dark matter and a potential test of the validity of general relativity at cosmological scales. It has been directly detected from CMB maps produced by WMAP [7] and by ACT [8], showing a preference for a cold dark matter model with a cosmological constant [9].

The non-linear effects act as contaminants of the primordial signal, which must be subtracted for an unbiased estimation of the cosmological parameters. Simultaneously, the non-linear effects probe the expanding universe and contain imprints of the interaction of the CMB photons with the large-scale structure on their way to the observer, thus providing indirect information on the physics of the early universe.

IV. The power spectrum

The primordial temperature fluctuations $\delta T = \Delta T/T$ are generated by random spatial fluctuations on the density and velocity fields of the plasma, hence the temperature anisotropies on the CMB must be analysed statistically. Assuming also that the primordial temperature fluctuations are Gaussian, all information on the anisotropies is encapsulated in the two-point temperature correlation function or equivalently in its angular decomposition in Legendre moments C_ℓ. The power spectrum of the primordial potential is often assumed to have the form of a power law in the wave number k, $P(k) \propto k^{n_s-1}$ where n_s is the spectral index. We predict C_ℓ by tracking the evolution of the temperature fluctuations on the surface where they are generated, to the temperature anisotropies which we observe on the sky. This evolution can be incorporated in a transfer function $T_\ell(k)$ relating the corresponding power spectra as $(2\ell + 1)C_\ell = \int d\ln[k]\, T_\ell^2(k)\, P(k)$. In Fig. 2 we plotted the C_ℓ from WMAP and ACT using data publicly available [10].

Acoustic oscillations are unavoidable if there are potential perturbations before the last-scattering surface, hence a common prediction of various cosmological models. Nonetheless, they can be used to discriminate between different models [5]. Depending on the initial conditions of the temperature fluctuations, i.e whether adiabatic (i.e. of the Neumann type) or isocurvature (i.e. of the Dirichlet type), different harmonics are triggered in the spectrum of acoustic oscillations. Thus the initial conditions can be distinguished by the angular scalar subtended by the sound horizon at last-scattering, which sets the fundamental angular scale, and the relation between the peaks. In particular, the locations of the peaks depend only on the background cosmology, mainly on the spatial curvature $\Omega_k h^2$, but also on a combination of the baryons $\Omega_b h^2$, the cosmological constant $\Omega_\Lambda h^2$ and the matter $\Omega_m h^2$ at last-scattering. (Here $\Omega_m = \Omega_b + \Omega_c$ includes both baryonic matter b and non-baryonic cold dark matter c.) Moreover, the difference in heights between the odd and even peaks is a robust probe of the baryons relative to the total matter at last-scattering, and possibly also of the number of massless neutrinos. Also, the damping scale probes the baryon content and the physics of recombination. Thus the detection of acoustic oscillations in the CMB data enables to measure various cosmological parameters and hence to constrain early universe cosmological models.

Parameter dependence

However, the determination of cosmological parameters from measurements of the CMB anisotropies is plagued with degeneracies among the parameters. An example is the geometric degeneracy, which leads to nearly identical CMB anisotropies in universes with different background geometries but identical matter constant [11]. Thus the geometric degeneracy imposes limits on the

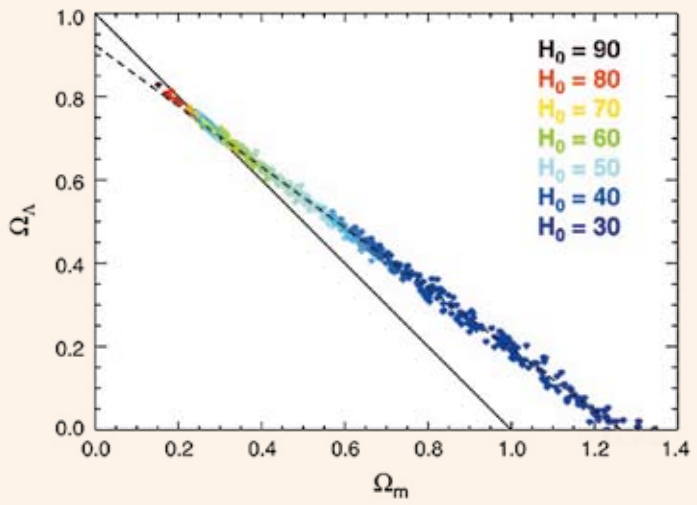

***Figure 3.* Degeneracy of Ω_Λ and Ω_m as a function of the Hubble constant, from WMAP 7-year data.** The black line is $\Omega_\Lambda + \Omega_m = 1$ and separates between closed and open universes. The dashed line is $\Omega_k = -0.2654 + 0.3697\Omega_\Lambda$ and parametrizes the geometric degeneracy in these data. The color points indicate the value of the Hubble constant for each non-flat model consistent with these data. If H_0 is known, then $\Omega_\Lambda + \Omega_m$ is fixed and vice-versa. Reprinted from Ref. [12].

measurement of the spatial curvature of the Universe and the Hubble constant from measurements of the CMB anisotropy only. This degeneracy can only be removed by the combination of constraints on the geometry of the Universe or from the effects of weak lensing on the CMB.

The accuracy of the relation between Ω_Λ and Ω_k depends on the ability to fix the position of the peaks. Improving the accuracy of the measurement simply causes the likelihood contours to narrow around the degeneracy lines. Simultaneously, the indeterminacy of Ω_Λ leads to an indeterminacy of H_0. If both $\Omega_m h^2$ and the relation between Ω_Λ and Ω_k are well constrained, then a constraint on H_0 implies a constraint on Ω_Λ. If $\Omega_m h^2$ is well constrained, then a constraint on the age of the Universe (which is a function of $\Omega_m h^2$, $\Omega_k h^2$ and $\Omega_\Lambda h^2$) implies a constraint on the geometrical degeneracy in the (Ω_k, Ω_Λ) plane. This is illustrated in Fig. 3 [12].

Restricting to spatially flat models $\Omega_k = 0$, the location of the first peak (at 1-degree scale) determines the degeneracy among Ω_Λ, Ω_c and Ω_b, whereas its height determines the degeneracy among Ω_c, Ω_b and n_s. WMAP brought the angular scale coverage to the degree scale, whereas the current generation of anisotropy experiments extends the angular scale coverage to the arcminute scale.

Cosmological parameters from WMAP

The results have been greatly improved by the observations from WMAP [10], which has produced sky maps from seven years of observation. Accurate measurements of the first few peaks in the angular power spectrum, in combination with other data sets, have allowed advances in the understanding of the universe [12]. Some of the results follow below.

a) The baryon density in the universe is now known to within 3% and agrees with the big-bang nucleosynthesis. Also, the first detection of pre-stellar Helium was reported, providing an important test of the big-bang theory, according to which most of the Helium in the Universe was synthesized in the hot early Universe and not in stars. Primordial Helium affects the time profile of recombination, which in turn affects especially the third acoustic peak of the CMB angular power spectrum.

b) Strong constraints were placed on the dark energy and geometry of the universe. The dark matter must be non-baryonic, according to nucleosynthesis, and interact only weakly with baryons and photons. Moreover, the universe is spatially flat to within 1%, as inferred from the combination with the local distance scale and the baryon acoustic oscillation (BAO) data [13].

c) Tighter limits were placed on the dark matter and cosmological constant for a flat universe. As a consequence, the Hubble constant is determined to within 3% in combination with BAO data.

d) The primordial fluctuations are adiabatic and nearly Gaussian, and its spectrum is slightly tilted (i.e. has a slight scale-dependence, with spectral index $n_s = 0.982^{+0.020}_{-0.019} < 1$).

e) New constraints were placed on the number of neutrino-like species in the early Universe, $N_{eff} > 2.7$ (95%CL), which were possible due to the improved measurement of the third peak.

Hence CMB observations strongly suggest that the universe is geometrically flat (with a Hubble constant $H_0 = 71.0 \pm 2.5$ km s^{-1} Mpc^{-1}), dominated by a dark energy component consistent with a cosmological constant $\Omega_\Lambda = 0.757 \pm 0.031$ and with about five times more cold dark matter than baryonic matter, respectively $\Omega_c = 0.222 \pm 0.026$ and $\Omega_b = 0.0449 \pm 0.0028$ [12]. A plethora of astronomical observations demonstrate not only that most of the matter of the universe is non-baryonic but also that the energy density of this form of matter is not enough to explain the observed flatness. Moreover, supernova observations suggest that the universe is expanding in an accelerated fashion [14]. These observations combined require a new form of energy capable of driving the accelerated expansion and of rendering the universe flat. The missing matter and energy suggest that important physics is missing from the cosmological model.

V. Conclusion

Observations from WMAP have placed robust constraints on fundamental cosmological parameters but little have they revealed about the dark components. Nonetheless, these observations can put constraints on specific models of dark matter and dark energy [15]. Since both dark components become dynamically

evident at most recent cosmological epochs only, we require higher-resolution experiments capable of probing the corresponding smaller scales of interest.

Ongoing observations by ACT [16] and SPT [17] are already showing results [8,18,19], whereas the data from PLANCK are awaited with a great promise of settling open questions due to their unprecedented resolution [20]. New insights are also expected from polarization, which introduces three additional power spectra to characterize the temperature anisotropies. In particular, measurements of the polarization can distinguish between scalar and tensor modes, as well as determine the redshift at which intergalactic medium was reionized, thus breaking other degeneracies among parameters.

Interesting times for cosmology are coming soon and they are here already.

Acknowledgments

The author is supported by Fundação para a Ciência e a Tecnologia, Ref. SFRH/BPD/65993/2009. The author thanks S. Basilakos, O. Bertolami, G. Contopoulos, I. Tereno and A. Zampeli for a careful reading of the manuscript and useful comments.

References

1. Wilson A.A. and Penzias R.W., ApJ 142, 419 (1965)
2. Fixsen D.J. et al., The Cosmic Microwave Background Spectrum from the Full COBE FIRAS Data Set, ApJL 473, 576 (1996); Fixsen D.J. and Mather J.C., The Spectral Results of the Far-Infrared Absolute Spectrophotometer Instrument on COBE, ApJ 581, 817 (2002)
3. Aihara H. et al., The Eighth Data Release of the Sloan Digital Sky Survey: First Data from SDSS-III, ApJS, 193, 29 (2011) [1101.1559 (astro-ph.IM)]
4. Hinshaw G. et al., Five-year Wilkinson Microwave Anisotropy Probe Observations: Data processing, sky maps and basic results, ApJS, 180, 225 (2009) [0803.0732 (astro-ph)]
5. Hu W., Wandering in the Background: a Cosmic microwave background explorer, (astro- ph/9508126)
6. Hicks A.D. et al., The Atacama Cosmology Telescope: Beam Profiles and First SZ Cluster Maps ApJS 191, 423 (2010) [0907.0461 (astro-ph.CO)]; Hand N. et al., The Atacama Cosmology Telescope: Detection of Sunyaev-Zel'dovich Decrement in Groups and Clusters Associated with Luminous Red Galaxies, [1101.1951 (astro-ph.CO)]
7. Smidt J. et al., Constraint on the Integrated Mass Power Spectrum Out to z = 1100 from Lensing of the Cosmic Microwave Background, ApJL 728, 1 (2011) [1012.1600 (astro-ph)]
8. Das S. et a., The Atacama Cosmology Telescope: Detection of the Power Spectrum of Gravitational Lensing, [1103.2124 (astro-ph.CO)]
9. Sherwin B. et al., The Atacama Cosmology Telescope: Evidence for Dark Energy from the CMB Alone, [1105.0419 (astro-ph.CO)]
10. http://lambda.gsfc.nasa.gov/
11. Efstathiou G. and Bond J.R., Cosmic confusion: Degeneracies among cosmological parameters derived from measurements of microwave background anisotropies, MNRAS 304, 75 (1999) [astro-ph/980713]
12. Larson D. et al., Sever-year Wilkinson Microwave Anisotropy Probe (WMAP) Observations: Power spectrum and WMAP-derived parameters, ApJS 192, 16 (2011) [1001.4635 (astro-ph.CO)]
13. Komatsu E. et al., Sever-year Wilkinson Microwave Anisotropy Probe (WMAP) Observations: Cosmological Interpretation, ApJS 192, 18 (2011) [1001.4538 (astro-ph.CO)]
14. Lampeitl H. et al., First-year Sloan Digital Sky Survey-II (SDSS-II) supernova results: consistency and constraints with other intermediate-redshift datasets, MNRAS 401, 2331 (2009) [0910.2193 (astro-ph.CO)]
15. Barreiro T., Bertolami O. andTorres P., WMAP5 constraints on the unified model of dark energy and dark matter, PRD 78, 043530 (2008) [0805.0731 (astro-ph)]
16. http://www.physics.princeton.edu/act/about.html
17. http://pole.uchicago.edu/
18. Das S. et al., The Atacama Cosmology Telescope: A Measurement of the Cosmic Microwave Background Power Spectrum at 148 and 218 GHz from the 2008 Southern Survey, [1009.0847 (astro-ph.CO)]
19. Keisler R. et al., A Measurement of the damping tail of the Cosmic Microwave Backgroun Power spectrum with the South Pole Telescope, [1105.3185 (astro-ph.CO)]
20. http://www.rssd.esa.int/index.php?pro ject=Planck

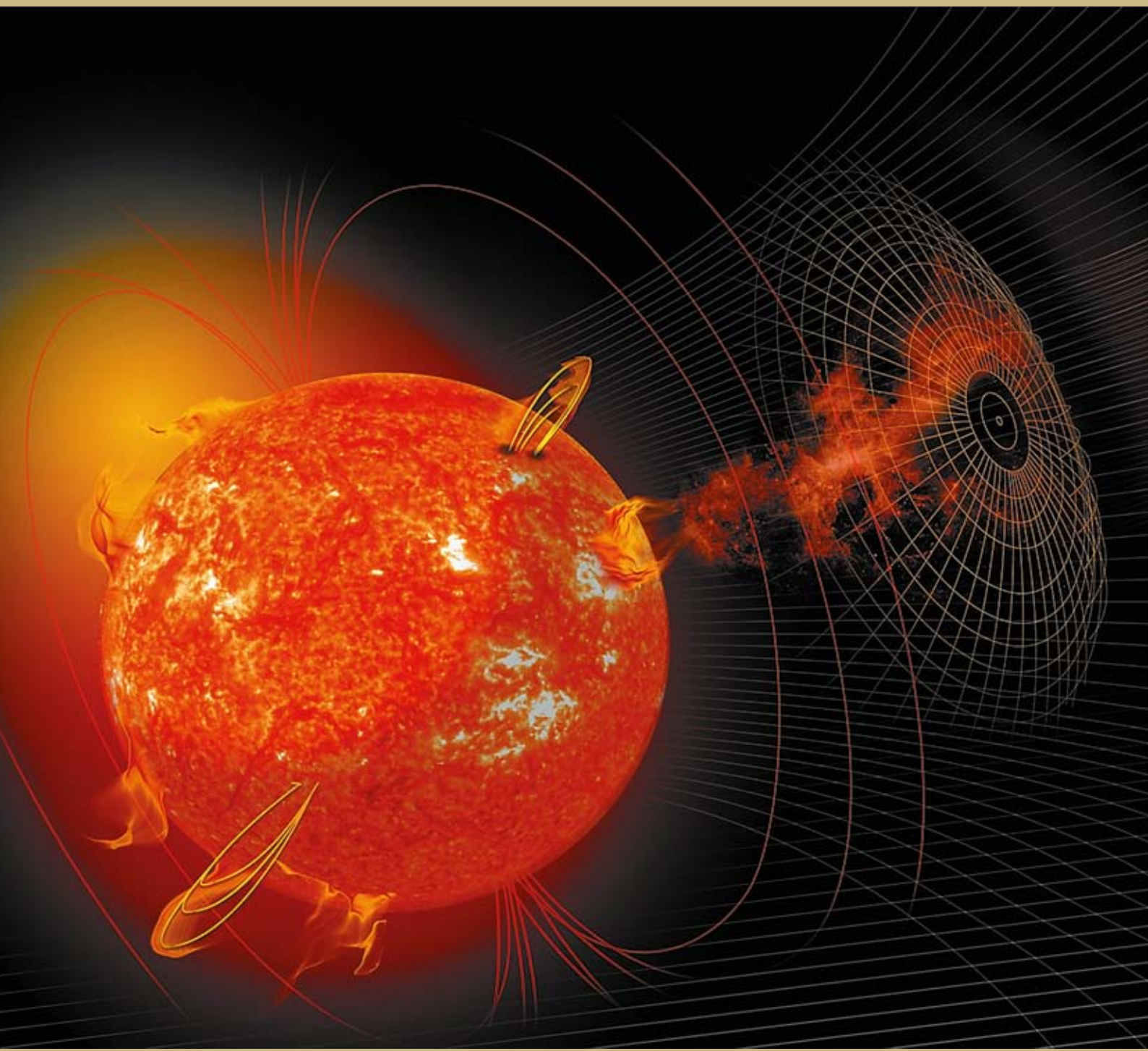

Heliophysics is the study of the Sun and its interactions with Earth and the solar system.
Credit: NASA
Source: http://www.nasa.gov/images/content/474966main_Heliophysics.jpg

Recent Advances in Heliophysics from Space-Based Observations

by Angelos Vourlidas

Space Sciences Division, Naval Research Laboratory, Washington DC, USA

Abstract

The Sun is the only star we can observe in detail and on the other hand, solar variability drives the heliosphere and influences the environment around our planet. Over the last 10-15 years, a large number of space missions have been providing a smorgasbord of observations from the photosphere to the outer reaches of the heliosphere. As a consequence, solar and space physics are being integrated into a joint research field, called heliophysics, and are tackling the mysteries of the Sun and the heliosphere with great success. In this short review, I discuss a few of those exciting advances in an attempt to capture the spirit of progress that permeates the field. Due to space restrictions, I left out many major results which may be addressed in future articles.

Figure 1. Currently-Operating Heliophysics Missions.

Mission	Daily Data Volume (GB)	Launch Date
SOHO	0.5	12/1995
RHESSI	1.6	02/2002
Hinode	7.0	09/2006
STEREO	12.0	10/2006
SDO	1500.0	02/2010

Table 1. Dypical Data Volumes from Heliophysics Missions.

The 'Great' Heliophysics Observatory

Perhaps the single most important force of progress in our discipline has been the sheer number of Solar or Solar-related, space observatories currently in operation. NASA's Heliophysics Division is operating 16 missions as of this writing, some of them in coordination with other space agencies (Figure 1). The spacecraft locations and their measurements span the whole heliosphere from the terrestrial magnetosphere (e.g., *THEMIS*) to the L_1 Lagrangian point (*SOHO*) to L_4 and L_5 (*STEREO*) to the edge of the heliopause (*Voyager*). The data from these missions are freely available of the internet and science investigations increasingly combine remote sensing and in-situ information for different probes. So another major change is afoot: the increasing fusion between the physics of the Sun and its local environment ('solar physics') and the physics of the inner heliosphere and the terrestrial environment ('space physics'). The spirit of this gradual change has been captured by the new term of 'heliophysics' which is the name of the NASA division responsible for solar and heliospheric studies and is now used extensively in the U.S. to describe our expanded community focus. I will use the term here in place of the old-fashioned 'solar physics' term because it describes better the science highlights in this article and expresses more clearly the future trends within our discipline.

With the large number of spacecraft and the variety of science measurements and locales covered by them comes the third major change in heliophysics: data deluge. Table 1 shows the daily data volume for five data-intensive

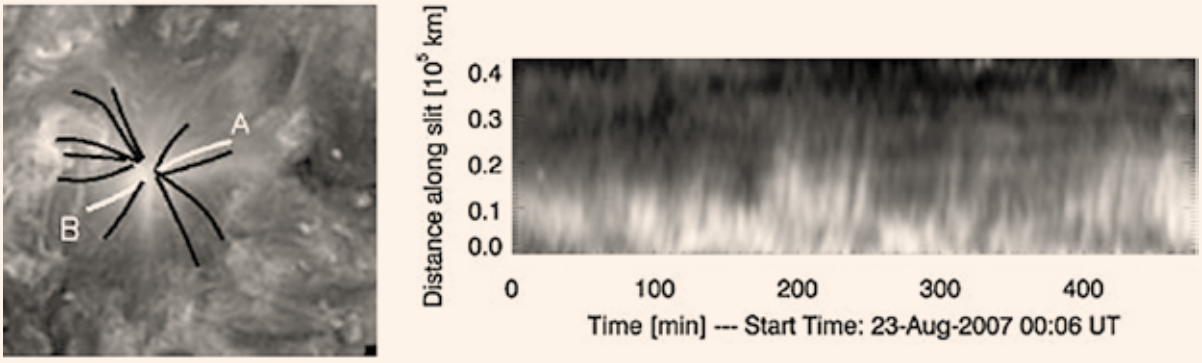

Figure 2. Detection of quasi-periodic fluctuations in active region. Left: EUV 195A image of an anemone active region on 23 August 2007. Right: The intensity time series is extracted along path A and plotted as a distance-time map. Each ridge corresponds to a fluctuation episode and the slope determines its speed. Most of the slopes in the figure correspond to about 70-120 km/s[5].

heliophysics missions. The data volumes haven been increasing steadily in the last 15 years and went to 'overdrive' with the launch of the Solar Dynamics Observatory (*SDO*) last year.

The large data volumes are not the only reasons for the increase in the science output in heliophysics research. Novel viewpoints and observing wavelengths, high temporal and spatial resolutions, long-term synoptic observations, and faster computers have accelerated research. The *Hinode*[1] mission employs the largest solar space telescope flown (0.5m diameter) and is exploring the solar photosphere and chromosphere with sub-arcsecond resolution. The *RHESSI*[2] spacecraft is mapping hard and soft X-ray sources using interferometric techniques. The unique mission design of the *STEREO*[3] mission provides us with a continuously varying, off the Sun-Earth line, perspective of solar and heliospheric activity 24 hours a day and with relatively high-cadence to boot. *SDO*[4] is providing full disk images of the corona in ten wavelengths at a cadence of 12 seconds with arcsecond resolution. *SOHO*[5] and *SDO* comprise the 'third eye' along the Sun-Earth line and provide both a long-term synoptic database going back to the previous cycle (*SOHO*) and large temporal and temperature coverage of the corona. MHD modeling on the other hand has been able to couple seamlessly models of the solar corona to the heliosphere and to the Earth creating a grand heliospheric modeling framework.

Heliophysics Advances in the Last 5 Years

The scope of heliophysics space research is large while the pages allocated to this article are restricted. Thus, the review discusses only a few topics which are indicative of the fresh air currently blowing in heliophysics, at least according to this author. The selection of the topics was based on whether they addressed longstanding questions, whether they opened new avenues of research, or because they reveal major trends in future heliophysics research. We focus on the last five years only when most of the discussed mission were launched.

An Old Debate on Coronal Heating Comes Into Focus: Waves or Flows?

The million Kelvin temperature of the solar corona has long been an outstanding issue in heliophysics with important implications for stellar physics as well. Uncovering the mechanism (or mechanisms) behind coronal heating has been the focus of many heliophysics missions since *Skylab* in the 1970's. Despite countless observations across most of the electromagnetic spectrum, a complete answer still eludes us. Is the corona heated by waves or by energy released through magnetic reconnection? Is it a discreet or a random process? Do the same processes operate across open and closed field regions? Does the energy originate in the corona and conducts downward towards the chromosphere or does the chromosphere do the heating thanks to its large mass and close magnetic coupling to the photosphere? The latter question may point to a potential 'turf war' between coronal and chromospheric researchers!

While the debate has not been settled yet, recent observations from space have provided a wealth of clues. Coronal spectroscopy has long given evidence for outflowing (blue-shifted) plasmas in active regions but the imaging context was missing or was of low spatial resolution. Thanks to more sophisticated extrapolation algorithms, comparisons of coronal magnetic field extrapolations to spectroscopic information from the SUMER instrument on *SOHO* led to the concept of coronal circulation [1] to explain the observed flows. In other words, the coronal plasma heats and moves upwards along field lines. At some height, it cools and returns to the chromosphere closing the loop. The problem is that the temperatures changes of the plasma and the small number and finite bandpasses of spectrometers and imagers makes it very difficult to follow the time history of a given parcel of plasma even at the easily resolvable scales of a few arcseconds (~1-2 Mm). The instruments record only intensity fluctuations which are just regular enough to indicate periodicity. Typical speeds are of the order of 50-100 km/s and periodicities of around 8-12 min. Since these structures occur in quick succession and the magnetic field within them is unknown, it is difficult to discriminate between true mass flows or overlapping waves sim-

1. http://hinode.nao.ac.jp/index_e.shtml
2. http://hesperia.gsfc.nasa.gov/hessi/
3. http://stereo.gsfc.nasa.gov
4. http://sdo.gsfc.nasa.gov/
5. http://sohowww.nascom.nasa.gov/

ply through spectroscopy. Additional constraints need to be used. Therefore, blue-shifted intensity fluctuations at the edges of active regions bordering coronal holes were interpreted as outflowing material possibly linked to solar wind [2]. Other analyses have detected periodicities and hence interpreted the fluctuations as waves[3]. However, neither the material nor the periodicities could be followed to large enough heights to check whether it escaped or returned (hence a flow) or dissipated away (hence a wave) leading to the current open issue: are the intensity fluctuations waves or mass outflows?

The answer may come from the great improvements in image processing techniques and instrumental sensitivities. Whereas early imaging observations from *TRACE* and *SOHO*/EIT have given hints of intensity fluctuations, today's imagers (EUVI, AIA) are literally seething with motion. Everywhere one looks, there is evidence of outflows (… or waves, of course). The online movie[6] shows an example from a 2-hr sequence of *SDO*/AIA 193Å images processed by a sophisticated wavelet algorithm [4] to remove the instrumental stray light and the stable large-scale structures. The movie sequence makes clear that the outflows occur in both open and closed field structures, in the quiet sun, active regions and coronal holes. Some of the outflows are larger scale jet-like structures occurring very intermittently but the majority of the outflow comprises small-scale repetitive fluctuations that can be followed almost to the edge of the field of view (~0.2 Rs or 140 Mm). Even with this amount of image processing, it is still difficult to follow individual plasma parcels. The sheer number of them would render any manual tracking method impossible. One solution is to resort to even more processing---computing power is cheap these days, anyway. Figure 2 shows an example of a distance-time map along a faint loop (labeled 'A') in an anemone active region[5]. The production of the map required a laborious procedure of wavelet-enhancing, region-of-interest extraction, background-subtraction in the distance-map plane, and edge-enhancement. The final result with the clearly-defined ridges of emission captures the intermittency and the extent of these outflows for the first time.

6. http://solphys.nrl.navy.mil/users/vourlidas/docs/ipparchos/20100613_aia193_21.mov

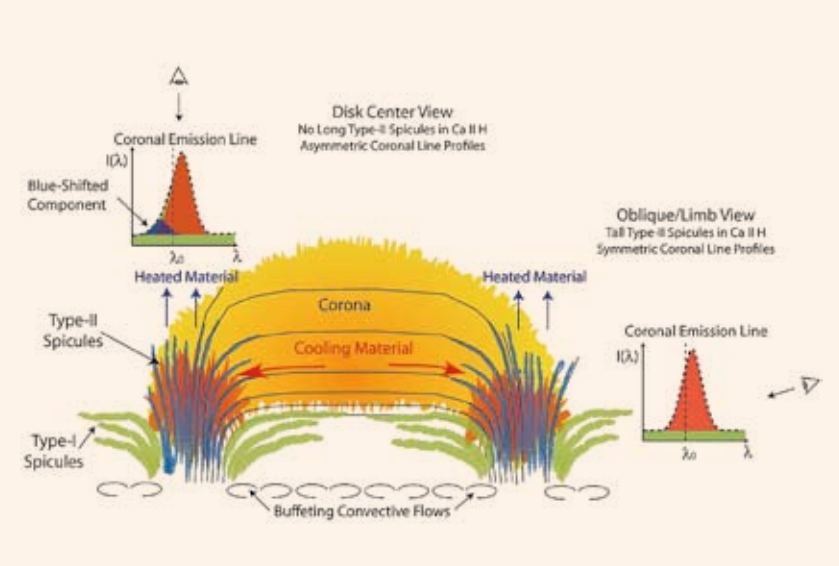

Figure 3. Mass and energy transport between the chromosphere, transition region, and corona, as deduced from SOT and EIS observations[9].

When one considers that the emission variation in Figure 2 represents just an 8-hour segment along a single 2000 km-wide loop in a single active region, one wonders about the scale of the problem at hand. The Sun is simply too close, too well-resolved, and too active. It is nothing short of a treasure trove for physics.

Returning to our discussion on flows versus waves, Figure 2 does suggest some periodicity in the fluctuations which comes to about 8 min after a wavelet decomposition analysis. Again we reach an impasse. We cannot tell with certainty whether the flows are waves or mass motions. It is most likely a combination of the two. Our discussion has focused only on the corona so far which is not an uncommon bias for coronal observers like the author. The chromosphere with its ready supply of plasma and its medium temperature is usually ignored because of the complexities of its partially ionized and neutral plasmas.

Thankfully, tantalizing clues have emerged about the transfer of mass and energy across the chromosphere-corona interface. Observations in the Ca II H (3968Å) line from the SOT telescope on the *Hinode* mission have uncovered a new class of spicules [6] in addition to those known for several decades[7]. These new, "Type-II" spicules with much shorter lifetimes (10-150 sec) than the 'traditional' spicules, are observed as thin jets (widths of 100-700 km or 0.1″ – 1″) shooting up in the atmosphere at high speeds (50-150 km/s). Type-II spicules disappear very rapidly from the Ca II bandpass suggesting plasma heating. Additional observations from the *Hinode*/EIS spectrometer and the *SDO*/AIA EUV images show substantial heating in Type-II spicules with some plasma reaching coronal temperatures: they could be the ultimate source of coronal mass and heat[8] (Figure 3). If the material is indeed heated to coronal temperatures and is prevalent enough to play a role in coronal thermodynamics, then it should be detected by EUV imagers after it is ejected by the cool chromosphere. Unfortunately, such idealized sequence of events is only rarely observed (Figure 4).

To make things more complicated, both types of spicules seem to be constantly permeated by waves manifested as transverse oscillations of the order of 10-25 km/s and periods of 100-500 s[8]. It is not clear whether these oscillations are related to the waves in the corona we discussed above. It is generally difficult for waves to propagate across the chromosphere/corona interface because the sudden change in the physical parameters (density, temperature, magnetic field) tends to reflect them.

Thus the question of how the corona is heated is still left open despite the plethora of spectroscopic and imaging observations. This simply means that the solution is not an obvious one but lies within the fine structures and high variability of the solar atmosphere that makes solar imaging so impressive. There is no doubt that the questions of whether the omni-

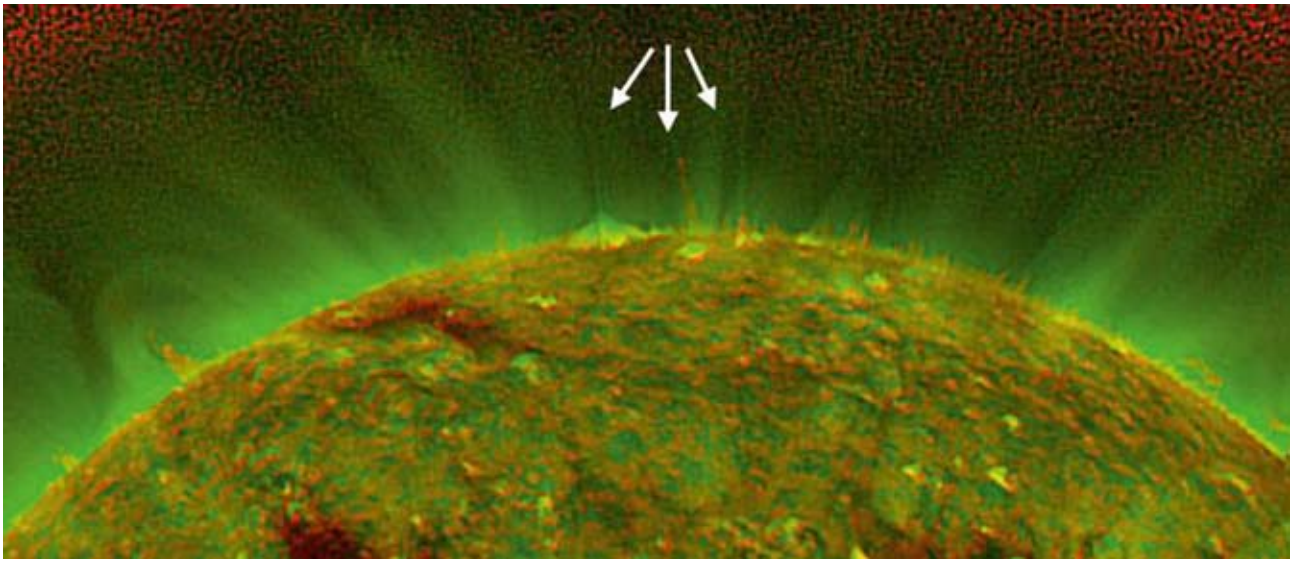

Figure 4. Two-temperature image of outflows within a coronal hole. The green colors show emission at the FeXII 195 Å line (formed at 1.4 10^6 K) and the red color comes from He II 304 Å (80,000 K). The arrows point to three types of ejections: A hot jet (left), a cool jet (middle), and a combination of a hot jet with cool plasma at its base (right). The latter is the signature expected by the De Pontieu et al. scenario. The images are from the STEREO EUVI-A telescope and have been enhanced by a wavelet technique.

present coronal fluctuations are waves or mass flows, the role of the chromosphere in heating the corona, and the origins of the solar wind will be at the forefront of heliophysics for the near future.

A Unification Theory for Solar Explosions

Coronal mass ejections (CMEs) and flares are the most energetic phenomena in the solar system. Flares can convert several times 10^{32} ergs of magnetic energy into heat and light across the electromagnetic spectrum and they accelerate copious amount of energetic particles up to GeV energies, all within a matter of minutes. With a similar timescale, CMEs can expel 10^{16} gr of magnetized coronal plasma with speeds of up to 3000 km/s into the interplanetary space. The shocks driven by these ejections can also accelerate particles to high energies and they can do so for days as they cross the inner heliosphere. Both phenomena extract their energies in more or less equal amounts (a few x 10^{32} ergs) from the magnetic field energy stored in the corona. Being of coronal origin, they are best observed from space telescopes in the EUV and X-ray and visible wavelengths. Flares, especially large ones, often occur in tandem to CMEs but the timing is not consistent. Sometimes the flare precedes the ejection, sometimes it follows it, and many times the intensity of the flare (as

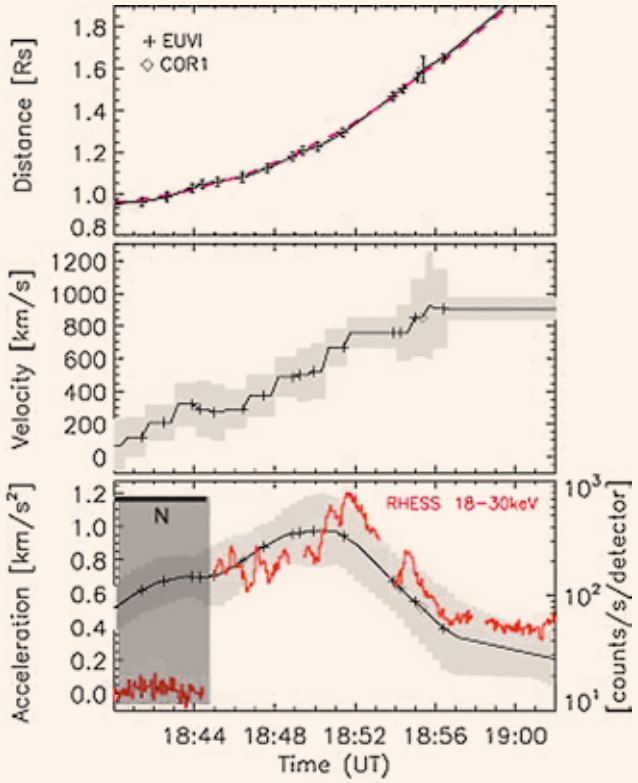

Figure 5. Comparison of CME kinematics to Hard X-ray light curves (red) for a CME/flare event on 25 March 2008. The X-ray curves come from RHESSI which was in the night until 18:44 UT (bar labeled 'N'). The gray swaths mark the uncertainty in the speed and acceleration derived from the height-time plots. Note the very close correspondence between the CME acceleration and HXR curves[10].

measured in soft X-rays, for example) does not match the size or speed of the accompanying CME. On the other hand, CMEs are observed at relatively large heights (>2 Rs) making hard to connect the CME structures, propagation path and acceleration history to the site and evolution of the flare. These observational uncertainties fueled an intense debate in the '80s and '90s on whether CMEs were the results of flares or vice versa. The prize at stake was the 'bragging rights' to the most important phenomenon in the heliosphere (…and possibly to more funding).

The debate seems to have been settled now. CMEs are the main contributors to the short term variability of the heliosphere with their echoes detected all the way to the heliopause. Flares, however, play an important role as efficient particle accelerators and short-term drivers of the thermosphere through their sudden EUV outbursts. The growing number of concurrent CME and flare observations is driving a fundamental change in our view of the two phenomena as separate entities.

We can now measure the acceleration profile of a CME with almost the same cadence and at the same height where the flare takes place [10]. Figure 5 shows an example from a CME/flare event on 25 March 2008. The CME was observed by the EUV and coronagraphs on the *STEREO* mission and the Hard X-ray (HXR) emission was recorded by the *RHESSI* satellite which was in the night during the beginning of the event. Note the very close correspondence between the CME acceleration profile and HXR light curve. The HXR emission originates from localized brightenings of a few arcseconds width (~5000 km across) very low in the corona while the CME measurements are taken at successively larger distance (0.1 R_s = 70,000 km). The Hard X-rays are due to bremsstrahlung emission emitted when non-thermal electrons accelerated by flares collide with ambient protons. Because of the bremsstrahlung density dependence, the strongest HXR emission comes when the electrons impact the chromosphere. The propagation paths of those electrons can be derived by time-of-flight measurements which show that the electrons are accelerated in beams high in the corona. As the CME accelerates and expands outwards, the HXR brightenings also expand along the surface signifying an intimate relationship between CME size (and evolution) and electron acceleration.

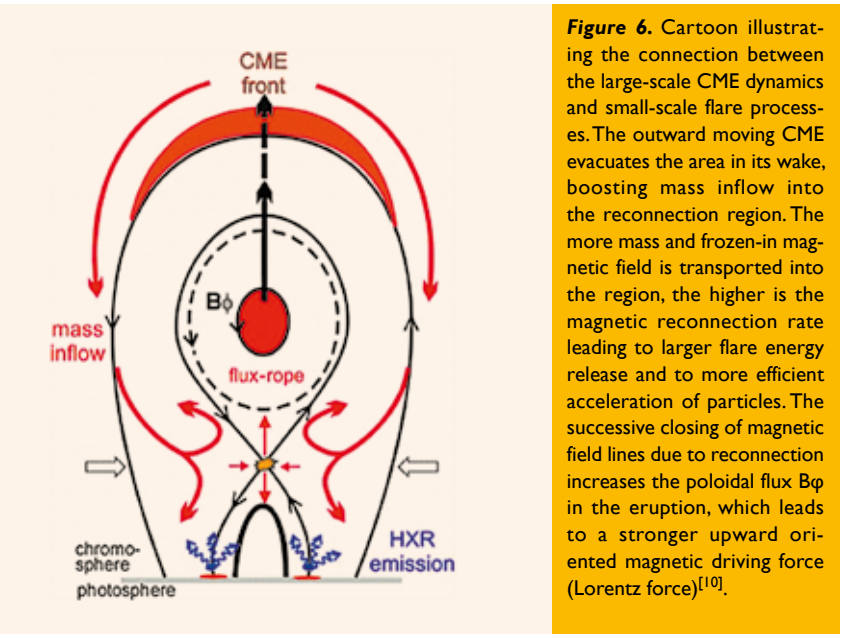

Figure 6. Cartoon illustrating the connection between the large-scale CME dynamics and small-scale flare processes. The outward moving CME evacuates the area in its wake, boosting mass inflow into the reconnection region. The more mass and frozen-in magnetic field is transported into the region, the higher is the magnetic reconnection rate leading to larger flare energy release and to more efficient acceleration of particles. The successive closing of magnetic field lines due to reconnection increases the poloidal flux Bφ in the eruption, which leads to a stronger upward oriented magnetic driving force (Lorentz force)[10].

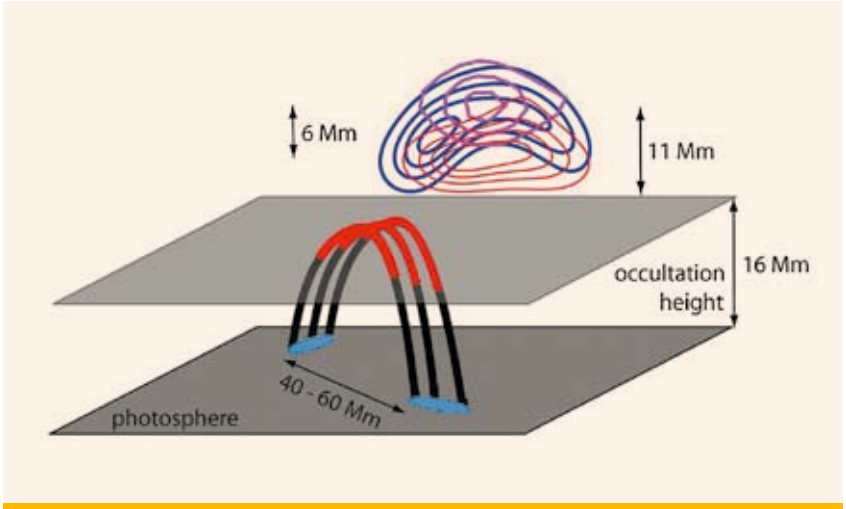

Figure 7. Cartoon of the impulsive phase of the 31 Dec 2007 flare. The dark gray plane is the photosphere, while the parallel plane in lighter gray gives the occultation height of the ***RHESSI*** observations. The flare loops are shown in black with the top part visible by ***RHESSI*** colored red. The contours of the HXR and microwave images are projected on the plane behind the flare loops. Source sizes and altitudes are roughly to scale[12].

This close connection has been verified by numerous studies[11] and constitutes one of the major findings in coronal physics in the last ten years. It suggests that flares and CMEs are not separate phenomena but they could be described by a unified picture (possibly Figure 6). In a nutshell, photospheric motions and flux emergence are continually shuffling the coronal fields above until reconnection is induced across a highly sheared neutral line. Magnetic reconnection is nothing more than a topological reconfiguration of the field but during the process the sheared coronal field relaxes to a lower state. The resulting change in magnetic energy, estimated in the order of $10^{33\text{-}34}$ ergs, is more than sufficient to accelerate the CME out of the solar gravitational field, thermalize the CME and flare plasma, and accelerate the electrons and protons to near-relativistic energies. In other words, CMEs and flares are nothing more than the mass and heat manifestations of the ejection of magnetic energy from the Sun. As the cartoon in Figure 6 suggests,

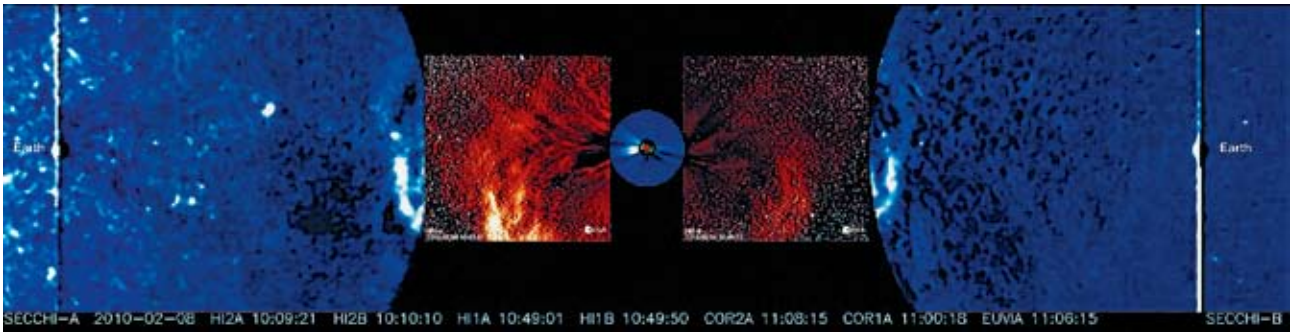

Figure 8. The inner heliosphere viewed by the twin STEREO imaging suites. The Sun is in the center and the inner circle (blue) shows the corona out to 15 solar radii. The heliospheric imagers HI-1 (red), HI-2 (outer blue) cover the heliosphere along the sun-earth line. Images from STEREO-Ahead (Behind) are shown on the left (right). The Earth is also shown. A CME heading towards Earth can be seen in this snapshot taken on February 8, 2010. The solar disk is barely visible in this scale.

the energy release site must lie somewhere between the bottom of the CME and above the flaring loops. Detecting this region would then provide strong support towards the aforementioned scenario. *So, where is it?*

Looptop HXR Sources

RHESSI observations of looptop HXR sources have shown that these sources are visible whenever the bright emission from the flaring footpoints is occulted. Some HXR sources are located up to 100 arcsec (~70,000 km) or more above the surface and may contain a surprising number of non-thermal particles. How are these particles accelerated and where do they come from?

When combined with EUV observations, the HXR sources tend to lie close to the post-CME current sheet. So the HXR source and the post-CME current sheet may be closely related. But how are the HXR sources related to the CME formation?

A careful analysis of a recent occulted flare (Figure 7) reached the surprising conclusion that all of the around 10^{35} electrons in the looptop source were non-thermal with a total energy of 10^{29} ergs[12]. These numbers were consistent with estimates of the pre-event coronal densities and magnetic field and current reconnection models. However, the acceleration process must be extremely efficient in converting magnetic energy into non-thermal electrons. The nature of that process is unknown and should be the subject of intense theoretical focus as we expect more observations of such looptop sources. It is hard to dismiss the HXR observations as a solar oddity. Radio imaging observations also show sources above the flaring loops and in some cases they show them splitting into a stationary and a radially propagating component. The outward-moving component is associated with the bottom of the ejected CME fluxrope where increased densities are expected according to the scenario on Figure 6. Although we still do not have an event with clear imaging in all three regimes (EUV, radio, HXR), the amount and consistency of the various analyses so far clearly support the unified scenario of CME and flare.

Spatial relation between the small-scale flare and the large-scale CME

The problem with cartoons, such as Figure 6, is their simplicity. They cannot easily capture the complexity of the solar conditions. In this case, the cartoon places the flaring site symmetrically beneath the erupting CME due to its two-dimensionality. In reality, the flare can be anywhere behind the CME and the CME does not have to propagate radially or expand self-similarly. Neither of these effects could be studied accurately until the launch of the *STEREO* mission making it very difficult to associate CMEs and flares. The ability to observe the corona simultaneously from two viewpoints afforded by the *STEREO* observations has revolutionized our understanding of the three-dimensional evolution of these eruptions. The realization that CMEs can expand non-linearity during the first few minutes of their formation has been the most important contribution of *STEREO* observations to our discussion here. Three-dimensional fitting of expanding EUV bubbles in very impulsive events showed that the CME lateral expansion reaches speeds of 1000 km/s and lasts only 1-5 minutes while the front of the CME rises at moderate speeds (~500 km/s)[13] . The lateral expansion is unlikely to be seen from a single viewpoint creating the impression that the CME grows in size slowly which the CME may double its size in a matter of minutes. The lateral expansion solves several problems in the flare-CME relationship in one stroke: (i) it explains the discrepancy between CME widths in the outer corona and the extend of flaring loop arcades in the lower corona, (ii) it explains how a CME may appear displaced by several degrees from the flaring site since the CME may expand laterally into low magnetic field regions over the quiet Sun which are not conducive to flaring. (iii) It explains the appearance and short lifetimes of radio sources that appear as drifting spectral emission in metric wavelengths and are interpreted as emission from shock-accelerated electrons. Their drivers (thermal blast from a flare or ejected CME fluxrope) have been debated for decades. The fast lateral expansion could easily drive shocks in the low corona while it lasts.

To summarize, space observations from a multitude of spacecraft have shown that flares and CMEs are not really two separate phenomena but they are manifestations of sudden energy release in the corona. If there is enough energy available, part of the preexisting loops are ejected as a magnetized fluxrope structure which piles up the

overlying corona into a CME. If not, then a small part of the loop system is heated and emits light in a large range of wavelengths. If the event occurs in a low magnetic field region, the timescale of the eruption lengthens somewhat allowing the slow rise of the fluxrope to a larger height where force imbalance and ideal processes (e.g., torus instability) can eventually release the CME. The accompanying heating of the post-CME loops is very low and hence unlikely to be easily detected. Of course, there are many details that need to be addressed in the above simplistic picture. It may be time to join the 'flare' and 'CME' term into the more appropriated term of *Flaring Magnetic Ejection* or FME.

Imaging of the Solar Wind

Perhaps, the most significant breakthrough of the past few years may be the direct imaging of the solar wind by a new type of telescope, called heliospheric imagers (HI). These are large-angle telescopes, operating in the visible, imaging the inner heliosphere starting several degrees away from sun center. The first prototype, the Solar Mass Ejection Imager (SMEI)[7], was flown in 2003. The technique came of age, however, only with the operation of the Heliospheric Imagers aboard the *STEREO* mission since 2007. The *STEREO*-HIs image the inner heliosphere along the Sun-Earth line, from 4^0 to 90^0 elongation from the Sun. As the Earth-Sun-spacecraft angle changes, the HI field of view extends to Earth and beyond. Because of their design---the HIs do not receive any direct sunlight, unlike coronagraphs—and their long exposures, the HIs are the highest sensitivity visible-light telescopes ever flown reaching background levels 15 orders of magnitude below the brightness of the Sun. In other words, the HIs can detect stars down to 12^{th} magnitude within 20^0 from the Sun, which is beyond the capability of any astronomical telescope at this time.

With such performance, the telescopes provide direct images of CMEs, Corotating Interactions Regions (CIRs), shock waves, and even of the fine structure of the quiescent solar wind itself, as they propagate all the way from the Sun to Earth and beyond (Figure 8 and online movie[8]).

Although the STEREO mission was launched during an unusually low solar minimum, the HI images showed a wealth of structures and propagating fronts even in the absence of CMEs. It was quickly recognized [14,15] that the fronts were created by the slow solar wind pileup against the fast solar wind streams originating by large-scale and long-lived equatorial corona holes. In other words, the HI images were our first view of the formation and shape of CIRs. In addition, the fronts could be tracked in elongation-distance plots and their arrival at Earth was predicted easily and with high accuracy[14,15]. This capability opened up new avenues of research both on the physics of CIRs as well as on predicting their Space Weather impacts. Further work into the internal structure of these solar wind entities revealed the surprising fact the many CIRs contained small-scale CMEs, apparently trapped by the fast wind as they were ejected from the tips of the coronal streamers[16]. The resulting magnetic field enhancements may be one of the reasons for the geo-effectiveness of CIRs but it was not recognized before.

STEREO's ability to image the faint outflow from streamers using two vantage points showed that many of the ejections that appeared as amorphous blobs in the LASCO images are highly structured magnetic fluxropes. In other words, they are mini-CMEs with typical widths of less than 10^0 and masses of less than 10^{12} gr, compared to a typical CME of 45^0 width and mass of 10^{15} gr. This finding implies that a large part of the slow solar wind may form as a result of an intermittent impulsive process rather than through the gradual release of plasma caused by the high temperature of the corona. This finding has large implications for long-established theories of slow solar wind formation including the role of coronal heating and the interplay between coronal holes and streamers in the release of magnetic field in the heliosphere.

The heliospheric imaging of CMEs and their shocks through larger parts of the heliosphere has created yet another research focus. It provides the opportunity to directly compare imaging and in-situ measurements of the same events and solar wind features. Past studies were only able to extrapolate speed and direction measurements from coronagraphs close to the sun to in-situ measurements at 0.3 AU at best. Even so, they proved that strong heliospheric shocks are driven by CMEs, thus settling a long debate. Now, we can perform such studies routinely and can even image the structures at the same time as they are sampled in-situ. When we take into account the capability of determining the three-dimensional quantities for the size and propagation direction for the larger structures afforded by the dual *STEREO*-HI observations, we end up with an extremely powerful arsenal for understanding the evolution and interaction of solar structures in the inner heliosphere. A recent analysis[17] serves as a useful demonstration of the joint use of HI and in-situ data and modeling to understand the longitudinal distribution of Solar Energetic Particle (SEP) fluxes across more than 140^0 of separation. The CME driven shock was imaged by the HIs allowed careful tracking of its expansion along the ecliptic. At the same time, SEPs were detected by both STEREO spacecraft and the ACE spacecraft at L1 but with different fluxes, intensity gradients and times of arrival. The CME and its shock properties were calculated based on the HI and coronagraphs measurements and were used as input constraints for a global MHD model that simulated the CME from the Sun to Earth. The model was also able to follow the magnetic connectivity of each spacecraft to the Sun. Since SEPs follow the magnetic field lines, it was expected that the y would be detected when the CME shock encountered the appropriate field line. Indeed, the model results showed that the SEP detections and intensities rose when the imaging measurements suggested that the shock encountered the magnetic field line passing by the spacecraft. For one case, the shock reached the field line late in the event when it had lost most of its strength. The observation readily explained the extremely low SEP intensities. In other words, the observations were fully consistent with particles accelerated by the CME shock and not by a flare. Such clear determination of the origin of SEPs is one of the major implications of such comprehensive studies. They have the potential to clear up the confusion of the SEP origin (flare or CME) that has bogged down our under-

7. http://smei.nso.edu/image_info.html

8. http://solphys.nrl.navy.mil/users/vourlidas/docs/ipparchos/all_201002_larger.mpg

standing of particle acceleration in the heliosphere.

Space Weather and the Evolution of Heliophysics

Solar effects on Earth, collectively called Space Weather, have become a major research focus in the last decade thanks to better observations and increased public awareness. The great improvement in remote sensing and in-situ coverage of the inner heliosphere has allowed scientists to correlate solar phenomena to their in-situ signatures. Specifically, observations from the *SOHO* and *ACE* satellites have established CMEs as the main drivers of Space Weather. At the same time, society's increasing dependence on space-based assets, such as GPS and telecommunications satellites, has drawn the attention of the political, and military authorities and of course of the public to Space Weather and consequently to its solar sources. The ready availability of solar images[9] and movies on the internet[10] continue to feed a growing awareness of our intimate relationship to our star, the Sun. Public attention may be a double-edge sword, however.

On one hand, it justifies investments in heliophysics research and eases the communication of our science to the public and especially to the younger generation of prospective scientists. Heliophysicists are in the enviable position to be able to relate easily the results of their work to the public rather than being burden with the common (mis)conception of a scientist as the privileged denizen of an ivory tower.

On the other hand, the increasing applicability of Space Weather research is signaling a shift away from basic research towards an operational approach for some aspects of heliophysics research, such as the solar wind-magnetosphere interaction or the CME heliospheric propagation research. Such 'research-to-operations' or R2O endeavors are still in their infancy in heliophysics. There seems to be some confusion as to who is supposed to contact such research or which organization is supposed to fund it (NASA, NOAA, or DoD in the case of the U.S.A) or even whether it still constitutes basic research (and therefore should be contacted by bona-fide heliophysicists) or operations (and should be left to operators) . This dichotomy is not unlike the debate that captured atmospheric scientists during the 1960's when a spade of research satellites in geostationary orbits (i.e., the *Nimbus* program) transformed atmospheric physics into robust and actionable weather prediction (with the advent of the *GOES* program). Is our field going to spun off its own meteorologists or shall we call them…*space-weatherlogists?* Time will tell but it is sure that change is afoot in our discipline and it has come out of the impressive space observations of the last years.

Future

Reaching the end of this review, we have barely scratched the surface of the latest heliophysics research. We left out exciting results on the direct measurements of magnetic reconnection in the heliosphere and within the Earth's magnetosphere. We did not discuss the *THEMIS* mission (led by one of our Greek colleagues, Dr. Aggelopoulos) success in uncovering how CMEs trigger geomagnetic storms and produce the spectacular polar lights We left out the discovery of a belt of Energetic Neutral Atoms (ENAs) at the edge of the heliosphere nor did we have space to discuss the crossing of the heliopause by the intrepid…and indestructible *Voyager* 1 and 2 spacecraft which continue to provide measurements 40 years after their launch. Maybe a future article will give these successes their proper forum. It is clear, however, that heliophysics is a very active field of research under a fast pace of evolution. The huge amounts of data and new observing capabilities paint a bright future for the younger generation of heliophysicists. Already, two missions to observe the Sun from two new vantage points are in the development phase. The ESA-NASA *Solar Orbiter* mission will observe the sun from 0.28 AU and slowly rise to 30^0 above the equator while NASA's *Solar Probe Plus* mission will go to the unprecedented distance of 9.5 Rs from the solar surface where the solar flux is 400 times higher than at Earth and will directly sample the coronal properties of a star. The future of heliophysics is indeed bright!

Acknowledgements

I like to thank the editors of Hipparchos for giving me the opportunity to discuss heliophysics research. Much of this research would be impossible without NASA's open data policy. The work of the author was supported by NASA Contract S-13631-Y.

9. http://www.solarmonitor.org/index.php
10. http://www.youtube.com//SDOmission2009

References

1. Marsch, Eckart, Hui Tian, Jian Sun, Werner Curdt, and Thomas Wiegelmann. "Plasma Flows Guided by Strong Magnetic Fields in the Solar Corona." *Astrophysical Journal* 685 (2008): 1262-1269. http://adsabs.harvard.edu/abs/2008ApJ...685.1262M.
2. Doschek, G. A., H. P. Warren, J. T. Mariska, K. Muglach, J. L. Culhane, H. Hara, and T. Watanabe. "Flows and Nonthermal Velocities in Solar Active Regions Observed with the EUV Imaging Spectrometer on Hinode: A Tracer of Active Region Sources of Heliospheric Magnetic Fields?" *Astrophysical Journal* 686 (2008): 1362-1371. http://adsabs.harvard.edu/abs/2008ApJ...686.1362D.
3. Wang, T. J., L. Ofman, J. M. Davila, and J. T. Mariska. "Hinode/EIS observations of propagating low-frequency slow magnetoacoustic waves in fan-like coronal loops." *Astronomy and Astrophysics* 503 (2009): L25-L28. http://adsabs.harvard.edu/abs/2009A%26A...503L..25W.
4. Stenborg, G., A. Vourlidas, and R. A Howard. "A Fresh View of the Extreme-Ultraviolet Corona from the Application of a New Image-Processing Technique." *The Astrophysical Journal* 674, no. 2 (2008): 1201–1206.
5. Stenborg, G., E. Marsch, A. Vourlidas, R. Howard, and K. Baldwin. "A novel technique to measure intensity fluctuations in EUV images and to detect coronal sound waves nearby active regions." *Astronomy and Astrophysics* 526 (2010): 58. http://adsabs.harvard.edu/abs/2011A%26A...526A..58S.
6. de Pontieu, Bart, et al, Theodore D. Tarbell, Alan M. Title, et al. "A Tale of Two Spicules: The Impact of Spicules on the Magnetic Chromosphere." *Publications of the Astronomical Society of Japan* 59, 655 (2007). http://adsabs.harvard.edu/abs/2007PASJ...59S.655D
7. Athay, R.G. & Holzer, T. E., ApJ, 255, 743, "The Role of Spicules in Heating the Solar Atmosphere"
8. De Pontieu, B., S. et al. "The Origins of Hot Plasma in the Solar Corona." *Science* 331, 55 (2011). http://adsabs.harvard.edu/abs/2011Sci...331...55D.
9. De Pontieu, Bart, Viggo H. Hansteen, Scott W. McIntosh, and Spiros Patsourakos. "Estimating the Chromospheric Absorption of Transition Region Moss Emission." *Astrophysical Journal* 702 (September 1, 2009): 1016-1024. http://adsabs.harvard.edu/abs/2009ApJ...702.1016D
10. Temmer, M., A. M. Veronig, E. P. Kontar, S. Krucker, and B. Vršnak. "Combined STEREO/RHESSI Study of Coronal Mass Ejection Acceleration and Particle Acceleration in Solar Flares." *The Astrophysical Journal* 712 (2010): 1410-1420. http://adsabs.harvard.edu/abs/2010ApJ...712.1410T.
11. Zhang, J., and K. P. Dere. "A statistical study of main and residual accelerations of coronal mass ejections." *The Astrophysical Journal* 649, no. 2 (2006): 1100–1109.
12. Krucker, Säm, H. S. Hudson, L. Glesener, S. M. White, S. Masuda, J.-P. Wuelser, and R. P. Lin. "Measurements of the Coronal Acceleration Region of a Solar Flare." *The Astrophysical Journal* 714 (2010): 1108-1119. http://adsabs.harvard.edu/abs/2010ApJ...714.1108K.
13. Patsourakos, S., A. Vourlidas, and B. Kliem. "Toward understanding the early stages of an impulsively accelerated coronal mass ejection. SECCHI observations." *Astronomy and Astrophysics* 522 (2010): 100. http://adsabs.harvard.edu/abs/2010A%26A...522A.100P..
14. Sheeley, N. R., A. D. Herbst, C. A. Palatchi, Y.-M. Wang, R. A. Howard, J. D. Moses, A. Vourlidas, et al. "Heliospheric Images of the Solar Wind at Earth." *Astrophysical Journal* 675 (March 1, 2008): 853-862. http://adsabs.harvard.edu/abs/2008ApJ...675..853S.
15. Sheeley, N. R., A. D. Herbst, C. A. Palatchi, Y.-M. Wang, R. A. Howard, J. D. Moses, A. Vourlidas, et al. "SECCHI Observations of the Sun's Garden-Hose Density Spiral." *Astrophysical Journal* 674 (February 1, 2008): L109-L112. http://adsabs.harvard.edu/abs/2008ApJ...674L.109S.
16. Rouillard, A., P. Savani, J. Davies, B. Lavraud, R. Forsyth, S. Morley, A. Opitz, et al. "A Multispacecraft Analysis of a Small-Scale Transient Entrained by Solar Wind Streams." *Solar Physics* 256, no. 1 (May 1, 2009): 307-326. http://dx.doi.org/10.1007/s11207-009-9329-6.
17. Rouillard, A., P. et al. "White-light observations of a bow wave forming ahead of a coronal mass ejection.", *Astrophysical Journal*, 2011, in press.

Visit our website

http://www.helas.gr

The above web server contains information, both in greek and english, about the Hellenic Astronomical Society (Hel.A.S.), the major organization of professional astronomers in Greece. The Society was established in 1993, it has more than 250 members, and it follows the usual structure of most modern scientific societies. The web pages provide information and pointers to astronomy related material which would be useful to both professional and amateur astronomer in Greece. It contains a directory of all members of the Society, as well as an archive of all material published by the Society such as the electronic newsletters, past issues of "Hipparchos", and proceedings of Conferences of Hel.A.S. The server is currently hosted by the University of Thessaloniki.

13TH EUROPEAN SOLAR PHYSICS MEETING

SCIENTIFIC ORGANIZING COMMITTEE

S. POEDTS (CHAIR)
G. CAUZZI
L. FLETCHER
K. GALSGAARD
M. GEORGOULIS
V. MELNIKOV
D. MUELLER
V. NAKARIAKOV
H. PETER
P. RUDAWY
J. TRUJILLO-BUENO
A. VERONIG
M. COLLADOS (EAST)
N. CROSBY (SWWT)
A. HANSLMEIER (JOSO)
S. POHJOLAINEN (CESRA)

ESPM-13
12 - 16 SEPTEMBER 2011
RHODES, GREECE

LOCAL ORGANIZING COMMITTEE

M. GEORGOULIS (CO-CHAIR)
G. TSIROPOULA (CO-CHAIR)
C. GONTIKAKIS
S. PATSOURAKOS
K. TZIOTZIOU
L. VLAHOS

http://astro.academyofathens.gr/espm13

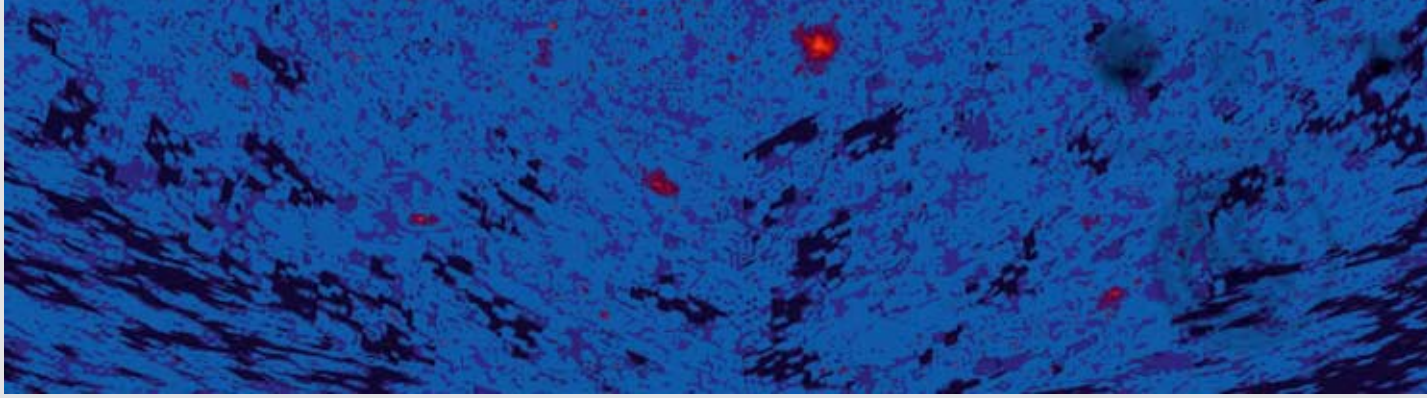

IMPRS
for Astronomy and Astrophysics

PhD Positions in Astronomy

Call for Applications
Deadline: November 15th, 2011

International Max Planck Research School (IMPRS) for Astronomy and Astrophysics
at the Universities of Bonn and Cologne

MAX-PLANCK-GESELLSCHAFT

universitätbonn

General

The International Max Planck Research School (IMPRS) for Astronomy and Astrophysics, is funded by the German Max Planck Society and is operated by the Max-Planck-Institut für Radioastronomie (MPIfR) in collaboration with the Argelander-Institut für Astronomie (AIfA) of the University of Bonn and the I. Physikalisches Institut at the University of Cologne. It offers three-year financed PhD courses. The official language is English. Currently it hosts roughly 40 students from 17 countries around the world.

IMPRS astronomy & astrophysics Bonn and Cologne

Fields of Research

The IMPRS for Astronomy and Astrophysics offers a broad spectrum of topics in observational and theoretical, galactic and extragalactic astrophysics, observational and theoretical cosmology, fundamental physics with astronomical tools and instrumentation.

Some examples:
– AGN Astrophysics – Structure and Kinematics of AGN Jets
– Extragalactic Relativistic Flows – Multi-band Blazar Astrophysics
– Multi-frequency AGN Polarimetry – VLBI Studies of AGNs
– Infrared Interferometry of Disks and Jets of Young Stars
– Protoplanetary Disks – Radiative Transfer Modeling – Galactic Masers
– Infra-Red Interferometry of AGN – Gravitational Lensing
– Galactic and Extragalactic Magnetic Fields – High Precision Astrometry
– Stellar Astrophysics and Stellar Evolution
– Supermassive Binary Black Holes in AGN
– Stellar Population Studies – Astro-chemistry
– Galactic Dynamics – Binary Pulsars – Neutron Stars
– Experimental tests of gravity – Transient Radio Sky
– Faraday Galaxy Tomography – Radio Pulsars
– Gravitational Wave Detection with Pulsar Timing
– Stellar Custer Dynamics – Dark Matter
– Galactic Center Studies.

Besides the expertise in radio astronomy of the MPIfR the IMPRS for Astronomy and Astrophysics provides the opportunity for scientific activity in almost all fields of contemporary astrophysics, techniques and energy bands.

Training

The IMPRS for Astronomy and Astrophysics offers a competitive PhD program on the basis of a tightl structured curriculum, including:

- Advanced lectures on fundamental astrophysical fields
- Soft skill seminars (e.g. presentation skills, time management, scientific reading)
- Weekly students seminars
- Annual, "students-only" workshop where they develop team activities aside from their main research interests
- Colloquia at the three hosting institutions given by experts from all over the globe
- University courses
- Thesis committees monitor the progress of each student and provide scientific feedback to the PhD course

Furthermore, the students are strongly encouraged and funded to travel to international schools, conferences and the best observing facilities around the world. They are exposed to the most advanced techniques and methods using state-of-the-art earth-bound or space observatories, such as the unique 100-m radio telescope in Effelsberg and the most advanced instruments in millimeter, sub-millimeter and high-energy bands, such as the APEX 12 m telescope, the Large Binocular Telescope and many more.

The call for applications is open until November 15, 2011. Encouraged to apply are students with a M.Sc. degree or diploma (including a written thesis) in Physics or closely related subjects. Solid astrophysical background is highly favored.

More details on the IMPRS program and the admission requirements and process can be found at the IMPRS website:

www.mpifr.de/imprs | www.youtube.com/user/imprstube

Max-Planck-Institut für Radioastronomie | Auf dem Hügel 69 | D-53121 Bonn, Germany | Tel. +49 228 525 456 | imprs@mpifr-bonn.mpg.de

Background image: All-sky map at gamma-rays observed with LAT on-board Fermi-GST. Credit: NASA, International LAT Team

Back issues of Hipparchos

Hipparchos is the official newsletter of the Hellenic Astronomical Society. It is distributed by post to the members of the society.

You can download back issues from:

http://www.helas.gr/news.php